

ENVIRONMENTAL SIGNIFICANCE OF ISOTOPIC  
AND TRACE ELEMENTAL VARIATIONS  
IN BANDED CORALS

043  
CHA  
15140

Thesis submitted to

*The Maharaja Sayajirao University of Baroda*

for the Degree of

Doctor of Philosophy

in

Geology

by

Supriya Chakraborty

*December 1993*

Physical Research Laboratory  
Navrangpura  
Ahmedabad 380 009  
Gujarat (INDIA)

043

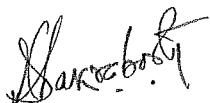


B15140

043  
CHA  
15/40

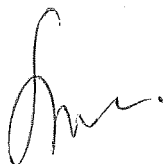
## CERTIFICATE

This is to certify that the contents of this thesis is the original research work of the candidate and have at no time been submitted for any other degree or diploma.



(Supriya Chakraborty)

Candidate



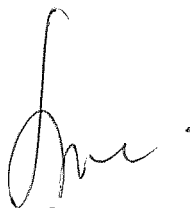
(Prof. S. J. Desai)

Co-Guide



(Prof. S. Krishnaswami)

Guide



(Prof. S. J. Desai)

Head

Dept. of Geology

M.S. University of Baroda

*Dedicated to*  
*my mother*  
*and fond memory*  
*of my late father*

...the intellect, it is said, is man's highest instrument and he must think and act according to its ideas. But this is not true; the intellect needs an inner light to guide, check and control it quite as much as the vital. There is something above the intellect which one has to discover and the intellect should be only an intermediary for the action of that source of true Knowledge.

Sri Aurobindo



## Acknowledgements

I wish to express my gratefulness to R Ramesh who initiated me to the wonderful world of geochemistry and palaeoclimatology and also for his tireless efforts and countless discussions in shaping the entire work. I like to express my deep sense of gratitude to S Krishnaswami, who with his great insight in the field of geochemistry guided me the finer intricacies of data analysis and their presentation. I am thankful to S J Desai for his constant encouragement and inspiration.

I express my appreciation and indebtedness to M M Sarin who taught me with great patience, the complicated methodology of cadmium geochemistry and also to R Rengarajan who extended full cooperation in this endeavour. I am beholden to S K Bhattacharya for his comments and criticisms and reviewing of this thesis. B L K Somayajulu has been a constant source of inspiration throughout this work. I am benefitted by the suggestions given by V Satyan.

I remember with pleasure the association of R Bhushan who shared the credit in establishing the Radiocarbon laboratory in the Chemistry Building and helped me in various stages of radiocarbon analyses. In this context I must acknowledge the inevitable and timely cooperation of M Yadav and S Kusumgar. I am also very much indebted to J P Bhavsar and R A Jani for their technical help in various stages, from sample collection, instrument handling to sample measurements.

I am extremely thankful to J M Lough for providing a coral sample belonging to Great Barrier Reef along with its density data and also for her continued support in various aspects of this thesis work. Thanks are due to M V M Wafar who provided me a coral sample collected from the Kavaratti lagoon. My sincere thanks go to G B Pant for providing a tree ring sample and also to R Shetye. I am benefitted receiving various data and useful comments from them. I thank M I Patel and J Veron for the identification of coral species.

It is a pleasure to acknowledge R B Dunbar and J E Cole who were kind enough to give me an opportunity in attending the coral workshop, the first of its kind held at La Parguera, Puerto Rico in Nov '92. I am also grateful for being invited by D Sheu and W C Wang to attend the PAGES workshop at Taipei in Apr '93. Both these workshops helped me a lot in widening my knowledge in the field of 'coral climatology'.

I wish to thank G T Shen who showed keen interest in the Cd work of Lakshadweep coral and provided valuable suggestions during the establishment of Cd geochemistry at PRL. I received helpful gestures and lot of encouragements from E R M Druffel, J E Cole, T McConnaughey, and D W Lea during the course of this work.

I would like to express my thankfulness to N Sinha and Deomurari for their technical cooperation in coral cutting and sampling. In this aspect I would like to thank J N Goswami for his kind permission in using his laboratory and also for his

suggestions and advice as (ex) Academic Committee chairman in academic as well as in non-academic affairs. I will always remember the sincere and timely effort of A R S Pandian, N R Manchanda and B L Panchal for their help in maintaining and smooth functioning of various instruments. Sai Iyer has always been a valued friend for his expertise in software handling. My special thanks go to G P Patel and V Ranganathan for their friendly cooperation in some aspects of this work. I am thankful to J T Padia, K Pande, N Bhandari, P N Shukla, J R Trivedi, T R Venkatesan, S V S Murty, R K Pant, A K Singvi, P Sharma, S K Gupta, V G Shah, K R Nambiar, K V Haridas, P G Thomas, G Kori and Arjun Premji for their cooperation in various aspects.

I also gratefully acknowledge the help rendered by P K Kurup & K K Shivshankaran and P G Ubale & his coworkers for their inevitable supports in glassware and hardware fabrication. D Ranpura was always active with smiling face in making several photographs. S C Bhavsar made my job easy by drafting many figures. I thank them all. I wish to express my appreciation to R R Bharucha and all other library staff for their quick and kind response in providing library materials and other documentation. I gratefully acknowledge the cooperations extended by the staff members of the computer centre, liquid nitrogen plant and the despatch section.

It is a pleasure to remember many happy moments with lively and educative discussions with Srini and Sarkar. I shared the joy in many academic affairs having discussion and association with Gopal, Renga, Bhushan, Avijit, Guru, Krishnan, Manoj, Debashis, Seema, Yadav, Somesh, Rama, Rajen, Sushma, Subrata, Jyoti, Yajna, Debabrata. During the agonizing days of thesis writing I especially remember the valued friendship of Himadri and the moral support of Pauline. I think myself fortunate having friendship with Ratan at the last stage of the hectic days of thesis writing. I thank my all other friends who extended help in some way or other, kept me jolly and cheerful and above all provided friendly and lively association in PRL which I will never forget. My sincere thank goes to P Chakraborty for her effort in the improvement of the thesis writing. Partial financial support for this work was provided by the Department of Ocean Development and INSA young scientist grant to R Ramesh.

# CONTENTS

	Page
List of Figures	iv
List of Tables	vii
List of Abbreviations	ix
Chapter I <b>Introduction</b>	1
I.1              Corals:a source of past environmental records	2
I.2              Proxy climate records in corals	2
I.2.a            Stable oxygen isotopes	4
I.2.b            Stable carbon isotopes	6
I.2.c            Radiocarbon in annual bands of corals	7
I.2.d            Trace elements	8
I.3              Scope of the present work	9
Chapter II <b>Experimental Techniques</b>	12
II.1             Sampling and chronology	12
II.2             Stable isotope measurements	15
II.2.a           Sampling and pretreatment	15
II.2.b           Mass spectrometric measurements	17

II.3	Radiocarbon measurements	20
II.3.a	Sample preparation	20
II.3.b	Benzene synthesis	21
II.3.c	Radiocarbon counting	22
II.3.d	$^{14}\text{C}$ blanks and standard	23
II.3.e	Reporting of radiocarbon activity	27
II.3.f	Intercalibration and repeat measurements	27
II.4	Cadmium measurements	28
II.4.a	Sample cleaning	28
II.4.b	Coprecipitation of Cd with APDC and atomic absorption analysis	28
II.4.c	Measurement of Cd concentration	30
II.5	Summary	32
 Chapter III	 <b>Results and Discussion</b>	 33
III.1	X-radiographic analysis	33
III.2	Stable isotopic studies	37
III.2.a	Lakshadweep corals	37
III.2.b	Gulf of Kutch coral	57
III.2.c	Effects of sampling on the retrieval of climatic signal	64
III.2.d	Stanley reef coral	72
III.3	Radiocarbon results	83

III.3.a	Gulf of Kutch coral	83
III.3.b	Tree rings	85
III.3.c	Air-Sea CO <sub>2</sub> exchange rate (ASCER) in the Gulf of Kutch	87
	Appendix-I	99
	Appendix-II	99
	Appendix-III	100
	Appendix-IV	101
	Appendix-V	101
III.4	Cadmium analyses	102
III.5	Synthesis	104
Chapter IV	Summary and Conclusions	106
	Scope for further work	110
	References	112
	Appendix A	
	List of Publications	A22

## List of Figures

No.	Caption	Page
2.1a	Location of corals from the Indian coast and tree sampled for proxy climate records	13
2.1b	Coral sample location (Stanley Reef, Australia)	14
2.2	Coral sectioning and sampling for X-radiography and tracer measurements	16
2.3a	Reproducibility of oxygen and carbon isotopic ratios of Z-Carrara	18
2.3b	Reproducibility of oxygen and carbon isotopic ratios of Makrana marble	19
2.4	$^{14}\text{C}$ blank (background) count-rates of marble	24
2.5	Count-rates of NBS Oxalic acid II standard (4990C)	26
2.6	Determination of Cd concentration by standard addition method	31
3.1	X-ray positive of a coral slice <i>P. compressa</i> , from the Lakshadweep Is.	34
3.2	Variations in bandwidth with time in corals from the Lakshadweep, Gulf of Kutch and Stanley Reef	36
3.3	Variations in $\delta^{13}\text{C}$ and $\delta^{18}\text{O}$ with distance in <i>P. compressa</i> (KV-1) from the Kavaratti lagoon, Lakshadweep islands	39

3.4	Mean monthly SST, salinity, $\delta^{18}\text{O}$ of water and expected $\delta^{18}\text{O}$ of coral carbonate for the Lakshadweep region	41
3.5	Plot of observed vs. calculated SST using coral thermometry	44
3.6	$\delta^{18}\text{O}$ and $\delta^{13}\text{C}$ variations with time in a 25 year old <i>P. compressa</i> coral (KV-2) from the Kavaratti lagoon, Lakshadweep Is.	46
3.7	Plot showing observed and calculated SST based on coral (KV-2) $\delta^{18}\text{O}$	48
3.8	Intercomparison of the $\delta^{18}\text{O}$ of the two <i>P. compressa</i> corals from the Lakshadweep region (1983-1987)	50
3.9	Relationship between $\delta^{13}\text{C}$ and extension rate in coral KV-2	55
3.10	$\delta^{13}\text{C}$ and $\delta^{18}\text{O}$ records of the coral <i>F. speciosa</i> from the Gulf of Kutch	58
3.11	Seasonal SST variations in the Gulf of Kutch near the coral site	60
3.12	$\delta^{18}\text{O}$ and $\delta^{13}\text{C}$ minima of the GK coral and interannual rainfall variability in the Kutch & Saurashtra region	62
3.13	Sampling of the sine curve representing coralline oxygen isotopic variations	65
3.14	Result of the simulation study on the dependence of retrieved $\delta^{18}\text{O}$ seasonal amplitude on sampling parameters for a constant annual increment; $g=5$ mm	67
3.15	Result of the simulation study on the dependence of retrieved $\delta^{18}\text{O}$ seasonal amplitude on sampling parameters for a constant annual increment; $g=10$ mm	69

3.16	Plot of retrieved amplitude vs growth rate	69
3.17	Result of the simulation study on the dependence of retrieved $\delta^{18}\text{O}$ seasonal amplitude on sampling parameters for variable annual increment	71
3.18	Relationship between calcification rate and extension rate in the coral <i>P. lutea</i> from the Stanley Reef	73
3.19	Covariation of SST and $\delta^{18}\text{O}$ of <i>P. lutea</i>	75
3.20	Growth rate variability in Tr-1 and Tr-2 in the coral <i>P. lutea</i>	77
3.21	Density, $\delta^{18}\text{O}$ and $\delta^{13}\text{C}$ variations along Tr-1 of <i>P. lutea</i>	79
3.22	Density, $\delta^{18}\text{O}$ and $\delta^{13}\text{C}$ variations along Tr-2 of <i>P. lutea</i>	81
3.23	$\Delta^{14}\text{C}$ time series in coral <i>F. speciosa</i> from the Gulf of Kutch	84
3.24	$\Delta^{14}\text{C}$ time series of NH and Thane (near Bombay) air	86
3.25	Calculated time variations of radiocarbon activity in the Gulf of Kutch considering only air-sea exchange of $\text{CO}_2$	91
3.26	Two box model of the northern Arabian Sea	93
3.27	Calculated time variations of radiocarbon activity in the mixed layer of the northern Arabian Sea	95
3.28	Calculated time variations of radiocarbon activity in the Gulf of Kutch	97
3.29	Temporal variations in Cd concentration and $\delta^{18}\text{O}$ in coral KV-1	103



## List of Tables

No.	Caption	Page
I.1	Proxy environmental indicators in corals	3
II.1	Isotopic analysis of Z-Carrara and Makrana marble standard	20
II.2	Net count-rates of NBS oxalic acid standard II (4990-C)	25
II.3	Reproducibility of blank and Cd standard absorbance measurements	29
II.4	Reproducibility of Cd measurements in "spiked" coral solution	31
II.5	Summary of measurements made in corals and tree rings in this work	32
III.1	Mean and range of bandwidths in coral samples analyzed	37
III.2	$\delta^{18}\text{O}$ data of coral KV-1 & Am and giant clam GC	A1
III.3	$\delta^{13}\text{C}$ data of coral KV-1	A7
III.4	Comparison between observed and derived SST	47
III.5	$\delta^{18}\text{O}$ and $\delta^{13}\text{C}$ data of KV-2 coral	A9
III.6	The average carbon isotopic composition of high and low density bands in coral KV-2	54
III.7	$\delta^{18}\text{O}$ and $\delta^{13}\text{C}$ data of GK coral	A14
III.8a	$\delta^{18}\text{O}$ , $\delta^{13}\text{C}$ , and density records of SR coral (Tr-1)	A16
III.8b	$\delta^{18}\text{O}$ , $\delta^{13}\text{C}$ , and density records of SR coral (Tr-2)	A19
III.9	Correlations among the stable isotopes and the density variations in coral <i>P. lutea</i>	80

III.10	$\Delta^{14}\text{C}$ minima, maxima and peak-shifts for different oceanic regions	88
III.11	Symbols, units and values of different parameters used in the box model calculation	92
III.12	$\Delta^{14}\text{C}$ records in annual bands of GK coral and Thane tree rings	A21

## List of abbreviations

Abs	Absorbance
APDC	Ammonium pyrrolidine-dithiocarbamate
Am	A four year old coral ( <i>P. compressa</i> ) from the Amini lagoon, Lakshadweep Is.
ASCER	air-sea CO <sub>2</sub> exchange rate
COADS	Comprehensive Ocean Atmospheric Data Set
cpm	counts per minute
DIC	dissolve inorganic carbon
FS	Foram standard carbon dioxide
GBR	Great Barrier Reef, Australia
GC	A giant clam ( <i>Tridacna maximus</i> ) from the Amini lagoon, Lakshadweep Is.
GK	A 41 old coral ( <i>F. speciosa</i> ) from the Gulf of Kutch, northern Arabian Sea
GKh	Gulf of Kutch
HD	high density band
KV-1	A 5 year old coral ( <i>P. compressa</i> ) from the Kavaratti lagoon, Lakshadweep Is.
KV-2	A 25 year old coral ( <i>P. compressa</i> ) from the Kavaratti lagoon, Lakshadweep Is.
LD	low density band
LDP	Lakshadweep archipelago
LLCM	Low level count mode
MMB	Makrana marble
PDB	Belemnite PeeDee formation
POPOP	2, 2'-p-phenylene-bis-5 phenyl oxazole
PPO	diphenyloxazole
rpm	revolution per minute

SR	An 18 year old coral ( <i>P. lutea</i> ) from the Stanley Reef, Australia
SST	Sea surface temperature
SWM	South west monsoon
ThTR	A 20 year old teak tree ( <i>Tectona grandis</i> ) from Thane
ZC	Z-Carrara

# INTRODUCTION

It is well established that the Earth's climate has changed in the past, both on short and on long time scales. Reconstruction of past climates provides not only snap shots of conditions that prevailed during that time but also a tool to test climate models. Availability of instrumental records of climate are limited to the past several decades at isolated sites. Hence for a better understanding of natural climate variability it is necessary to extend the available limited instrumental climatic records both in space and time, using different natural archives as proxy indicators of climate. Long lived hermatypic corals preserve in them high quality, high resolution records of "ocean climate" for the past few centuries. The study of isotopic and chemical tracers in the annual bands of corals has been shown to provide accurate records of seasonal and interannual variability of meteorological and oceanographic parameters such as the sea surface temperature (SST), salinity, upwelling, rainfall and air-sea gas exchange (Fairbanks & Dodge 1979; Dunbar & Wellington 1981; Druffel & Suess 1983, Druffel 1985, 1987; Pätzold 1984; Cember 1989; McConnaughey 1989; Shen *et al.* 1987, 1992; Cole & Fairbanks 1990). Recognizing the importance of corals in providing high resolution proxy climate records for the past several centuries, their study has been brought under the umbrella of the International Geosphere Biosphere Programme (IGBP). One of IGBP's core project is Past Global Changes (PAGES) which aims to reconstruct high resolution ( $\leq 1$ yr) palaeoclimatic information for the last 2000 years from corals and a few other repositories, *e.g.* tree rings, varved and coastal sediments.

The present work focuses on the study of corals from the northern Indian Ocean region to explore their potential as a source of high resolution climatic and environmental records.

## I.1 CORALS : A SOURCE OF PAST ENVIRONMENTAL RECORDS

Corals are marine organisms that grow in shallow sea water in tropical regions. They deposit aragonitic calcium carbonate, and are mainly classified as hermatypic and ahermatypic corals. The hermatypic corals form reefs and host endosymbiotic algae called zooxanthellae (*e.g. Gymnodinium microadriaticum*). These corals generally grow at rates of a few mm to a few cm per year with alternate high and low density growth bands. In many coral species, a high density and low density band together constitute a year's growth (Dodge & Thompson 1974). The mechanism of band formation is not fully understood. Wellington and Glynn (1983) proposed that banding in corals is a complex phenomenon governed by endogenous processes (*e.g. reallocation of energy from growth to reproduction*) mediated by exogenous factors (*e.g. light intensity and productivity*). Highsmith (1979) suggested that variable density banding is a result of differential calcification rates mediated by the effect of light and temperature on zooxanthellar activity and by the effect of temperature on extracellular  $\text{CaCO}_3$  precipitation rate. Despite the complexity in understanding the density band formation, they provide a means of accurately determining the chronology of coral growth. These density bandings can be revealed by X-radiography (Knutson *et al.* 1972; Buddemeier *et al.* 1974; Macintyre & Smith 1974; Barnes & Lough 1989; Lough & Barnes 1990) and their annual nature ascertained through stable isotope systematics (Fairbanks & Dodge 1979). Many corals, thus are easily datable and can provide high resolution (~months) records of climate and environmental history of the region where they grow.

## I.2 PROXY CLIMATIC RECORDS IN CORALS

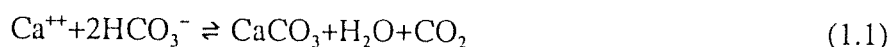
During the past 1-2 decades, several studies have demonstrated that corals contain in them several isotopic and chemical tracers which can serve as proxy climatic indicators. Table I.1 lists some of these well established and promising tracers in corals for the retrieval of past environmental parameters.

Table I.1 Proxy environmental indicators in corals

Tracer	Index of	Reference
Oxygen isotopes	SST, salinity, rainfall	Fairbanks & Dodge 1979; Dunbar & Wellington 1981; Pätzold 1984; Druffel 1985; McConnaughey 1989; Cole & Fairbanks 1990
Carbon isotopes	insolation, nutrient dynamics, CO <sub>2</sub> air-sea exchange	Nozaki <i>et al.</i> 1978; Druffel & Suess 1983; Aharon 1985; Cember 1989
Sr/Ca	SST	Smith <i>et al.</i> 1979; Beck <i>et al.</i> 1992; de Villiers <i>et al.</i> 1993
Ba/Ca	nutrient dynamics, runoff	Shen <i>et al.</i> 1992
Cd/Ca	upwelling, nutrient dynamics	Shen <i>et al.</i> 1987; Lea <i>et al.</i> 1989; Shen & Sanford 1990; Cole <i>et al.</i> 1992; Shen <i>et al.</i> 1992

Of the tracers listed in Table I.1, oxygen isotopes are the most well established and commonly used tracers for climatic reconstruction.

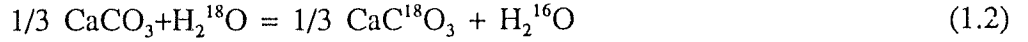
Different environmental parameters influence the coral calcification, their isotopic ratios and abundances of trace elements. Among them are temperature, light intensity, nutrient supply, isotopic and chemical composition of sea water, turbidity, ocean mixing and runoff. The calcification can be expressed by the reaction:



The symbiotic algae (zooxanthellae) which reside in hermatypic corals consume CO<sub>2</sub> for photosynthesis thus favouring the forward reaction *i.e.* calcification (Swart 1983). During the calcification process the corals incorporate in them different chemical and isotopic tracers of climatic and environmental importance.

### I.2.a Stable oxygen isotopes

The oxygen isotopic ratio in the coral  $\text{CaCO}_3$  is a function of two parameters, the SST and the oxygen isotopic ratio of the ambient sea-water. During  $\text{CaCO}_3$  precipitation there is an exchange reaction of oxygen isotopes between  $\text{CaCO}_3$  and  $\text{H}_2\text{O}$ :



The equilibrium constant for this reaction is given by

$$K = [\text{CaC}^{18}\text{O}_3]^{1/3} [\text{H}_2^{16}\text{O}] / [\text{CaCO}_3]^{1/3} [\text{H}_2^{18}\text{O}] \quad (1.3)$$

Since the equilibrium constant (K) depends on temperature (T), calcium carbonate precipitated from water of a constant oxygen isotopic composition but at different temperatures, will have different  $^{18}\text{O}/^{16}\text{O}$  ratios. This is the basis underlying the quantitative determination of palaeotemperatures of ocean water from oxygen isotopes studies of  $\text{CaCO}_3$  (Urey 1947).

The isotopic fractionation that occurs during various physico-chemical processes is described in terms of fractionation factor  $\alpha$ , which is defined as:

$$\alpha_{a-b} = R_a/R_b \quad (1.4)$$

where R is the ratio of the abundance of the heavy to that of the light isotope. The subscripts a and b refer to two phases, A and B. The ratio R, in the different phases is reported in terms of the deviation of the isotopic ratio of the sample relative to that of a standard. This deviation,  $\delta$ , is expressed in parts per thousand (or permil) as given below:

$$\delta(\text{‰}) = [(R_s/R_r) - 1] \cdot 10^3 \quad (1.5)$$

where  $R_s$  and  $R_r$  are the  $^{18}\text{O}/^{16}\text{O}$  (or  $^{13}\text{C}/^{12}\text{C}$ ) in the sample and the standard respectively. The empirical relationship between  $\delta^{18}\text{O}$  of the inorganically precipitated  $\text{CaCO}_3$  and temperature was initially established by Epstein *et al.* (1953), and was later modified by Craig (1965). This has the following form:

$$T = a + b(\delta_c - \delta_w) + c(\delta_c - \delta_w)^2 \quad (1.6)$$

where T is the temp of the water in  $^{\circ}\text{C}$ , in which the precipitation of  $\text{CaCO}_3$  occurs.  $\delta_c$  is



the  $\delta^{18}\text{O}$  of  $\text{CO}_2$  obtained from the carbonate by reacting it with 100% phosphoric acid at 25°C.  $\delta_w$  is the  $\delta^{18}\text{O}$  of  $\text{CO}_2$  equilibrated isotopically at 25°C with water from which the carbonate was precipitated; both  $\delta$ 's measured relative to the same laboratory standard  $\text{CO}_2$ .

This equation was applied successfully for the determination of the palaeotemperature of ocean water based on oxygen isotopic studies in foraminiferal shells in ocean sediments. Though the equation was derived originally for calcite-water-bicarbonate system, it was shown to be equally valid for aragonite-water-bicarbonate system *i.e.* corals and bivalves (Grossman & Ku 1986).

The biologically precipitated  $\text{CaCO}_3$  in equilibrium with sea water has a temperature coefficient of  $-0.22\text{‰}$  per °C, *i.e.*  $\delta^{18}\text{O}$  of the  $\text{CaCO}_3$  decreases by  $0.22\text{‰}$  for every degree rise in water temperature (Epstein *et al.* 1953). In corals the biological processes mediated by endosymbiotic activity also control the isotope fractionation. These processes deplete the oxygen isotopic ratio in the coral skeleton with respect to that expected from the isotopic equilibrium. This depletion or offset is shown to be generally constant within a coral genus. The pioneering work of Weber & Woodhead (1972) established the  $\delta^{18}\text{O}$ -SST relationship for 44 genera of corals of Indo-Pacific origin. Subsequently various investigators (Fairbanks & Dodge 1979; Dunbar & Wellington 1981; Pätzold 1984; McConnaughey 1989) showed that the coral  $\delta^{18}\text{O}$  can be used for the accurate reconstruction of past SST variations. It was also used to investigate climatic features like the El Niño and the Southern Oscillation (Druffel 1985).

As mentioned earlier, in addition to temperature, the  $\delta^{18}\text{O}$  of ambient sea water also controls the coralline  $\delta^{18}\text{O}$ . Therefore in principle it should be possible to determine the sea water  $\delta^{18}\text{O}$  variations based on coral  $\delta^{18}\text{O}$  if independent estimates of SST variations are available. However in general this is not a major application of oxygen isotope studies in corals as most of the tropical oceanic regions show minimal changes in surface water  $\delta^{18}\text{O}$ . Therefore, such studies are restricted to oceanic regions having significant  $\delta^{18}\text{O}$  variability resulting from evaporation, precipitation and runoff. Recently, Cole & Fairbanks (1990) showed that in the Tarawa Atoll coral  $\delta^{18}\text{O}$  was controlled mainly by the sea-water isotopic composition. Intense precipitation in this region changes the sea water isotopic composition which is recorded in the coral  $\delta^{18}\text{O}$ . There is a

significant negative correlation between  $\delta^{18}\text{O}$  and rainfall, making it a useful index of rainfall variability in this region.

Summarizing, the coral  $\delta^{18}\text{O}$  is a powerful tool for quantitatively assessing historical variations in SST, salinity, rainfall and thus provides a measure of "ocean climate" of the recent past.

### I.2.b Stable carbon isotopes

The use of  $\delta^{13}\text{C}$  signal in coral skeletons as an environmental indicator often poses difficulties due to the complicated interaction of physiological processes within the coral-algae system, which produces large and variable disequilibrium-isotopic-fractionation of carbon isotopes. The parameters controlling carbon isotopic systematics in coral  $\text{CaCO}_3$  are: (i) the isotopic composition of seawater  $\Sigma\text{CO}_2$  (Nozaki *et al.* 1978; Aharon 1985) (ii) the coral geometry and growth rate (Land *et al.* 1975; McConnaughey 1989) and (iii) the endosymbiotic photosynthesis (Weber & Woodhead 1972; Goreau 1977; Fairbanks & Dodge 1979). The  $\delta^{13}\text{C}$  of sea water (from which corals precipitate  $\text{CaCO}_3$ ) is controlled by photosynthesis and respiration, air-sea  $\text{CO}_2$  exchange and varying contribution of upwelled waters. The endosymbiotic photosynthesis and respiration are critical factors in controlling the  $\delta^{13}\text{C}$  of coral  $\text{CaCO}_3$ . Photosynthesis preferentially removes light isotopes from sea water thereby enriching the residual inorganic carbon pool in  $^{13}\text{C}$  causing an increase in the skeletal  $\delta^{13}\text{C}$ . On the other hand respired  $\text{CO}_2$  which is depleted in  $\delta^{13}\text{C}$  relative to dissolved inorganic carbonate (DIC) makes the carbon pool lighter and hence also the coral skeleton lighter in  $^{13}\text{C}$ . Summarizing, one can say that the isotopic composition of coral skeleton results from the mixing of two carbon components. One of these components consists of DIC, whereas the other is the metabolic  $\text{CO}_2$ . However the extent of the contribution of the metabolic  $\text{CO}_2$  is not known, but could be significant, and probably varies with species.

Endosymbiotic photosynthesis which depends largely on the light intensity provides qualitative information on cloudiness and hence insolation. The  $\delta^{13}\text{C}$  in coral  $\text{CaCO}_3$  is in someway controlled by endosymbiotic photosynthesis and hence may provide information on cloudiness and insolation. Indeed in many places coralline  $\delta^{13}\text{C}$  shows a covariation

with the seasonal insolation variation (Pätzold 1984; McConnaughey 1989). Fairbanks & Dodge (1979) observe that the  $\delta^{13}\text{C}$  of the *Montastrea annularis* of Bermuda covaries with insolation.

Though the application of coralline  $\delta^{13}\text{C}$  to retrieve climatic parameters is not straightforward, it appears to be a useful tracer for obtaining qualitative information on insolation and surface ocean productivity.

### I.2.c Radiocarbon in annual bands of coral

The radiocarbon content of surface ocean water at any location is a dynamic balance between its supply and removal processes such as the air-sea exchange, lateral transport and upwelling. Corals contain in them a chronological record of  $^{14}\text{C}$  variations of surface sea water, analogous to  $\delta^{13}\text{C}$ . These records provide details of air-sea exchange of  $\text{CO}_2$ . Information on the rate of air-sea  $\text{CO}_2$  exchange is critical to determine the fate of fossil fuel  $\text{CO}_2$ , and hence models related to the greenhouse warming. The air-sea  $\text{CO}_2$  exchange rate (ASCER) is influenced by physical, chemical and biological processes occurring in the oceans.

The natural distribution of radiocarbon in the environment was perturbed considerably by the injection of large quantities of  $^{14}\text{C}$  in the atmosphere through nuclear (bomb) tests conducted primarily during the late 50's and early 60's. The abundance of bomb carbon in the atmosphere has been decreasing since ~1963, resulting from its exchange with ocean. From a knowledge of the rate of change of bomb  $^{14}\text{C}$  activity in the atmosphere and in surface sea water it is possible to determine ASCER (Stuiver 1980; Druffel & Suess 1983; Cember 1989). The temporal evolution of surface water bomb-radiocarbon activity can be obtained from dated coral bands and that of the atmospheric bomb radiocarbon variation can be retrieved from tree rings. Following this approach Druffel & Suess (1983) made detailed studies of ASCER in the west Atlantic and the equatorial Pacific region and Cember (1989) in the Red Sea. In addition to determining the air-sea exchange of  $\text{CO}_2$ , radiocarbon in corals can also provide information on water mass renewal and ventilation rates (Druffel 1989). All these studies have demonstrated that

the measurement of radiocarbon activity in coral bands is useful for monitoring surface water radiocarbon activity, which helps in understanding the ocean mixing processes and the determination of air-sea  $\text{CO}_2$  exchange rate.

#### I.2.d Trace elements

Corals incorporate in their skeleton various minor and trace elements such as Mg, Sr, Ba and Cd during calcification process. All these elements are cations with charge +2, and can substitute for Ca in the  $\text{CaCO}_3$ . The ratio of the (metal/Ca) incorporated in the  $\text{CaCO}_3$  by and large depends on their abundance ratio in the ambient water and the SST. Elements like Cd and Ba, have nutrient like distribution in sea water (*i.e.* concentration increases from surface to deep waters mimicking nutrient (phosphates and nitrate) profiles (Bruland 1983)) and their concentrations in surface water is influenced by upwelling and biological activities. Therefore, through a high resolution (~ 2-3 months) studies of Ba/Ca and Cd/Ca in corals it is possible to obtain information on upwelling characteristics in the region of coral growth (Cole *et al.* 1992). The Sr/Ca ratio, on the other hand, has been shown to be a sensitive index of SST, analogous to oxygen isotopes (Smith *et al.* 1979; Beck *et al.* 1992; de-Villiers *et al.* 1993). The Sr/Ca in coral (*P. clavus*) has a temperature coefficient of  $-6.245 \times 10^{-5} \text{ } ^\circ\text{C}^{-1}$  (Beck *et al.* 1992). High precision measurement of Sr/Ca ratios is required for its use as a monitor of SST.

##### I.2.d(i) Cadmium

Chemical analysis of lattice bound cadmium in scleractinian corals has been shown to be a sensitive tracer of oceanic upwelling. Cadmium is a nutrient-like element, depleted in the surface ocean relative to deeper waters. (Boyle *et al.* 1976, Shen *et al.* 1987).

The lattice bound Cd in corals from the eastern equatorial Pacific has been shown to be correlated with sea surface temperature changes associated with interannual ENSO variability (Shen *et al.* 1992). Similarly various investigators have reported the use of Cd as an upwelling indicator and its usefulness in understanding nutrient dynamics (Shen *et al.* 1987; Cole *et al.* 1992).

### 1.3 SCOPE OF THE PRESENT WORK

As mentioned earlier, the aim of this thesis is to explore the potential of corals in the northern Indian Ocean for extracting high resolution palaeoclimatic data.

Moore & Krishnaswami (1974) first reported isotopic studies on a coral from this region. They used environmental radionuclides ( $^{228}\text{Ra}$ ,  $^{210}\text{Pb}$ ,  $^{90}\text{Sr}$ , and  $^{14}\text{C}$ ) to determine coral growth rate (Moore *et al.* 1973) and compared the results with the band thickness measurements based on X-radiography. Taxonomic analysis of corals and their demographic distributions in the seas around India are available (Wafar 1986; Pillai & Patel 1988). There is, however no earlier work from this region on the use of corals as a source of proxy climate indicators. It was, therefore thought worthwhile to make a detailed study of corals from this region to assess their utility as a source of palaeoclimatic and environmental records. This was prompted by the results from other oceanic regions mentioned in the earlier sections. The following paragraphs summarize some of the scientific problems in the Arabian Sea region which are amenable to examination using coral isotopic data.

One of the characteristic climatic features over the Arabian Sea is the occurrence of monsoon. The south west monsoon (SWM) occurs during summer, Jun-Sep and the north east or winter monsoon prevails during Nov-Feb. The SWM is associated with intense winds which results in large scale surface circulation in the Arabian Sea and the monsoon rainfall in the Indian subcontinent. One of the consequences of the SWM is the upwelling of cool, nutrient rich water in several areas of the Arabian Sea, notably in the Somali basin, off the coast of Arabia and to some degree along the westcoast of India. Thus the SWM causes high biological productivity in the Arabian Sea. The high productivity and the strong winds also produce intense air-sea exchange of  $\text{CO}_2$ .

This unique climatic characteristic of the Arabian Sea makes it an interesting oceanic region for studying the behaviour of the monsoon over interannual to century time scales. Compared to the mid-latitude weather systems, the prediction of the tropical monsoon system is extremely difficult. This difficulty is accentuated by the absence of adequate spatial and temporal coverage of climatological data set including SST.

Some of these problems can be addressed through detailed high resolution studies

of isotopic and chemical tracers in corals as they have been proven to be sources of climatic indices in other oceanic regions. Corals, as discussed earlier, are known to incorporate various physical and chemical signatures of "ocean climate" (SST, salinity, rainfall etc.) on different time scales. The corals having high growth rates ( $>10$  mm/yr) are ideally suited for monitoring seasonal features with a resolution as high as about a month. The proxy records obtained from their growth bands can extend "ocean climate" data to several centuries in the past, much longer than those available from the instrumental records.

Corals occur in several regions in the northern Indian ocean (Wafar 1986; Pillai & Patel 1988); two regions were selected for the present study, The Lakshadweep (LDP) sea and the Gulf of Kutch (GKh). The climate of these two regions are influenced by different processes. The SST variations in LDP are influenced by the monsoon induced cooling in summer, whereas those in the GKh are mainly controlled by summer heating and winter cooling. Different species of corals grow around these coastlines. In the adjoining seas and lagoons of LDP they form huge reefs and colonies, in the GKh they grow in isolated patches. We collected coral samples of different genera and species from these two regions. In addition, we also analyzed one coral sample from the Stanley Reef of the Great Barrier Reef of Australia. The main goals are:

- 1) to identify corals from LDP and GKh areas that can provide high resolution record of climate and environmental parameters. Towards this, growth rates of corals were determined by X-radiography and oxygen isotope cyclicities. In addition to the growth rate an important constraint in retrieving high resolution records is the sampling thickness and the sampling interval (for mass spectrometric measurements). A model simulation study was made to determine the effects of sampling on the retrieval of climatic signal from the coral  $\delta^{18}\text{O}$  record.
- 2) to determine the extent of isotopic disequilibrium in  $\delta^{18}\text{O}$  in *Porites*, the most abundant coral genus in the LDP region, to establish an empirical relation between SST and  $\delta^{18}\text{O}$  of this coral species and assess the usefulness of this relation in the reconstruction of SST (LDP sea) on seasonal time scales by comparing this with available instrumental

data.

3) to examine the influence of monsoon rainfall on coral  $\delta^{18}\text{O}$  and its possible implications.

4) to determine the air-sea  $\text{CO}_2$  exchange and water mass mixing rates in the GK<sub>h</sub> region from the radiocarbon time series data from coral bands and tree rings. Such data find application in modelling the oceanic uptake of fossil fuel  $\text{CO}_2$ , and

5) to determine Cd concentrations with sub-seasonal resolution in one of the LDP corals and to explore its use as a tracer to investigate upwelling phenomena in this region.

In addition to the above studies of corals from the Indian coast, stable oxygen and carbon isotope analyses of a coral from the Stanley Reef of the Great Barrier Reef was carried out to assess the intraband-isotopic-variability, and the factors influencing the density band formation.

During the course of this investigation the author participated in the setting up of a new radiocarbon laboratory. He also established the capability for measuring nanogram levels of Cd in corals. Such a comprehensive analysis of corals has been done for the first time in the country.

The following chapters describe the measurements made to address the above goals and their interpretations.

# EXPERIMENTAL TECHNIQUES

The primary goal of this thesis, as outlined in the earlier chapter, is to analyze recent corals from the Indian coast for their proxy climatic records. Such a study involves the collection of corals, determination of their chronology and their analysis. The proxies chosen for measurements in this work are: stable oxygen and carbon isotopes, radiocarbon and cadmium. This chapter briefly outlines the procedures used in this work for sample collection and their analyses. Wherever possible the procedures available in literature were used, in some cases they were modified to suit our requirements.

## II.1 SAMPLING AND CHRONOLOGY

Live coral heads were collected from two locations in the Indian coast viz., Covered and Amini islands belonging to Lakshadweep archipelago ( $10^{\circ}\text{N}, 73^{\circ}\text{E}$ ) and from the Pirotan island ( $22.6^{\circ}\text{N}, 70^{\circ}\text{E}$ ) in the Gulf of Kutch (Fig 2.1a). These corals were collected from depths of  $\sim 1$  m during low tide. In addition to samples from these two sites, another coral from the Stanley Reef ( $19^{\circ}15' \text{ S}, 148^{\circ}07' \text{ E}$ ) was also analyzed, the location of which is shown in Fig 2.1b. This coral was provided to us by Dr J M Lough for stable isotopic analyses. The corals (from the Indian coast) were dislodged from their site of growth with a hammer and chisel and brought ashore. The polyps were removed by washing with tap water. The coral head was air dried and cut into two halves (Fig 2.2).

To obtain time series records of proxy climate parameters preserved in the coral it is essential to determine its chronology precisely. We have done this through X-radiography and oxygen isotope systematics.

X-radiography of coral skeleton, originally developed by Knutson *et al.* (1972) is widely used to determine their growth rates and pattern. For X-radiography, a section of about 1 cm thick (Fig 2.2) was sliced along the principal growth axis from the cut



# EXPERIMENTAL TECHNIQUES

The primary goal of this thesis, as outlined in the earlier chapter, is to analyze recent corals from the Indian coast for their proxy climatic records. Such a study involves the collection of corals, determination of their chronology and their analysis. The proxies chosen for measurements in this work are: stable oxygen and carbon isotopes, radiocarbon and cadmium. This chapter briefly outlines the procedures used in this work for sample collection and their analyses. Wherever possible the procedures available in literature were used, in some cases they were modified to suit our requirements.

## II.1 SAMPLING AND CHRONOLOGY

Live coral heads were collected from two locations in the Indian coast viz., Covered and Amini islands belonging to Lakshadweep archipelago ( $10^{\circ}\text{N}, 73^{\circ}\text{E}$ ) and from the Pirotan island ( $22.6^{\circ}\text{N}, 70^{\circ}\text{E}$ ) in the Gulf of Kutch (Fig 2.1a). These corals were collected from depths of  $\sim 1$  m during low tide. In addition to samples from these two sites, another coral from the Stanley Reef ( $19^{\circ}15' \text{ S}, 148^{\circ}07' \text{ E}$ ) was also analyzed, the location of which is shown in Fig 2.1b. This coral was provided to us by Dr J M Lough for stable isotopic analyses. The corals (from the Indian coast) were dislodged from their site of growth with a hammer and chisel and brought ashore. The polyps were removed by washing with tap water. The coral head was air dried and cut into two halves (Fig 2.2).

To obtain time series records of proxy climate parameters preserved in the coral it is essential to determine its chronology precisely. We have done this through X-radiography and oxygen isotope systematics.

X-radiography of coral skeleton, originally developed by Knutson *et al.* (1972) is widely used to determine their growth rates and pattern. For X-radiography, a section of about 1 cm thick (Fig 2.2) was sliced along the principal growth axis from the cut

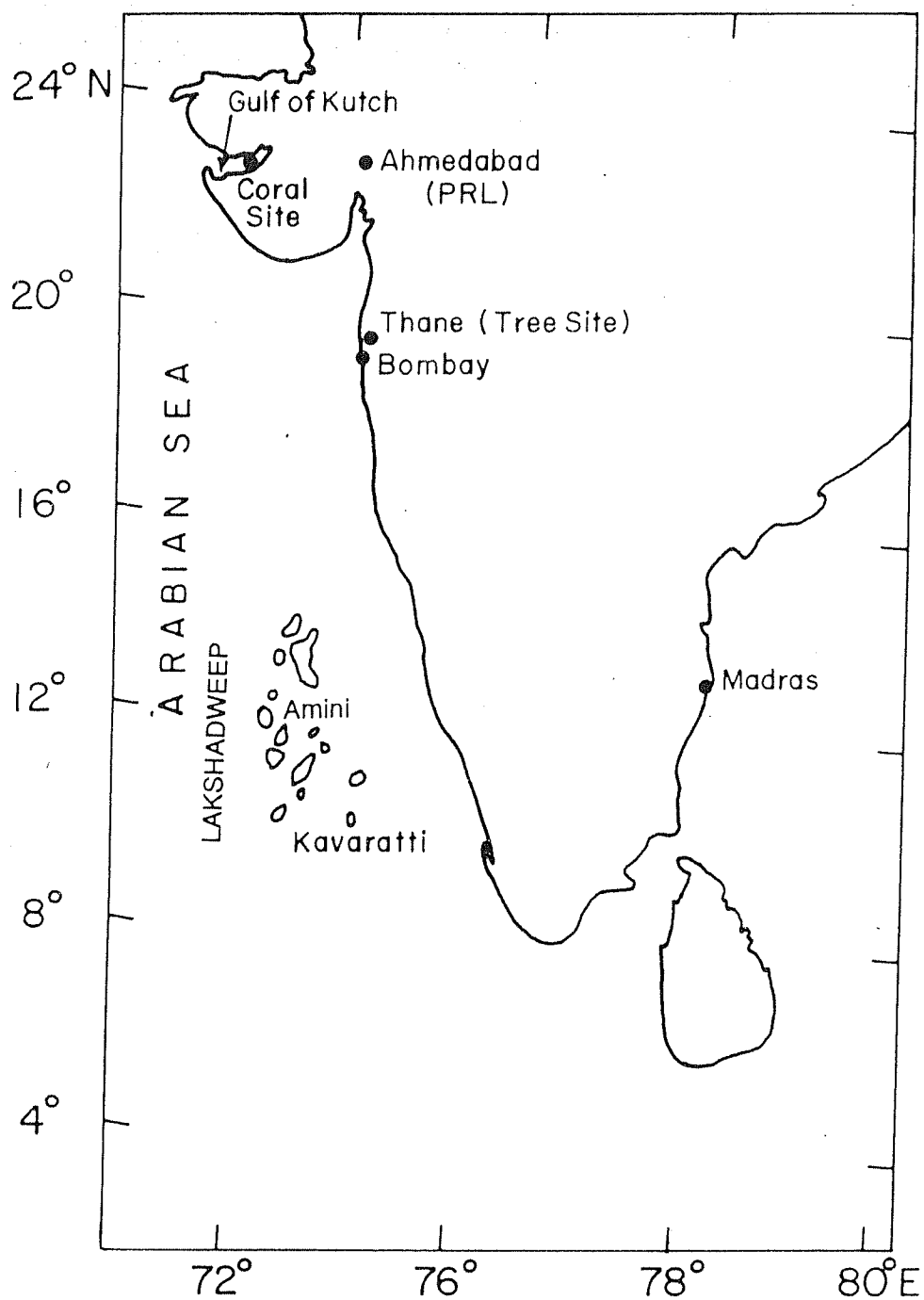


Fig 2.1a Location of corals from the Indian coast and tree sampled for proxy climate records. The tree stem slice was provided by Dr G B Pant of the Indian Institute of Tropical Meteorology.

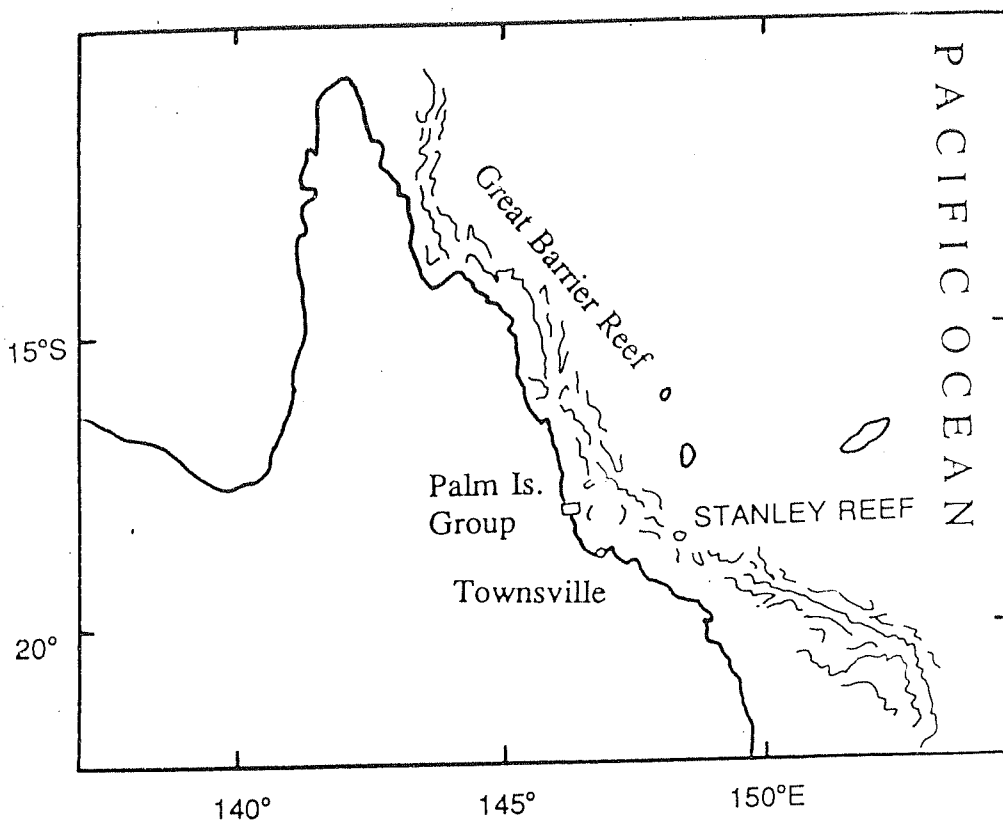


Fig 2.1b Location of coral sampled from the Stanley Reef, western Pacific. The sample was provided for isotopic studies by Dr J M Lough of the Australian Institute of Marine Science.

face of one of the halves. The slice was washed thoroughly with tap water and then in distilled water, followed by ultrasonic agitation to remove adhering particles. The cleaned slice is dried at 90°C for ~12 hours. This slice is X-rayed on Kodak medical film at a source to film distance of one metre and an applied voltage of about 46-48 KVp with an exposure time of 0.08 sec. The X-ray positive is then used to identify the band structure.

## II.2 STABLE ISOTOPE MEASUREMENTS

### II.2.a Sampling and pretreatment

For stable isotope measurements, a thin strip (~1cm × 1cm) was sliced from the coral section used for X-radiography. This strip was taken along the central growth axis (Fig 2.2). Sampling for mass spectrometric measurements of oxygen and carbon isotopes using dental drill is a popular technique since the pioneering work of Emiliani (1956). However there is some concern about possible isotopic exchange between the metastable aragonite and atmospheric gases and moisture, by the heat produced at the point of drilling (Aharon 1991). Leder *et al.* (1991) claim that such isotopic fractionation is produced only at high pressure and/or if dull drill bits are used. In this work, initially we used slow speed drilling and in the later phases the subsampling was done using a needle file. The use of a needle file enables high resolution sampling and may minimize problems of fractionation as the heat generation is less compared to that in drilling. The sampling resolution varies from 0.5 to 1.5 mm depending on the nature and texture of the sample. About 1 mg CaCO<sub>3</sub> powder was filed out for mass spectrometric measurements. The CaCO<sub>3</sub> samples were stored in labelled glass thimbles and covered with parafilm till they were subjected to mass spectrometric analysis.

The sample pretreatment is an important prerequisite for the mass spectrometric measurements of carbon and oxygen isotopes. This is because coral powder may contain a small amount of organic matter, which needs to be removed to avoid possible exchange of carbon and oxygen isotopes with the CO<sub>2</sub> evolved from the carbonate during acid treatment. Towards this, prior to acidification, the samples were roasted under vacuum at 350 °C for one hour to remove any volatile material that might be present.

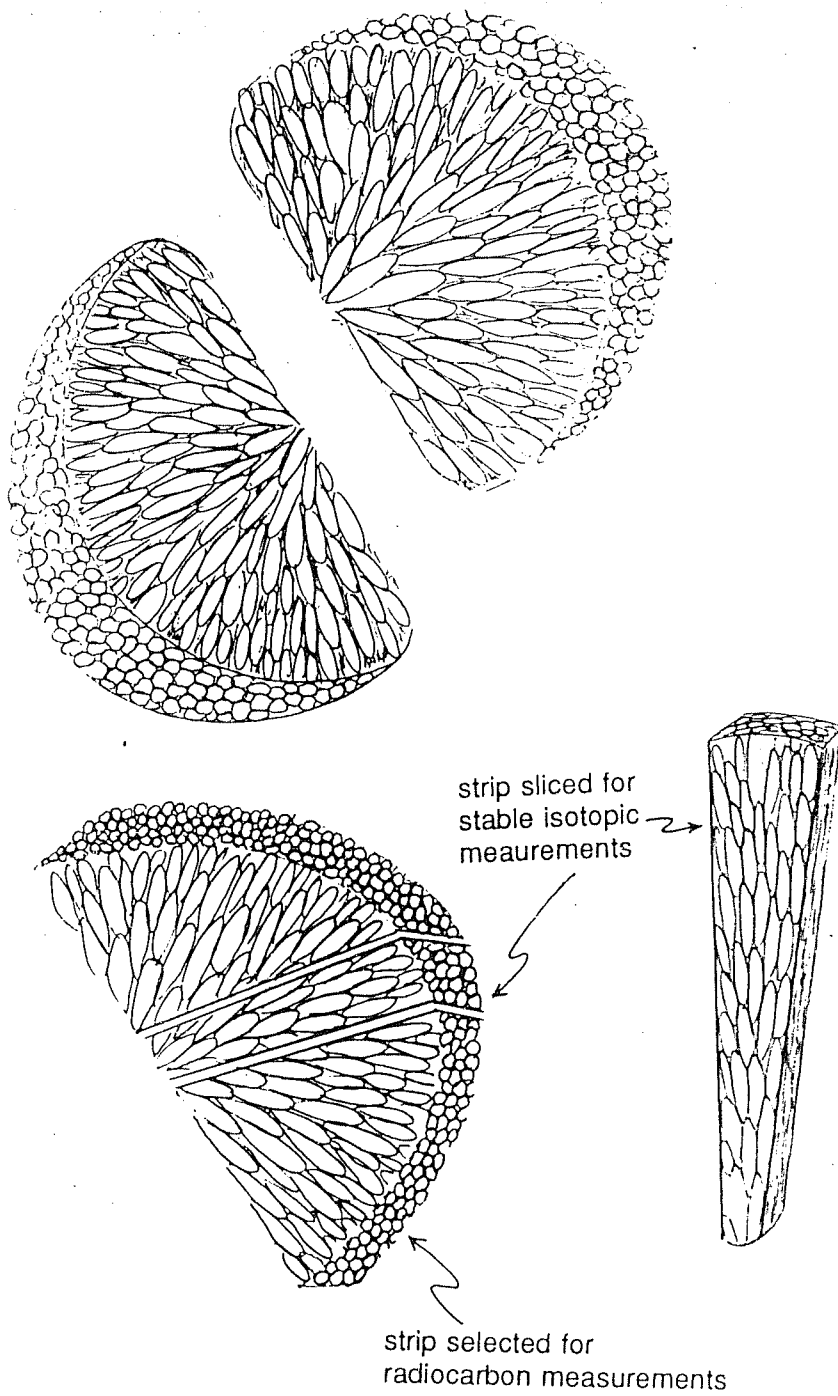


Fig 2.2 Coral sectioning and sampling for X-radiography and tracer measurements

## II.2.b Mass spectrometric measurements:

Stable isotopic measurements were performed on two corals from the Covered island (KV-1, KV-2), one coral (Am) and one giant clam (GC) from the Amini island, one coral each from the Gulf of Kutch (GK) and the Stanley Reef (SR).

Measurements of stable isotopic ratios of oxygen and carbon were carried out using a VG Micromass 602D mass spectrometer. The measurements were made relative to an internal standard, the foram standard  $\text{CO}_2$  (FS). This standard was prepared by reacting a large quantity of foraminifera separated from the Arabian sea sediments with  $\text{H}_3\text{PO}_4$ (100%) at room temperature (Sarkar, 1989). The FS was stored in a large volume (5 l) flask connected to the reference side of the mass spectrometer. To check the constancy of the isotopic composition of FS with time and the reproducibility of the isotopic measurements, two other standards, Makrana Marble (MMB) and Z-Carrara (ZC) whose  $\delta$  values are well established wrt PDB (*op cit.*), were also run routinely. Z-Carrara standard was provided by Prof N J Shackleton and was run only during the early phase of this work as its availability was limited. However measurements on MMB were made throughout this work and its long term average  $\delta$  values showed very good agreement with those measured at the Godwin Laboratory, Cambridge, UK. Table (II.1) lists the  $\delta$  values of MMB and Z-Carrara (wrt PDB) run during this thesis work. The \* marked numbers are the delta values of MMB and ZC analyzed in Godwin Laboratory, Cambridge UK (quoted by Sarkar, 1989) and n stands for number of measurements.

Fig 2.3 shows the delta values of ZC and MMB measured during the course of this work. For all standards and samples isobaric interferences were corrected using the equation of Craig (1957) and the  $\delta$  values are reported relative to PDB.

During Aug '91 the mass spectrometer was updated to triple collector system (903). The same reference gas (FS) was continued for oxygen and carbon isotopic measurements and found to give consistent and reproducible results.

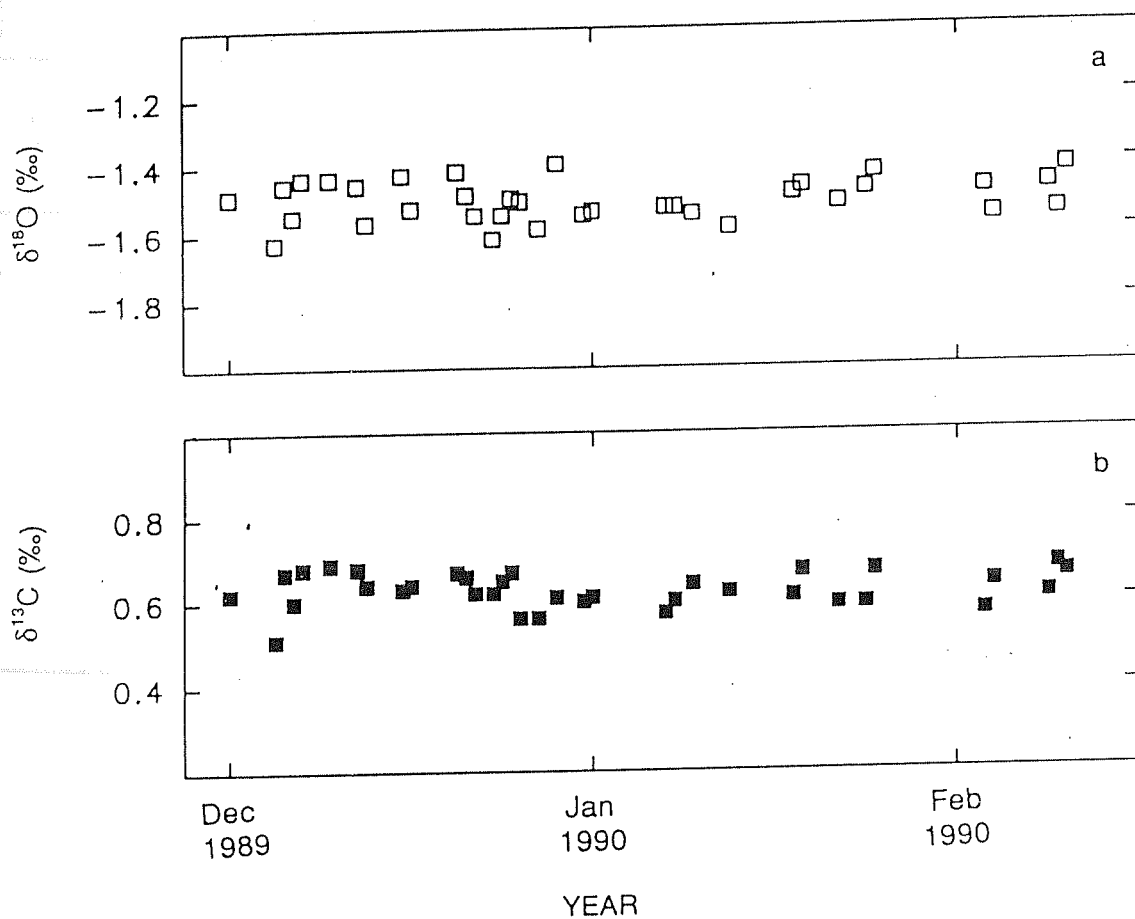


Fig 2.3a Oxygen (a) and carbon (b) isotopic ratios of Z-Carrara (relative to machine standard). The reproducibility over the period of analysis is  $\pm 0.06\text{‰}$  and  $\pm 0.04\text{‰}$  for  $\delta^{18}\text{O}$  and  $\delta^{13}\text{C}$  respectively.

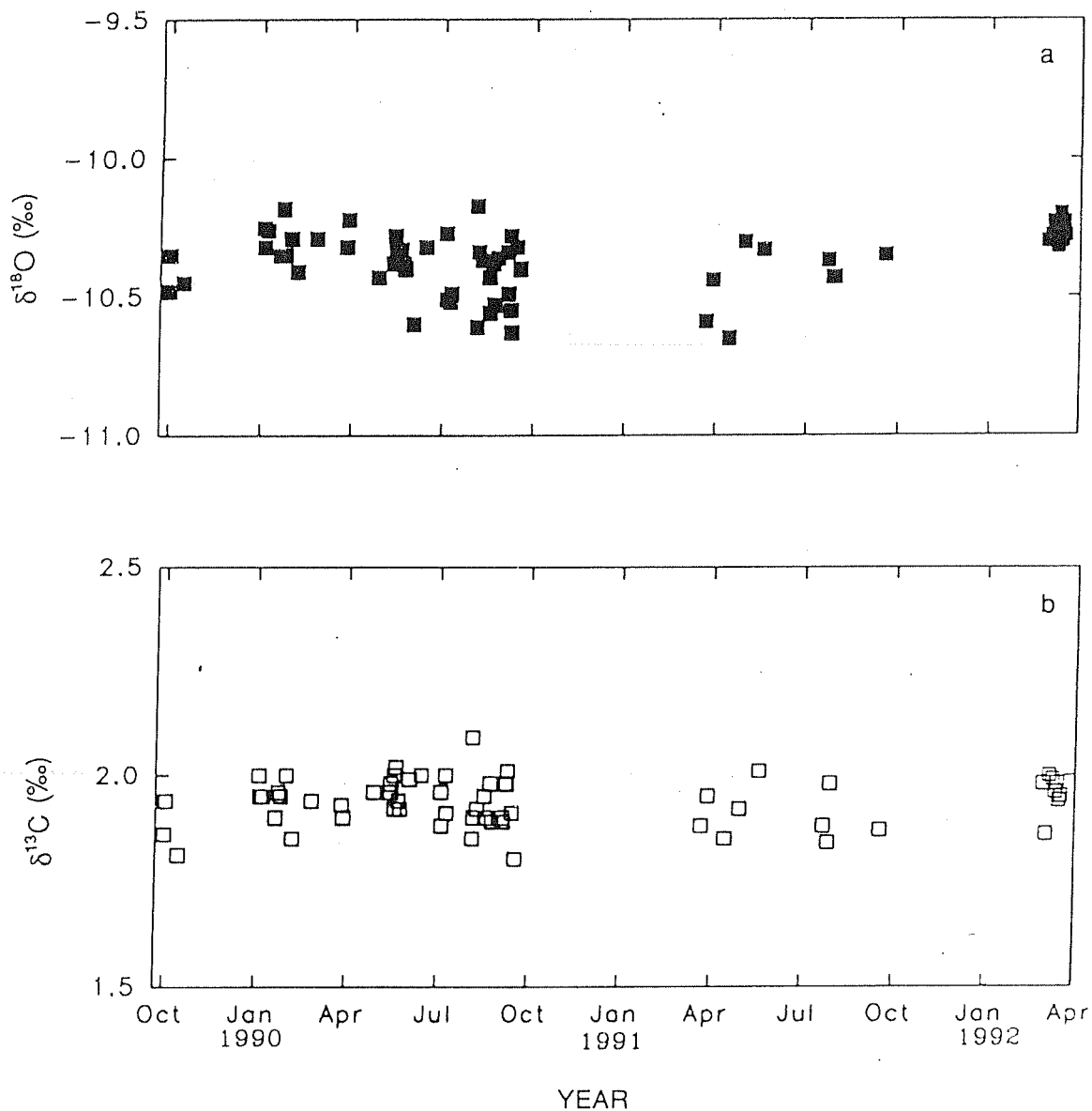


Fig 2.3b Oxygen (a) and carbon (b) isotopic ratios of Makrana marble (relative to machine standard). The reproducibility of measurements over a two year period is  $\pm 0.13\%$  and  $\pm 0.07\%$  for  $\delta^{18}\text{O}$  and  $\delta^{13}\text{C}$  respectively.



Table II.1 Isotopic analysis of Z-Carrara and Makrana Marble standards

	n	$\delta^{18}\text{O}_{\text{PDB}} (\text{‰})$	$\delta^{13}\text{C}_{\text{PDB}} (\text{‰})$
Z-Carrara	37	$-1.78 \pm 0.04$	$2.09 \pm 0.06$
	-	$-1.79^*$	$2.18^*$
MMB	80	$-10.61 \pm 0.13$	$3.88 \pm 0.07$
	18	$-10.5 \pm 0.2^*$	$3.9 \pm 0.1^*$

\* Analyses done in Cambridge, U.K.

For the triple collector system, a different set of Craig equations was used (Gat & Gonfiantini 1981). Internal laboratory standard (MMB) and several sample replicates were run routinely. For each sample the purity of  $\text{CO}_2$  in the mass spectrometer was also ascertained from the peaks at various masses. If there was any spurious peak, such as in mass 43 due to water contamination during the extraction of  $\text{CO}_2$  (Sarkar 1989) in the sample, the run was rejected. Such occurrences, however, were very rare. All  $\delta$  values are reported with respect to PDB. Errors (0.1‰) given are one standard deviation obtained for the working standard.

## II.3 RADIOCARBON MEASUREMENTS

### II.3.a Sample preparation

#### (i) Corals

Annual bands from the Gulf of Kutch coral sample (GK) and tree ring samples from a teak tree (ThTR) were analyzed for radiocarbon.

For radiocarbon analysis a ~1cm thick section along the growth axis of the coral was cut (Fig 2.2). From this slice depending on the growth rate, single or multiple annual bands were cut using a small diamond wheel (~1" diameter and < 1mm thickness) operated by an electric hand drill under a distilled water jet. The cut bands

were dried by heating overnight at 80-90°C, and powdered using a Tima mill. About 15g of this coral powder was used for radiocarbon measurements.

## (ii) Tree Rings

Radiocarbon measurements in tree rings were made to determine the time variation in atmospheric  $^{14}\text{C}$  activity near the coral site. The tree ring samples were taken from a teak tree (*Tectona grandis*) which grew at Thane (19°14'N, 73°24'E), near Bombay (Fig 2.1a). The chronology of the tree was established by Pant & Borgaonkar(1983). Hydrogen isotopic studies of this species of tree from this region were earlier made by Ramesh *et al.* (1989) to determine the relation between the isotope ratios and meteorological parameters. Annual rings were separated by chiseling from a ~2cm thick cross section of the tree stem. The individual rings were powdered using a Wiley mill. This powder was then treated by soaking in acetone for ~3 hrs with intermittent ultrasonic agitation. This was followed by 6-8 hrs soaking in 5% NaOH and finally in 1% HCl for ~ 6 hrs to remove the resinous and oily substances (Cain & Suess 1976). The sample was thoroughly washed with distilled water, dried and used for radiocarbon measurements. Following this pretreatment about 6g of the cleaned wood powder was used for benzene synthesis.

### II.3.b Benzene synthesis

Benzene was prepared from the coral and tree ring samples using a TASK Benzene Synthesizer following the methodology available in literature (Noakes *et al.* 1965, Gupta & Polach 1985). A brief description follows:

First, carbon dioxide is produced from the samples either by acid hydrolysis (in case of coral) or by dry combustion in an oxygen environment (tree ring samples). From some of the coral  $\text{CO}_2$  samples, an aliquot was taken for  $\delta^{13}\text{C}$  measurements. The results showed that the  $\delta^{13}\text{C}$  in this  $\text{CO}_2$  was same within the experimental uncertainty to that of the  $\delta^{13}\text{C}$  averaged over the portion of the band used for radiocarbon measurement. The remaining  $\text{CO}_2$  is then converted to  $\text{Li}_2\text{C}_2$  which is hydrolyzed to form  $\text{C}_2\text{H}_2$  (to minimize tritium contamination, the water used for the hydrolysis was obtained by double

distilling ground water collected from a 200 m deep well. This ground water is reported to have a  $^{14}\text{C}$  age of  $\sim 8200$  years, Bhushan *et al.* 1993). The acetylene is polymerized using alumina coated vanadium catalyst to produce benzene. The benzene is then transferred to a 7ml glass scintillation vial and weighed. Typically,  $\sim 1.5\text{g}$  (for coral) and  $\sim 2\text{g}$  (for wood samples) of benzene were obtained. Overall yield of benzene was typically 70%. To the sample benzene, scintillator grade non radioactive benzene was added by weight to make the volume to 3ml (2.637g) which is the standard volume used for counting. To this 0.5 ml of scintillator cocktail [42g/l PPO(diphenyloxazole) + 0.7 g/l POPOP (2, 2'-p-phenylene-bis-5 phenyl oxazole) in benzene] was added. The sample cocktail was mixed well and counted for  $^{14}\text{C}$  activity.

NBS oxalic acid was run 3 to 4 times a year to check the reproducibility and for  $\Delta^{14}\text{C}$  calculations.  $\text{CO}_2$  was liberated from the oxalic acid by  $\text{KMnO}_4$  oxidation as well as by dry combustion. The  $\text{CO}_2$  was converted to benzene as described above. We have run both NBS oxalic acid-I and II standards during the course of this work. The details of procedure and assay are given in Bhushan *et al.* (1993).

### II.3.c Radiocarbon counting

The benzene samples were counted in a Packard Tri-Carb Liquid Scintillator Analyzer, model 2250CA. This spectrometer operates in two modes, normal mode and low level count mode (LLCM). In LLCM, the background is reduced internally by electronic background discriminator using Three-Dimensional Spectrum Analysis (Kessler 1989).

More recently, in addition to electronic background reduction, Packard Instruments have introduced a scintillator sleeving (a low level PICO-XL vial holder) for the counting vial which further reduces the background drastically ( $\sim 40\%$ ) with a marginal reduction in  $^{14}\text{C}$  counting efficiency ( $\sim 5\%$ ). We operated the counter in LLCM mode with the sleeving.

The  $\beta$  particle of  $^{14}\text{C}$  atom has a maximum energy of 156 keV. If there is tritium (0 - 18.6 keV) contamination in the benzene sample, it would affect the  $^{14}\text{C}$  count rate. The tritium interference can be minimized by selecting an energy window for  $^{14}\text{C}$  counting

where contribution from tritium would be minimal and at the same time have high efficiency and low background for  $^{14}\text{C}$ . The Packard counter provides a built-in mechanism to select and optimize an energy region for  $^{14}\text{C}$  counting. Using the LLCM, the optimized region selected for  $^{14}\text{C}$  in our counter was 11 to 98 keV. In addition, the instrument has a three channel provision to measure the count rates. We had chosen the following energy intervals for the three channels.

Channel A 0.0 - 18.6 keV

Channel B 11 - 98 keV

Channel C 0.0 - 156 keV

Channel A is the energy window which would predominantly record tritium counts if any, from the sample. The higher energy betas (with energy 11-18.6 keV) from tritium fall in the  $^{14}\text{C}$  window, Channel B. Comparison of count-rates in Channel A of scintillation grade benzene and the marble blanks shows that they are same within experimental uncertainties. This suggests that there is no discernable tritium contamination during benzene synthesis.

### II.3.d $^{14}\text{C}$ blanks and standards

To ascertain the background count-rates for  $^{14}\text{C}$ , several blanks were run using marble from quarries of Rajasthan belonging to Raialo formation of the Precambrian Period. Fig 2.4 shows the variations in the count-rates of the  $^{14}\text{C}$  blanks over a period of  $\sim 2$  years.

From this figure it is seen that the background (or blank) count-rates are quite consistent (except in four cases which had count-rates  $\sim 25\%$  excess over the long term trend) and center around a value  $\sim 1.15$  cpm. The reason for the high count-rate in these four blank runs is not clear. The average of all numbers gives a background  $1.193 \pm 0.115$  cpm. Rejecting the counts beyond  $\pm 2\sigma$  of the mean and recalculation yields an average background count-rate of  $1.154 \pm 0.008$  cpm. This value has been taken as background activity and was used for all calculations. The background count-rate is typically 10% of coral and tree ring sample count-rate. In this context it must be

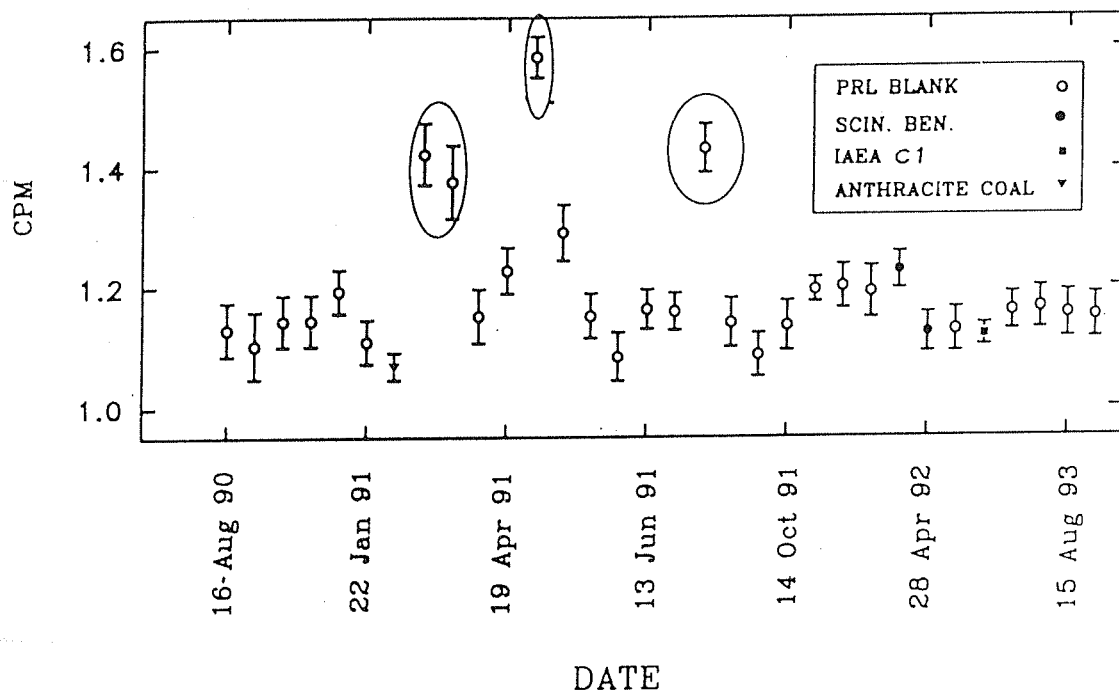


Fig 2.4  $^{14}\text{C}$  blank (background) count-rates of marble and other  $^{14}\text{C}$  free materials over a ~2 year period. The measured  $^{14}\text{C}$  blank count-rate excluding the four deviant (circled) points is  $1.154 \pm 0.008$  cpm. Error bar =  $\pm 2\sigma$ .

mentioned here that in the early phase of this work, scintillator grade commercially available benzene was also counted after mixing with scintillator cocktail. The count-rate of this commercial benzene was nearly identical to that of the marble blank. Analysis of IAEA carbonate sample (IAEA Quality Assurance Materials, sample C1, 1991), whose reported percent modern activity is  $\sim 0$  also yielded a count-rate of  $1.121 \pm 0.018$ , nearly identical to the mean background count-rate. Benzene synthesized from anthracite coal also gave similar count-rates (Fig 2.4)

NBS-Oxalic acid standard (SRM 4990C) was run 3-4 times per year. Table II.2 gives the net count-rates of the NBS Oxalic acid standard (cpm/3 ml benzene) during 1991 and 1992 when most of the measurements for this thesis work were made. (One of the oxalic acid runs (marked \* in the table below) had a count-rate of  $28.816 \pm 0.103$  which was significantly higher ( $>2\sigma$ ) than the mean of the all other measurements. For calculation of mean oxalic acid count-rate this run was excluded).

Table II.2 Net count-rates of NBS oxalic acid standard II-4990C

Date	Count-rate(cpm)
16.02.91	$28.052 \pm 0.127$
10.04.91	$28.816 \pm 0.103^*$
07.06.91	$27.762 \pm 0.102$
16.10.91	$28.077 \pm 0.078$
07.04.92	$28.064 \pm 0.087$
05.05.92	$27.748 \pm 0.091$
08.12.92	$27.760 \pm 0.115$
Mean	$27.911 \pm 0.069$

Fig 2.5 shows the pictorial representation of the data in Table II.2. The mean net oxalic acid count-rate calculated for the period (1991-1992) is  $27.911 \pm 0.069$  cpm (excluding

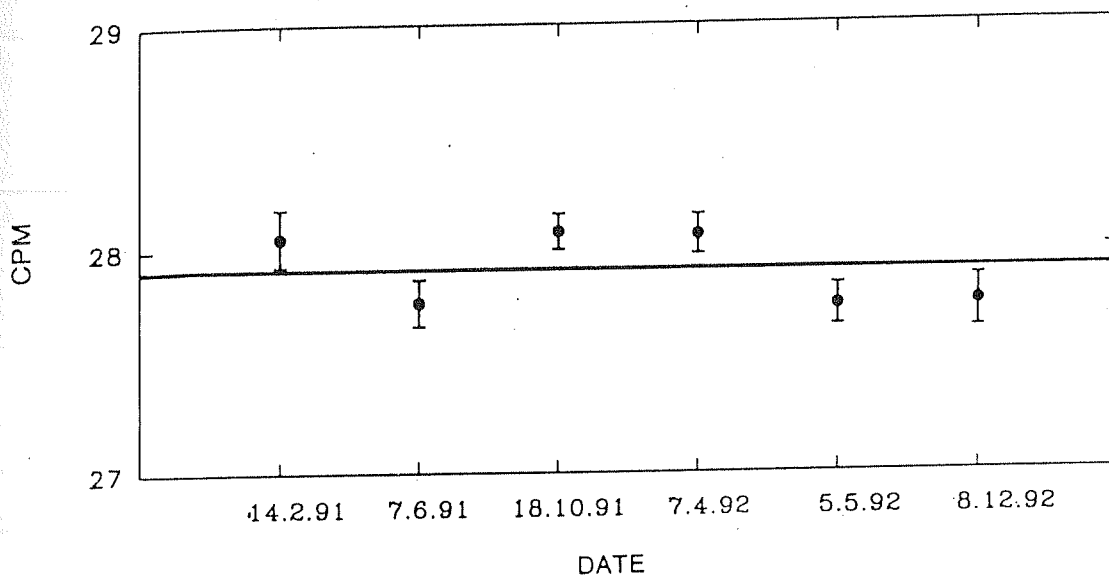


Fig 2.5 Count-rates of NBS Oxalic acid II standard (4990C) during 1991-1992. Error bars are  $\pm 1\sigma$ . The line drawn is the mean count-rate during the course of this work ( $27.911 \pm 0.069$  cpm).

the high count-rate sample; error is on the mean). This value was used for  $\Delta^{14}\text{C}$  calculations for all coral and tree ring samples.

### II.3.e Reporting of radiocarbon activity

For reporting of  $^{14}\text{C}$  activity we follow the notations described by Stuiver and Polach (1977).

$$\delta^{14}\text{C}(\text{‰}) = [(A_s e^{\lambda(y-x)} / A_{\text{abs}}) - 1] \cdot 1000 \quad (2.1)$$

and 
$$\Delta^{14}\text{C}(\text{‰}) = [(A_{\text{SN}} e^{\lambda(y-x)} / A_{\text{abs}}) - 1] \cdot 1000 \quad (2.2)$$

where  $\delta^{14}\text{C}$  is defined as the relative difference between the absolute international standard ( $A_{\text{abs}}$ ) and the sample activity ( $A_s$ ) corrected for age, and  $\Delta^{14}\text{C}$  is the ratio of sample and standard activity normalized to  $\delta^{13}\text{C} = -25\text{‰}$ . ( $A_{\text{SN}}$  = normalized sample activity,  $y$  = the year of measurement and  $x$  is the year of growth).

### II.3.f Intercalibration and repeat measurements

To check the reproducibility, four repeat measurements of a coral powder (Am, from Amini island, Lakshadweep) was run over a period of about two years. The replicate measurements ( $n=4$ ) gave a mean value of  $\Delta^{14}\text{C} = 50 \pm 11$ . The large error is because one of the samples deviated considerably from the other three. This sample was also analyzed at Birbal Sahni Institute of Palaeobotany, Lucknow using a gas proportional counter which yielded a value of  $\Delta^{14}\text{C} = 69 \pm 6$ . Further checks on our measurements were made by analyzing IAEA Quality Assurance Materials (carbonates and cellulose) for their  $^{14}\text{C}$  activities. The results (Bhushan *et al.* 1993) are in good agreement with the values published by IAEA.



## II.4 CADMIUM MEASUREMENTS

Cadmium measurements were made in a coral (KV-1, *P. compressa*) from the Kavaratti island. This coral had a life span of ~5 years, with an average band width of ~23 mm as determined by X-radiography. This coral was chosen for Cd measurements as it had a high growth rate, which allows subsampling over time intervals of a few months whereby it is possible to look for signatures of seasonal upwelling.

### II.4.a Sample cleaning

For Cd measurement ~0.5g of coral sample of 2-3 mm thick was chipped. These chips were thoroughly cleaned through a series of oxidative and reductive reaction sequences as suggested by Shen and Boyle(1988). First the coral chips were placed in distilled water in 20 ml glass vials and were subjected to ultrasonic agitation for 10 min. This was followed by treatment in 0.16N HNO<sub>3</sub> in ultrasonic bath for 3 min and then H<sub>2</sub>O rinse. Next the samples were cleaned in a mixture containing equal parts of 30% H<sub>2</sub>O<sub>2</sub> and 0.2 N NaOH to hydrolyze and oxidize organic coatings. After this the samples were kept in a boiling water bath for 20 min with repeated ultrasonic agitation. During this treatment, they were rinsed twice with distilled water. The next step was to remove oxide coatings with reducing agents (a mixture of 1 part hydrazine, 6 part conc. NH<sub>4</sub>OH, and 3 parts 0.3M solution of citric acid in 7N NH<sub>4</sub>OH) on a hot water bath with intermittent ultrasonic agitation. The cleaned samples were rinsed thoroughly with distilled water. In the final step, samples were again treated twice with 0.16N HNO<sub>3</sub> in ultrasonic bath followed by distilled water rinse each time. The samples were then dried under a laminar flow bench at temperature ~80°C.

### II.4.b Coprecipitation of Cd with APDC and atomic absorption analysis

The concentration of Cd in corals are too low (~5 nmol Cd/mol Ca) to be measured directly in a coral solution. Thus it needs to be pre-concentrated, which was done as follows. An accurately known amount (typically 0.25 g) of cleaned coral sample was dissolved with

4N HNO<sub>3</sub> and made to 10 ml. 1 ml aliquots of this solution were then transferred to four precleaned 15 ml polypropylene tubes and volume made to ~ 6ml. In three of these four aliquots a known amount of Cd (0.5, 1, 1.5 ng respectively) was added. CoCl<sub>2</sub> solution (containing ~ 0.1 mg Co) was added to each tube and pH of solution was adjusted to 4.5±0.5 with ammonium acetate buffer. Cobalt was precipitated as dithiocarbamate by adding a known amount of 1% solution of APDC. The polypropylene tubes containing precipitates were allowed to stand for 3-4 hours, at the end of which the precipitates were centrifuged (at 11,500 rpm) for 5 min. The Co-APDC precipitate was washed twice with distilled water and centrifuged each time to remove the Ca occluded in the precipitate. The precipitate was then transferred to a 5ml conical teflon cup using ~3ml of 8N HNO<sub>3</sub> and warmed at ~70 °C (under a laminar flow bench) to oxidize the organic matter. The residue was dissolved in 20µl of 4N HNO<sub>3</sub> and diluted with distilled water to a final volume 1020 µl.

Table II.3 Reproducibility of blank and Cd standard absorbance

Date	Blank (Abs)	Stand. (Abs)
12.01.93	0.003	0.012
21.01.93	0.004	0.013
24.01.93	0.003	0.012
25.01.93	0.007	0.011
28.01.93	0.002	0.014
30.01.93	0.002	0.011
01.02.93	0.002	0.012
09.02.93	0.01*	0.012
11.02.93	0.006	0.015
13.02.93	0.003	0.012

16.02.93	0.005	0.015
mean	0.0037±0.0017	0.013±0.0014
(* this number was excluded for calculating the mean)		

The reagents used throughout the coprecipitation were precleaned as suggested (*op cit.*). Along with each batch of samples reagent blanks and standards were also run.

The Cd measurement in the samples were made using an atomic absorption spectrophotometer (Perkin Elmer model 4000) attached to an HGA 500 graphite furnace. All analyses were performed employing the continuum background correction. Each sample and standard was measured 2-3 times with 20 µl injection. Table (II.3) gives the results of the replicate measurements of blank and a laboratory standard run during the sample measurements. This standard was a CaCO<sub>3</sub> solution made by dissolving 10g of coral sample in dilute nitric acid.

Inspite of the variability in the blank absorbance we see that the standard's absorbance is consistent (11% variability) which indicates that the occasional high blanks are due to some contamination. Rejecting the high blank (abs 0.01) we get the mean blank absorbance as ~ 0.004 (typical sample absorbance without Cd spiking is 0.018).

#### II.4.c Measurement of Cd concentration

The Cd concentration in the coral sample was determined by standard addition method (Beaty 1978). Blank was also ascertained in a similar way. Since the samples and blanks were made to identical volumes, the blank absorbance (0.0037) was subtracted from that of the sample. The Fig 2.6 shows a typical plot between the conc. of Cd added and the net sample absorbance. The regression line gives an intercept ( $x_{in}$ ) corresponding to the sample concentration in ng. This is then normalized to the known weight of CaCO<sub>3</sub> initially taken to express sample concentration in units of nmol Cd/mol Ca.

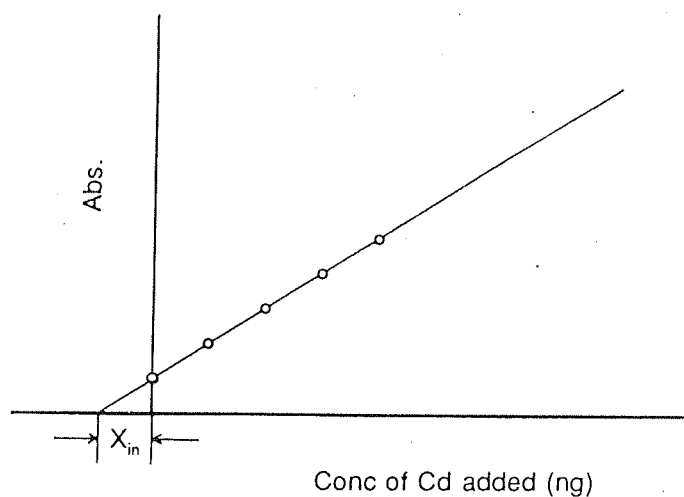


Fig 2.6 Determination of cadmium concentration by the standard addition method

In order to check the reproducibility on Cd concentration a coral sample was run three times. Following table (Table II.4) shows the results of these runs.

Table II.4 Reproducibility of Cd measurements in "spiked" coral solution

Date	conc.(nmol Cd/mol Ca)
20.01.93	10.7±1.65
23.01.93	11.1±1.34
25.01.93	12.3±0.82

## II.5 SUMMARY

As discussed above, time series measurements of stable isotopes of oxygen, carbon and radiocarbon, were made in corals and tree rings. Table II.5 summarizes the various measurements made on different samples in this work.

Table II.5 Summary of measurements made in corals and tree rings in this work

Sample Code	Genus/species	Lifespan (year)	Tracers measured
<u>Lakshadweep</u>			$\delta^{18}\text{O}, \delta^{13}\text{C},$
KV-1	<i>Porites compressa</i>	5	Cd
KV-2	<i>Porites compressa</i>	25	$\delta^{18}\text{O}, \delta^{13}\text{C}$
Am	<i>Porites compressa</i>	4	$\delta^{18}\text{O}$
GC	<i>Tridacna maximus</i>	4	$\delta^{18}\text{O}$
<u>Gulf of Kutch</u>			
GK	<i>Favia speciosa</i>	40	$\delta^{18}\text{O}, \delta^{13}\text{C}$ $\Delta^{14}\text{C}$
<u>Stanley Reef</u>			
SR	<i>Porites lutea</i>	18	$\delta^{18}\text{O}, \delta^{13}\text{C}$ Density*
<u>Thane (tree)</u>			
ThTR	<i>Tectona grandis</i>	20	$\Delta^{14}\text{C}$

\*Density measurements were made by Dr J M Lough of the Australian Institute of Marine Science, Townsville, Australia

## RESULTS AND DISCUSSION

In this chapter, the results of X-radiography and time series measurements of stable isotopes, radiocarbon and Cd made in various corals are presented and discussed. For clarity the chapter is divided into five sections.

The first section is on X-radiography and growth rates of corals. The second section deals with the results of stable isotope (O and C) data and their interpretation. Section three focuses on the determination of the air-sea carbon-dioxide exchange rate in the Gulf of Kutch based on radiocarbon analyses of coral bands and tree rings. Cadmium measurements are presented in the fourth section. The last section deals with the intercomparison and synthesis of the results of different corals analyzed.

### III.1 X-RADIOGRAPHIC ANALYSIS

X-radiography is a useful tool to obtain information on banding in corals and their growth rates. In the previous chapter we had mentioned in some detail the methodology used by us for mapping coral banding using X-ray photography. Here we present the results.

The first coral we analyzed was a *Porites compressa* (KV-1) from Lakshadweep region (LDP). It showed 5 bands with alternate high and low density growth rings, corresponding to dark and light colour respectively in the X-ray positive. From this X-ray picture we determined the average band width (made of one dark and the adjoining light band) as  $23.3 \pm 1.9$  mm. Oxygen isotope studies of this coral (discussed in the next section) showed that the bands are annual in nature. Such a high growth rate enabled us to subsample the bands with a resolution better than a fortnight for stable isotopic studies (average of 28 samples per band). Another *P. compressa* (Am) from the Amini island also showed 4 bands with an average thickness of  $22.5 \pm 3.7$  mm. In this coral, for stable



Fig 3.1 X-radiograph of the coral *Porites compressa* (KV-2) collected from Kavaratti lagoon, Lakshadweep islands. The average bandwidth of this coral is  $15 \pm 3.4$  mm.

isotopic measurements 9 samples per band were taken. The coral KV-2, also a *Porites compressa* from Kavaratti atoll on which extensive oxygen and carbon isotope measurements were made, showed 25 growth bands corresponding to 25 years of age. Its average growth rate was  $15 \pm 3.4$  mm/yr. Fig 3.1 shows a portion of the X-ray positive of this coral. This coral was sampled for stable isotopic studies with a resolution of 8 to 16 samples per band. The sample (GK) from the Gulf of Kutch, a *Favia speciosa*, had 40 growth bands. The mean band thickness of this coral was only  $4.3 \pm 1.3$  mm. Because of the smaller band width, the time resolution for isotopic studies in this coral was poorer compared to that of Lakshadweep corals. About 2 to 5 samples per band were analyzed. The sample (SR), a *Porites lutea* collected from the Stanley Reef of Great Barrier Reef, Australia (by Dr J M Lough) had 20 bands, with an average band width of  $11.7 \pm 3$  mm. Two tracks were chosen for isotopic and densitometric analyses. One close to growth axis ( $10^\circ$  off), other  $\sim 20^\circ$  off the growth axis. Fig 3.2 shows the variations of bandwidth in KV-2, GK and SR corals respectively. Also shown in this figure (inset) are the bandwidth variations of KV-1 and Am corals. Table 3.1 gives a summary of the bandwidth measurements. All the samples mentioned above formed a single band in a year. This was revealed by oxygen isotopic analysis presented in the following section; hence the bands represent annual skeletal extensions.

The species identification of Lakshadweep corals was done by Dr M V M Wafar of National Institute of Oceanography, Goa and Mr M I Patel of Gujarat State Fisheries Aquatic Sciences Research Station, Sikka, Gujarat and that of the Gulf of Kutch and Stanley Reef corals by Dr J Veron of Australian Institute of Marine Science, Townsville, Australia.



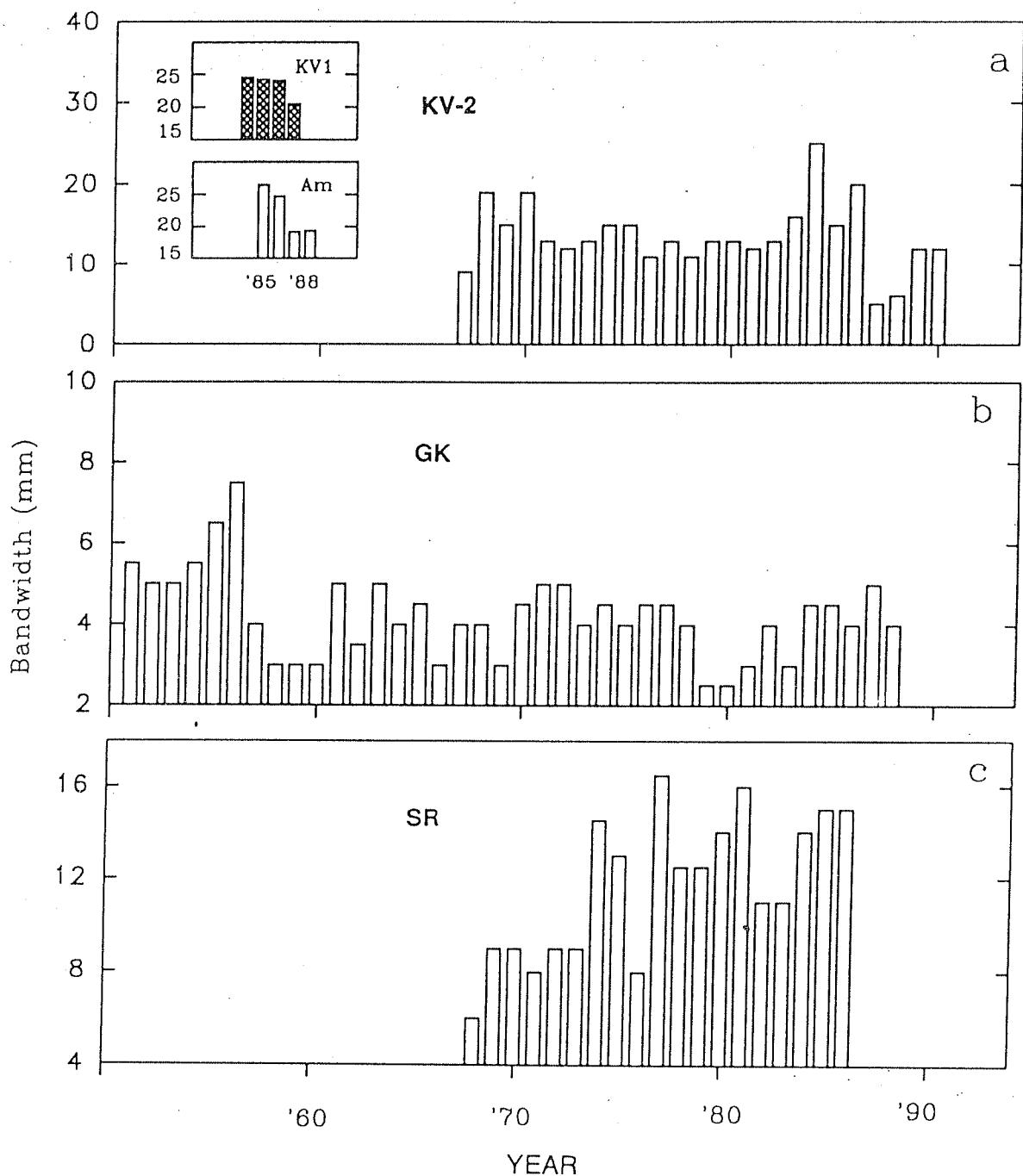


Fig 3.2 Variations in bandwidth with time in corals from (a) Kavaratti (Lakshadweep): (KV-2), (b) Gulf of Kutch, (GK) and (c) Stanley Reef, (SR) region. The insets in box a are for two younger corals from Kavaratti (KV-1) and Amini (Am) from the Lakshadweep. X-axis is not a calendar year but the year corresponding to one high + one low density band.

Table III.1 Range and mean bandwidths of various coral samples used in this work

Coral code	No. of bands	Bandwidth(mm)	
		Range	Mean $\pm 1\sigma$
KV-1	5	20.5-24.5	23.3 $\pm 1.9$
Am	4	19.2-26.5	22.5 $\pm 3.7$
KV-2	25	10-23	15 $\pm 3.4$
GK	41	2.5-7.5	4.3 $\pm 1.3$
SR	19	6-16.5	11.7 $\pm 3$

The variations in bandwidth or rates of coral growth which vary among the coral genera are controlled by various environmental parameters. The corals from Lakshadweep have higher growth rates compared to the Gulf of Kutch coral, possibly because Lakshadweep region has light and temperature conditions more suited for coral growth.

### III.2 STABLE ISOTOPIC STUDIES

As mentioned in the last chapter stable oxygen and carbon isotope measurements were made on corals from the Lakshadweep, the Gulf of Kutch and the Stanley Reef. The results are presented regionwise below.

#### III.2.a Lakshadweep corals

Stable isotopic measurements were made on three corals from the Lakshadweep islands; KV-1 & KV-2 from the Kavaratti island, Am and a giant clam (GC) from the Amini island.

The first sample analyzed was KV-1, a five year old *Porites*. This coral had an average bandwidth of 2.3 cm based on X-radiography (Table III.1). Oxygen and carbon isotope measurements were made on an average of about 28 samples per band. This

provided a time resolution of better than a fortnight per sample. The seasonal chronology was assigned to the  $\delta^{18}\text{O}$  profile of this coral using SST and  $\delta^{18}\text{O}$  of water. This was subsequently followed for all other *P. compressa* corals from this region. The results of Am and GC were used to quantify the disequilibrium offset (in  $\delta^{18}\text{O}$ ) and to standardize coral thermometry for retrieving SST of this region. The resulting equation was then applied to the  $\delta^{18}\text{O}$  signatures on the longer lived coral KV-2 to derive SST for the last seventeen years and compare the results with the instrumental records.

Time variations in  $\delta^{13}\text{C}$  and  $\delta^{18}\text{O}$  of the coral KV-1 are shown in Fig 3.3. Table-III.2 and III.3 in the Appendix-A list these data.

#### (i) *Oxygen isotopes*

The  $\delta^{18}\text{O}$  of this coral ranges from -5.6 to -4.8‰ (Fig 3.3). The seasonal changes in  $\delta^{18}\text{O}$  in coral  $\text{CaCO}_3$  are influenced both by SST and  $\delta^{18}\text{O}$  of water. To evaluate how in this region SST and  $\delta^{18}\text{O}$  of water control the  $\delta^{18}\text{O}$  of the coral  $\text{CaCO}_3$  we approach as follows. The monthly average values of SST are shown in Fig 3.4a. These are based on the COADS (Comprehensive Ocean Atmosphere Data Set) SST data for a location near to Kavaratti (10°N, 74°E, 2°×2° grid) for the period of 1974 to 1980 A.D. Data on the  $\delta^{18}\text{O}$  of water are not available for this region. Therefore we have derived the  $\delta^{18}\text{O}$  of water based on salinity. The available results (Duplessey *et al.* 1981) along the west coast of India, show that for every 1‰ increase in salinity, the  $\delta^{18}\text{O}$  of sea water increases by about 0.3‰ (used by Sarkar *et al.* 1990). Assuming that this relationship also holds for the Lakshadweep region, we have derived the  $\delta^{18}\text{O}$  of the water, using the salinity data from the bimonthly averages given in the Oceanographic Atlas (Wyrki 1971), the values for the sample location were obtained by reading between contours (0.5‰). The calculated  $\delta^{18}\text{O}$  values for the waters are given in Fig 3.4b (In order to check the assumption on the salinity- $\delta^{18}\text{O}$  relation mentioned above, we analyzed water samples collected from the Kavaratti lagoon during Apr 1988 and Dec 1988. The salinity difference between these two periods is 1‰. The observed  $\delta^{18}\text{O}$  difference is  $0.3 \pm 0.3$ ‰). The quoted error is not experimental uncertainties but sample to sample variability. We have analyzed a total of 7 samples for April and 12 samples for December.

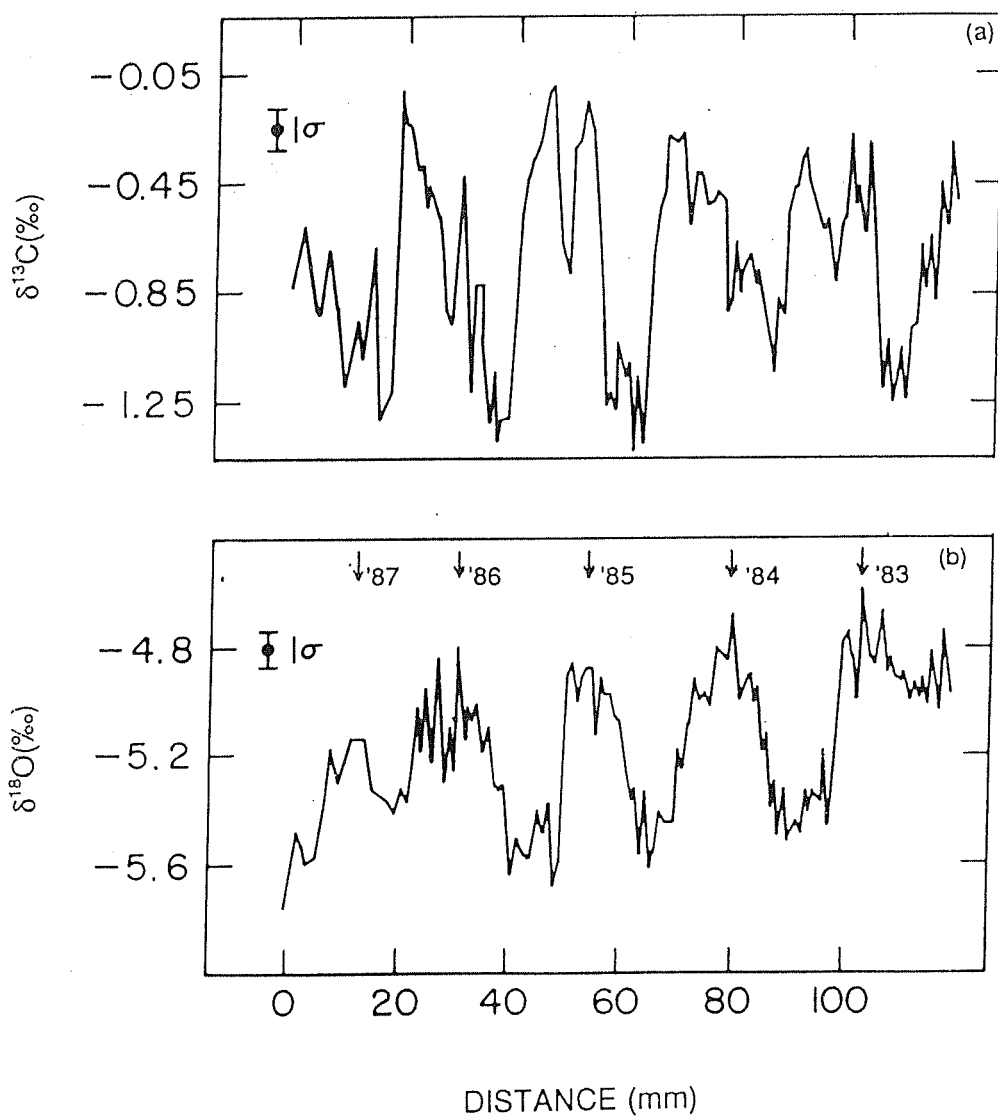


Fig 3.3  $\delta^{13}\text{C}$  (a) and  $\delta^{18}\text{O}$  (b) variations in the *Porites compressa* (KV-1) from the Kavaratti lagoon, Lakshadweep Is. Distance is measured inward, from the coral surface (live when collected) to its base. August of each year is marked by an arrow.

Based on the SST and  $\delta^{18}\text{O}$  of sea water (relative to PDB) during the course of the year, we can derive the  $\delta^{18}\text{O}$  in coralline  $\text{CaCO}_3$  (for calculation a temperature coefficient of  $-0.2\text{‰}$  per  $^{\circ}\text{C}$  is used). From Oct to Feb, the temperature is more or less constant at about  $28^{\circ}\text{C}$  (within one standard deviation, which represents the interannual SST variability). During this period the  $\delta^{18}\text{O}$  of seawater decreases by about  $0.3\text{‰}$ , causing a decrease of  $0.3\text{‰}$  in the  $\delta^{18}\text{O}$  of coral. From Feb to Apr, there is a steady increase in the SST by about  $2^{\circ}\text{C}$ , whereas the  $\delta^{18}\text{O}$  of water remains constant at around  $0.15\text{‰}$ . For this period we would expect the  $\delta^{18}\text{O}$  of coral  $\text{CaCO}_3$  to decrease by  $0.4\text{‰}$ . From May to Aug, due to monsoon induced upwelling, there is a reduction in SST by about  $3^{\circ}\text{C}$ , and an increase in  $\delta^{18}\text{O}$  of water by about  $0.3\text{‰}$ . The reduction in SST and increase in salinity both favour increase in  $\delta^{18}\text{O}$  of coral  $\text{CaCO}_3$ . Therefore during this period, the coral  $\delta^{18}\text{O}$  increases by  $0.9\text{‰}$ . From Aug to Oct the SST increases by  $1^{\circ}\text{C}$  and the  $\delta^{18}\text{O}$  of water decreases by  $0.15\text{‰}$ . Both these changes together cause a reduction in coral  $\delta^{18}\text{O}$  by about  $0.35\text{‰}$ .

Summing up, the pattern of variations of SST and  $\delta^{18}\text{O}$  of water should be reflected in the  $\delta^{18}\text{O}$  of coral  $\text{CaCO}_3$  by a minimum around Apr-May and maximum during Aug. The expected coral  $\delta^{18}\text{O}$  (seasonal) variation is ( $\sim 0.9\text{‰}$ ) as shown in Fig 3.4c. With this information it is possible to assign specific time slots (in terms of months) to the  $\delta^{18}\text{O}$  data shown in Fig 3.3b. The minimum value ( $-5.6\text{‰}$ ) in  $\delta^{18}\text{O}$  corresponds to Apr-May while the maximum value ( $\sim -4.8\text{‰}$ ) corresponds to Aug. The monsoon induced cooling is manifested as an increase in the  $\delta^{18}\text{O}$  value from about  $-5.6\text{‰}$  to  $-4.8\text{‰}$ , the range being  $0.8\text{‰}$  similar to the expected value of  $0.9\text{‰}$ .

To translate the  $\delta^{18}\text{O}$  time series in the coral  $\text{CaCO}_3$  to SST it is necessary to quantitatively assess the isotopic disequilibrium offset since corals do not precipitate  $\text{CaCO}_3$  in isotopic equilibrium (Weber 1974, Weber & Woodhead 1972, Swart 1983). The complex biological processes, such as metabolism and endosymbiotic photosynthesis, result in metabolic and/or kinetic fractionation. These processes deplete the isotopic composition (*i.e.* ratio of heavy to light isotopes) of coral  $\text{CaCO}_3$  relative to that expected for equilibrium precipitation. The deviation from the equilibrium precipitation can be represented by the following equation (Aharon 1991).

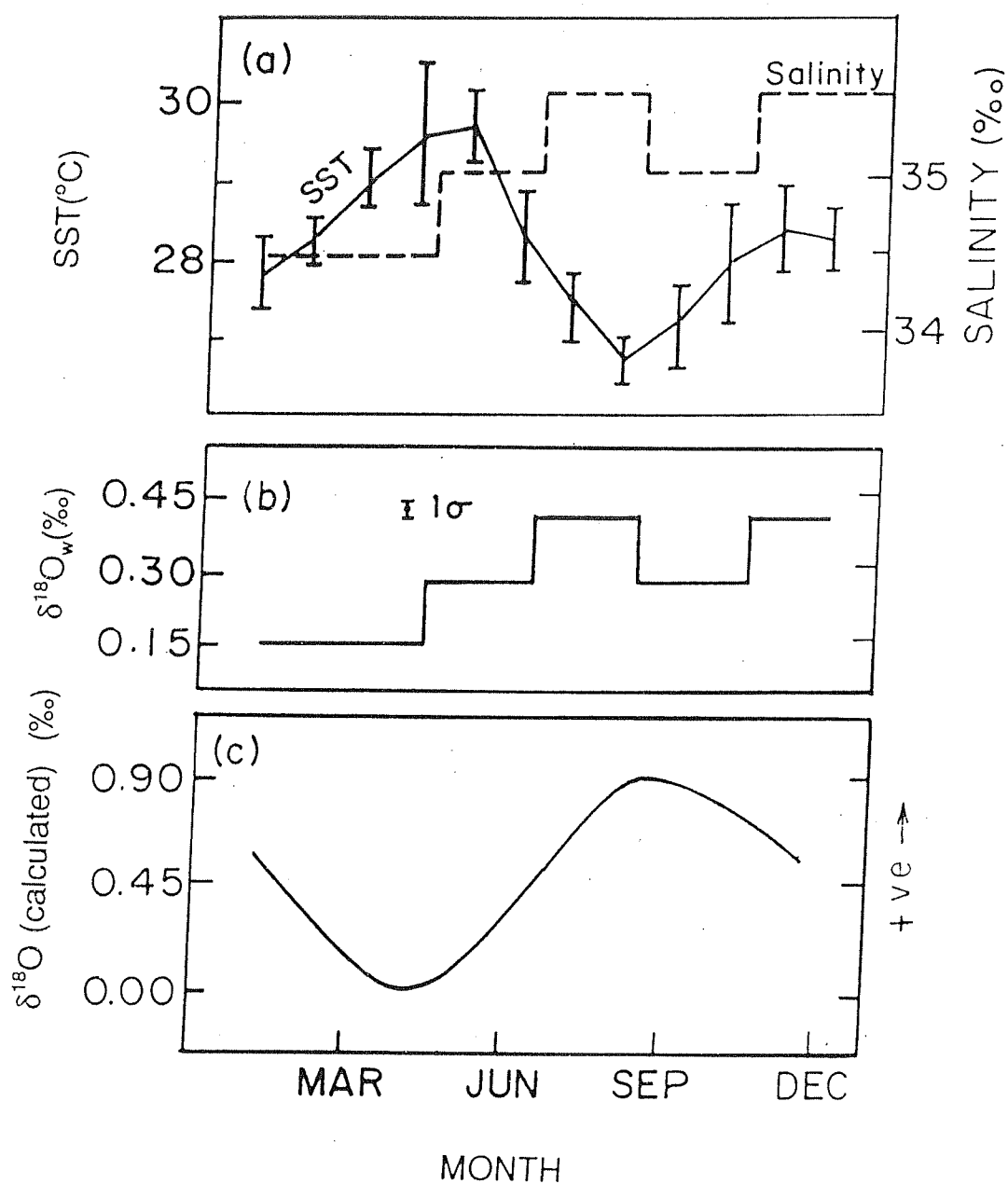


Fig 3.4(a) Mean monthly SST (solid line) and bimonthly averages of salinity (dotted line) for the region 10°N, 74°E. The error bars for SST show 1σ variations around the mean of 7 years. (b) δ¹⁸O of water (relative to PDB) calculated from salinity data and δ¹⁸O-salinity relation for this region (Duplessey *et al.* 1981). (c) estimated δ¹⁸O variations of coral based on SST and δ¹⁸O of water. Y-axis represents a relative scale.

$$\delta^{18}\text{O}_{\text{coral}} = \delta^{18}\text{O}_{\text{eq}} + \delta^{18}\text{O}_{\text{off}} \quad (3.1)$$

where  $\delta^{18}\text{O}_{\text{off}}$  is the "offset" term. This offset has so far been assumed to be constant with time, within the limits of experimental uncertainties for a given coral species. The offset from equilibrium value in symbiont bearing corals of Indo-Pacific origin ranges from -3.12 to -1.93‰ at 25°C among 44 coral genera analyzed by Weber & Woodhead (1972). Aharon (1991) obtained a value of -5.1‰ for *Porites* from the Palm Isles.

We determined the  $\delta^{18}\text{O}_{\text{off}}$  for *Porites* of Lakshadweep by comparing  $\delta^{18}\text{O}$  profiles in a coral (Am) from the Amini island with that in a giant clam (GC) that grew near the coral. It is known that the giant clam (*Tridacna*) precipitates its  $\text{CaCO}_3$  in isotopic equilibrium (Aharon & Chappel 1986; Romanek & Grossman 1989), hence it is possible to correct for the coral  $\delta^{18}\text{O}$  disequilibrium offset by comparing  $\delta^{18}\text{O}$  values in time contemporaneous samples of coral and a bivalve.

We collected a live coral head (*Porites*) and a giant clam (*Tridacna maximus*) from the Amini island (11°7'N, 72°44'E) in December 1988. Band assignment in the Amini coral was made following the procedure discussed earlier for the Kavaratti coral. This coral had a life span of about 5 years. In the case of *Tridacna*, year assignment was possible by identifying the annual zonation in the exoskeleton (Aharon & Chappel, 1986).  $\delta^{18}\text{O}$  data for the clam and the Amini coral are given in Table III.2 (Appendix A). We have estimated the disequilibrium offset in the *P. compressa* coral by comparing the  $\delta^{18}\text{O}$  values of the two during the life span of the coral, 1983-1988. Again, because of the difference in the growth rates, only the maxima, minima values of the two are compared. This yields a mean value of  $-4.47 \pm 0.23$ ‰ for the disequilibrium offset and ranges between -4.22 to -5.00‰. Note that all these disequilibrium factors are relative to aragonite equilibrium values. We consider our estimate of disequilibrium offset to be better than that available in literature (Aharon 1991) because the coral and the clam were growing very close to each other ~1m, compared to ~3km separation in earlier work. Our estimate of disequilibrium offset appears to be constant (within  $\pm 0.2$ ‰) with time.

From the available data on SST,  $\delta^{18}\text{O}$  of clam, and  $\delta^{18}\text{O}$  of sea water for April and August we derive a regression line of the form:

$$T(^{\circ}\text{C}) = A + B (\delta_c - \delta_w) \quad (3.2)$$

where  $\delta_c$  and  $\delta_w$  are the  $\delta^{18}\text{O}$  of the clam and sea water wrt PDB respectively. For this,

we have taken the  $\delta_w$  values to be 0.28 and 0.415 for May and August respectively (see Fig 3.4). This assumes that there is no year to year change in seasonal  $\delta_w$ . This can cause some uncertainty in the accurate evaluation of SST from the coral  $\delta^{18}\text{O}$ . This is discussed later.

Fitting of our measured yearly maximum and minimum oxygen isotope data of the clam with corresponding SST (for 1983-1988) yields:  $A=23.92\pm0.35$  and  $B=-4.68\pm0.33$ , with a correlation coefficient  $r=-0.92$  significant at 0.01 level. Substituting these values in Eqn (3.2) we get,

$$T(^{\circ}\text{C}) = 23.92 - 4.68 (\delta_c - \delta_w) \quad (3.3)$$

This is similar to the equation  $[T = 20.95 - 4.35(\delta_c - \delta_w)]$  obtained by Aharon & Chappel (1986) for tridacnid clams between temperatures of 23 to 28°C. The slopes of these two equations agree within analytical uncertainties, but the intercepts differ by 3°C. One possible explanation for this may be the difference in temperature ranges in the two localities. In Lakshadweep the maximum temperature exceeds 30°C in summer, occasionally it reaches even 35°C for a few days.

Substituting for  $\delta_c$  in Eqn (3.3) in terms of  $\delta_{\text{coral}}$  and the disequilibrium offset, we obtain the temperature equation for SST based on the coral  $\delta^{18}\text{O}$ .

$$T(^{\circ}\text{C}) = 3.0 - 4.68(\delta_{\text{coral}} - \delta_w) \quad (3.4)$$

where  $\delta_{\text{coral}}$  is the  $\delta^{18}\text{O}$  value of the *Porites* coral. This equation is quite similar to that reported for *Porites* from the Pacific (Aharon, 1991):

$$T = 2.81 - 4.76(\delta_{\text{coral}} - \delta_w) \quad (3.5)$$

The slope is also in agreement with that for *Porites* from the Atlantic (Druffel 1985). The uncertainties in estimating temperature using Eqn (3.5) are: (i) there may be small changes from equilibrium values even for the tridacnid clams ranging from 0.1 to 0.3‰ (Aharon 1991); this would correspond to 0.5 to 1.5 °C difference in the estimated SSTs, (ii) the SST values used by us for deriving the temp- $\delta^{18}\text{O}$  equation (Eqn 3.4) are not from the exact location of the clam. This may cause an additional uncertainty.

The estimated uncertainty in SST based on Eqn 3.4 is calculated to be 1.4°C considering the errors in  $\delta_w$  (0.2‰) and that in the disequilibrium offset (0.23‰). If the errors on the coefficients A, B are also taken into account the uncertainty in the SST



we have taken the  $\delta_w$  values to be 0.28 and 0.415 for May and August respectively (see Fig 3.4). This assumes that there is no year to year change in seasonal  $\delta_w$ . This can cause some uncertainty in the accurate evaluation of SST from the coral  $\delta^{18}\text{O}$ . This is discussed later.

Fitting of our measured yearly maximum and minimum oxygen isotope data of the clam with corresponding SST (for 1983-1988) yields:  $A=23.92\pm0.35$  and  $B=-4.68\pm0.33$ , with a correlation coefficient  $r=-0.92$  significant at 0.01 level. Substituting these values in Eqn (3.2) we get,

$$T(^{\circ}\text{C}) = 23.92 - 4.68 (\delta_c - \delta_w) \quad (3.3)$$

This is similar to the equation  $[T = 20.95 - 4.35(\delta_c - \delta_w)]$  obtained by Aharon & Chappel (1986) for tridacnid clams between temperatures of 23 to 28°C. The slopes of these two equations agree within analytical uncertainties, but the intercepts differ by 3°C. One possible explanation for this may be the difference in temperature ranges in the two localities. In Lakshadweep the maximum temperature exceeds 30°C in summer, occasionally it reaches even 35°C for a few days.

Substituting for  $\delta_c$  in Eqn (3.3) in terms of  $\delta_{\text{coral}}$  and the disequilibrium offset, we obtain the temperature equation for SST based on the coral  $\delta^{18}\text{O}$ .

$$T(^{\circ}\text{C}) = 3.0 - 4.68(\delta_{\text{coral}} - \delta_w) \quad (3.4)$$

where  $\delta_{\text{coral}}$  is the  $\delta^{18}\text{O}$  value of the *Porites* coral. This equation is quite similar to that reported for *Porites* from the Pacific (Aharon, 1991):

$$T = 2.81 - 4.76(\delta_{\text{coral}} - \delta_w) \quad (3.5)$$

The slope is also in agreement with that for *Porites* from the Atlantic (Druffel 1985). The uncertainties in estimating temperature using Eqn (3.5) are: (i) there may be small changes from equilibrium values even for the tridacnid clams ranging from 0.1 to 0.3‰ (Aharon 1991); this would correspond to 0.5 to 1.5 °C difference in the estimated SSTs, (ii) the SST values used by us for deriving the temp- $\delta^{18}\text{O}$  equation (Eqn 3.4) are not from the exact location of the clam. This may cause an additional uncertainty.

The estimated uncertainty in SST based on Eqn 3.4 is calculated to be 1.4°C considering the errors in  $\delta_w$  (0.2‰) and that in the disequilibrium offset (0.23‰). If the errors on the coefficients A, B are also taken into account the uncertainty in the SST

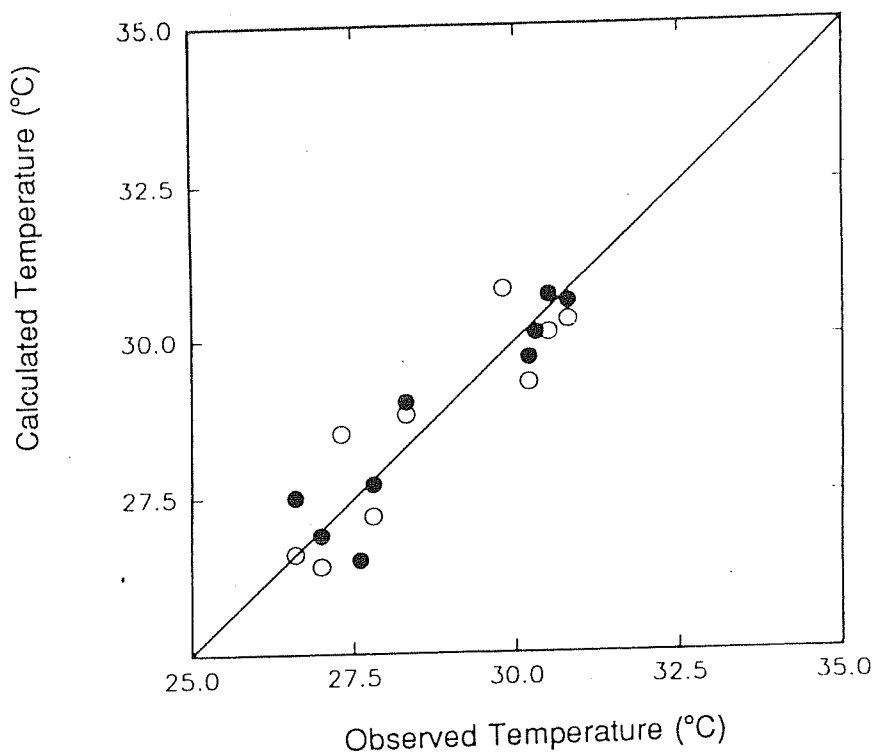


Fig 3.5 Plot of observed vs. calculated SST using coral thermometry. The data appear clustered as they represent the maxima and minima of SST. Filled circle: KV-1, open circle: Am coral. 45° line is drawn for comparison (it is not the best fit line). The observed temperatures are from a location near to the coral site.

estimate becomes  $1.9^{\circ}\text{C}$ . This is the maximum uncertainty in the estimation of SST taking into consideration the errors in  $\delta_w$ , disequilibrium offset, and in A and B.

Fig 3.5 shows the relationship between observed temperature and the calculated temperature using KV-1 and Am respectively. Please note that even though we have used the Amini coral  $\delta^{18}\text{O}$  data for calculating the disequilibrium offset, we include these data for comparison because the seasonal variations of the Amini coral  $\delta^{18}\text{O}$  data have not been used to find the temperature Eqn (3.3). The points scatter closely around the  $45^{\circ}$  line where the observed temperatures equal calculated temperatures. The mean error in the estimated temperatures is  $1.2^{\circ}\text{C}$ . This estimate is better than that anticipated based on the propagation of errors discussed above.

Now we test this temperature equation by applying it to another *P. compressa* KV-2 from Kavaratti, which had a 25 year long  $\delta^{18}\text{O}$  record. Its average growth rate based on X-radiography is  $15 \pm 3.4$  mm/yr. We have sampled the bands for isotopic studies to get a resolution of 3 to 6 weeks. (but each sample was  $\sim 1$  mm thick and corresponds to  $\sim 1$  month growth). Its oxygen isotopic time series is shown in Fig 3.6a and listed in Table III.5 (Appendix-A). Most of the  $\delta^{18}\text{O}$  values lie between  $-5.5$  to  $-4.8\text{‰}$ , similar to that observed in KV-1 and Am coral. We use the Eqn (3.4) derived earlier in this section based on the coral data for estimating the yearly maxima and minima in SST. For the  $\delta^{18}\text{O}$  of water (wrt PDB) for May and Aug we have used values of 0.28 and 0.415 respectively (Fig 3.4b).

Also shown in Table III.4 and Fig 3.7 are observed SST data based on ship record (COADS). Some of the data (during the period 1979-1990) are from Paul *et al.* (1992). As each sample used for  $\delta^{18}\text{O}$  analysis grew for period of 1 month, the monthly mean values of SST for May ( $\delta^{18}\text{O}$  minima) and August ( $\delta^{18}\text{O}$  maxima) are shown in Table III.4, for the sake of comparison. The observed and estimated SST values (from coral  $\delta^{18}\text{O}$ , using Eqn 3.4) are in good agreement within the quoted uncertainty. The difference between the observed and the calculated temperatures has mean values of  $0.0 \pm 0.9^{\circ}\text{C}$  for May and  $0.2 \pm 0.5^{\circ}\text{C}$  for August. The ranges are from  $-1.7$  to  $1.7^{\circ}\text{C}$  for May and  $-0.4$  to  $1.7^{\circ}\text{C}$  for August. These are less than the maximum estimated uncertainties of  $1.9^{\circ}\text{C}$ . Therefore we conclude that our palaeotemperature Eqn 3.4 is quite valid for *P. compressa* in this region. The discrepancy between the observed and calculated temperatures arises

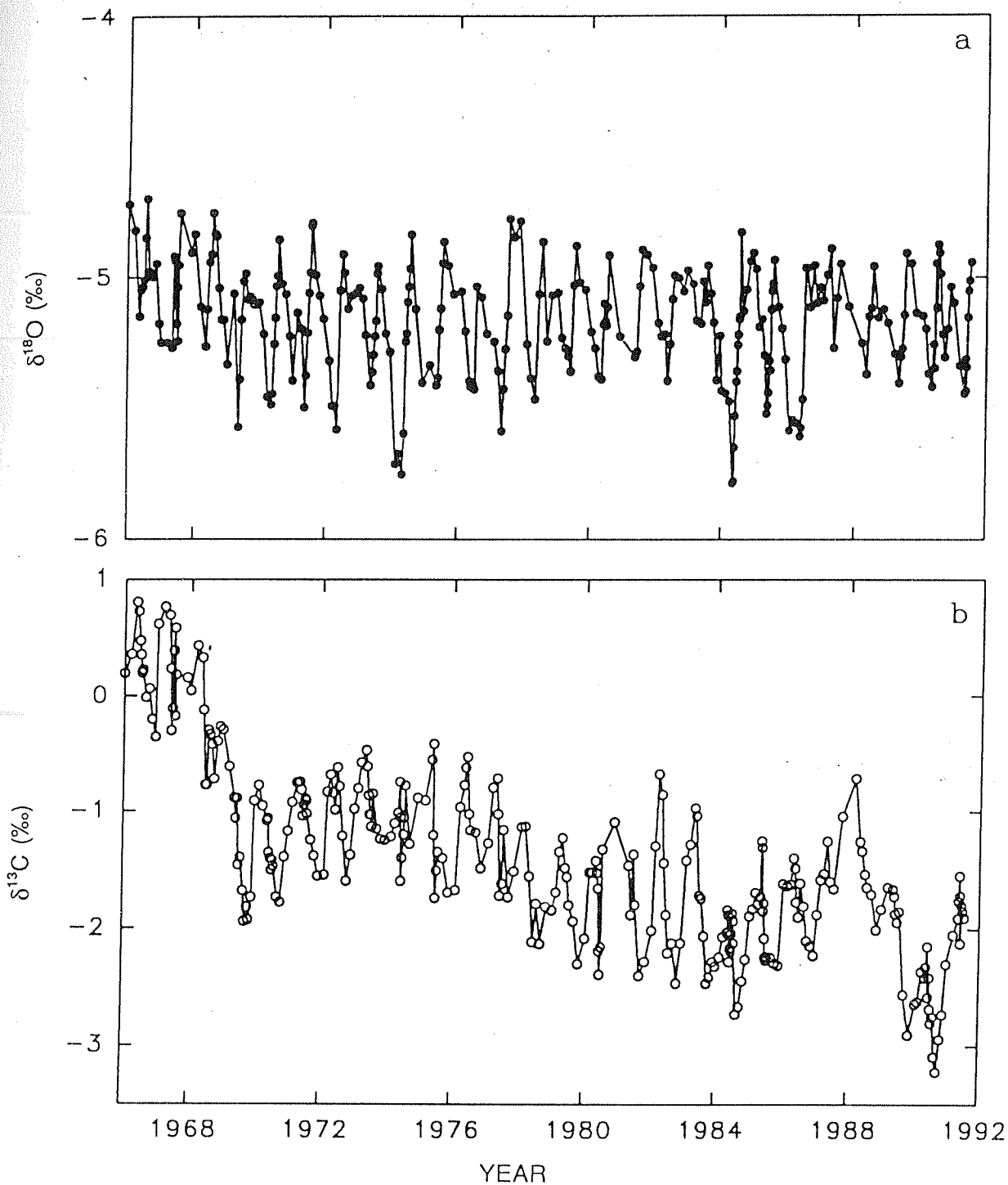


Fig 3.6  $\delta^{18}\text{O}$ (a) and  $\delta^{13}\text{C}$  (b) variations in *P. compressa* coral (KV-2) from the Kavaratti lagoon. The  $\delta^{13}\text{C}$  shows a decreasing trend with age of this coral.

because we have not considered the year to year variations in the  $\delta^{18}\text{O}$  of water ( $\delta_w$ ). The range of  $-1.7$  to  $+1.7$   $^{\circ}\text{C}$  in the discrepancy, can be caused by interannual variation in  $\delta_w$ .

Table III.4 Comparison between observed and derived SST

Month & Year	$\delta^{18}\text{O}$ (‰)	Derived Temp. $T_d$ ( $^{\circ}\text{C}$ )	Obs. Temp. $T_o$ ( $^{\circ}\text{C}$ )	$T_d - T_o$ ( $^{\circ}\text{C}$ )
May '74	-5.76	31.3	29.8	1.5
Aug '74	-4.84	27.6	27.0	0.6
May '75	-5.41	29.6	29.0	0.6
Aug '75	-4.86	27.7	26.5	1.2
May '76	-5.43	29.7	29.2	0.5
Aug '76	-5.04	28.5	26.8	1.7
May '77	-5.59	30.5	30.1	0.4
Aug '77	-4.78	27.3	27.0	0.0
May '78	-5.46	29.9	30.0	-0.1
Aug '78	-4.86	27.7	27.6	0.1
May '79	-5.30	29.1	29.4	-0.3
Aug '79	-4.88	27.8	27.3	0.5
May '80	-5.39	29.5	30.7	-1.2
Aug '80	-4.91	27.9	28.3	-0.4
May '81	-5.30	29.1	29.9	-0.8
Aug '81	-4.89	27.8	27.5	0.3
May '82	-5.40	29.5	30.2	-0.7
Aug '82	-4.99	28.3	28.3	0.0
May '83	-5.18	28.6	30.1	-0.5
Aug '83	-4.95	28.1	28.5	-0.4

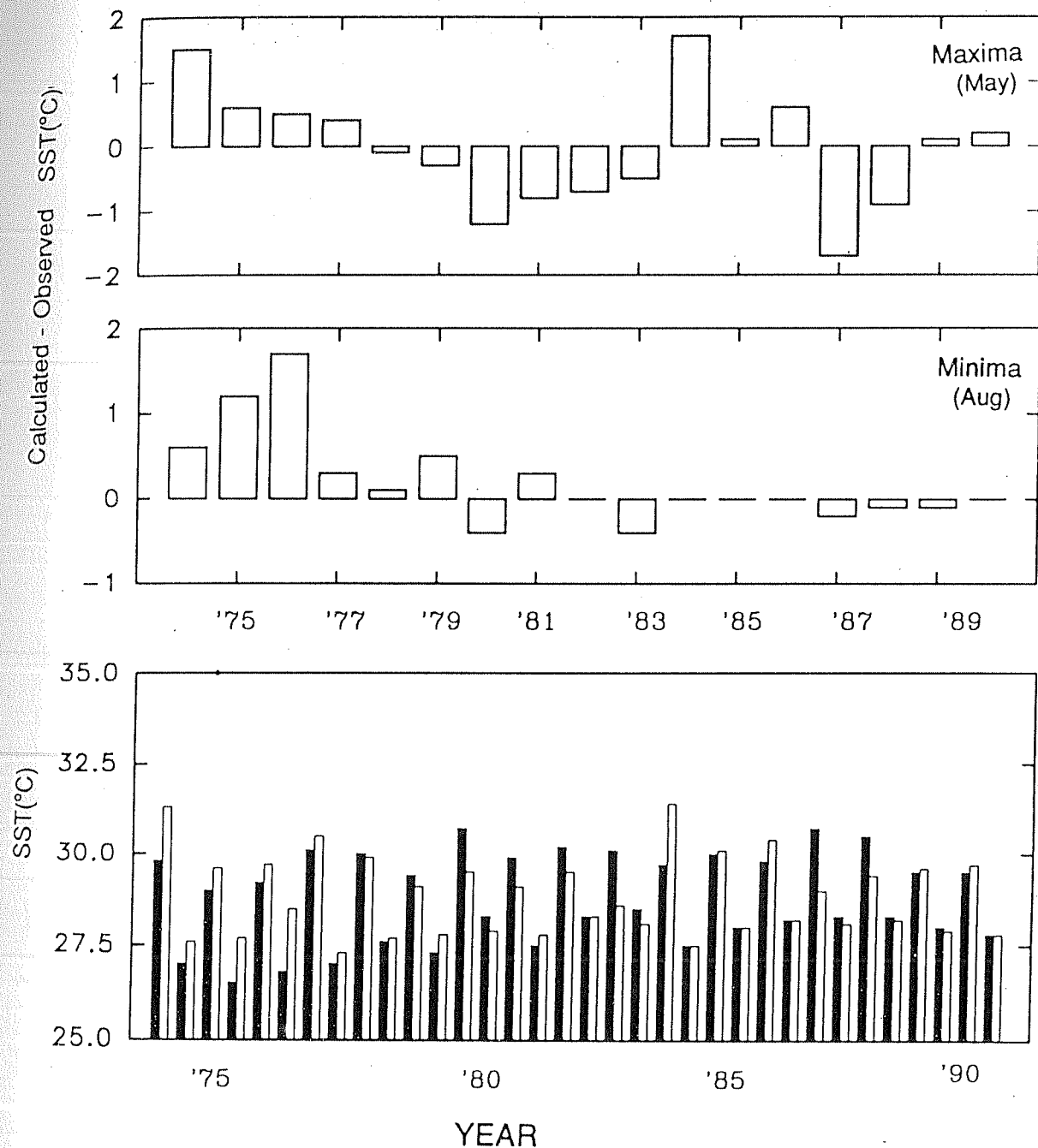


Fig 3.7 Plot showing the observed (filled bar) and calculated SST (open bar) based on coral  $\delta^{18}\text{O}$  (KV-2). For each year both the minima and the maxima SSTs are shown.

Top panel diagrams show the deviations of the calculated SSTs from the observed SSTs. Deviations for the May has a mean of  $0.0 \pm 0.9$  and for Aug it has a mean of  $0.2 \pm 0.5$  °C.

May '84	-5.79	31.4	29.7	1.7
Aug '84	-4.83	27.5	27.5	0.0
May '85	-5.52	30.1	30.0	0.1
Aug '85	-4.93	28.0	28.0	0.0
May '86	-5.58	30.4	29.8	0.6
Aug '86	-4.96	28.2	28.2	0.0
May '87	-5.27	29.0	30.7	-1.7
Aug '87	-4.95	28.1	28.3	-0.2
May '88	-5.37	29.4	30.5	-0.9
Aug '88	-4.96	28.2	28.3	-0.1
May '89	-5.40	29.6	29.5	0.1
Aug '89	-4.91	27.9	28.0	-0.1
May '90	-5.42	29.7	29.5	0.2
Aug '90	-4.88	27.8	27.8	0.0

Summing up, it can be said that the coral  $\delta^{18}\text{O}$  thermometry provides a fairly reliable estimation of SST in the LDP region. The uncertainty in the SST estimation is slightly better than the reported uncertainty ( $\pm 2.8^\circ\text{C}$ ) for coral  $\delta^{18}\text{O}$  as palaeothermometer (Aharon 1991). The present uncertainty of  $\pm 1.9^\circ\text{C}$  can be reduced further if we have monthly  $\delta^{18}\text{O}$  measurements of sea water.

Fig 3.8 shows  $\delta^{18}\text{O}$  time series of the two corals, KV-1 and KV-2 which grew in nearby regions and which are also of the same species. The data clearly show that there is a close resemblance in their oxygen isotope time series, with almost equal amplitudes for the seasonal variations,  $\sim 0.8\text{‰}$ . As discussed earlier this seasonal amplitude by and large results from SST changes caused by upwelling during SW monsoon. The magnitude of the  $\delta^{18}\text{O}$  amplitude for a drought year 1987, was found to be much less, about  $\sim 0.3\text{‰}$  in both KV-1 and KV-2. This observation prompted us to look for possible correlation between upwelling and rainfall, both of which are driven by the south-west monsoon. If such a correlation exists then one would expect reduced seasonal amplitude in coral  $\delta^{18}\text{O}$

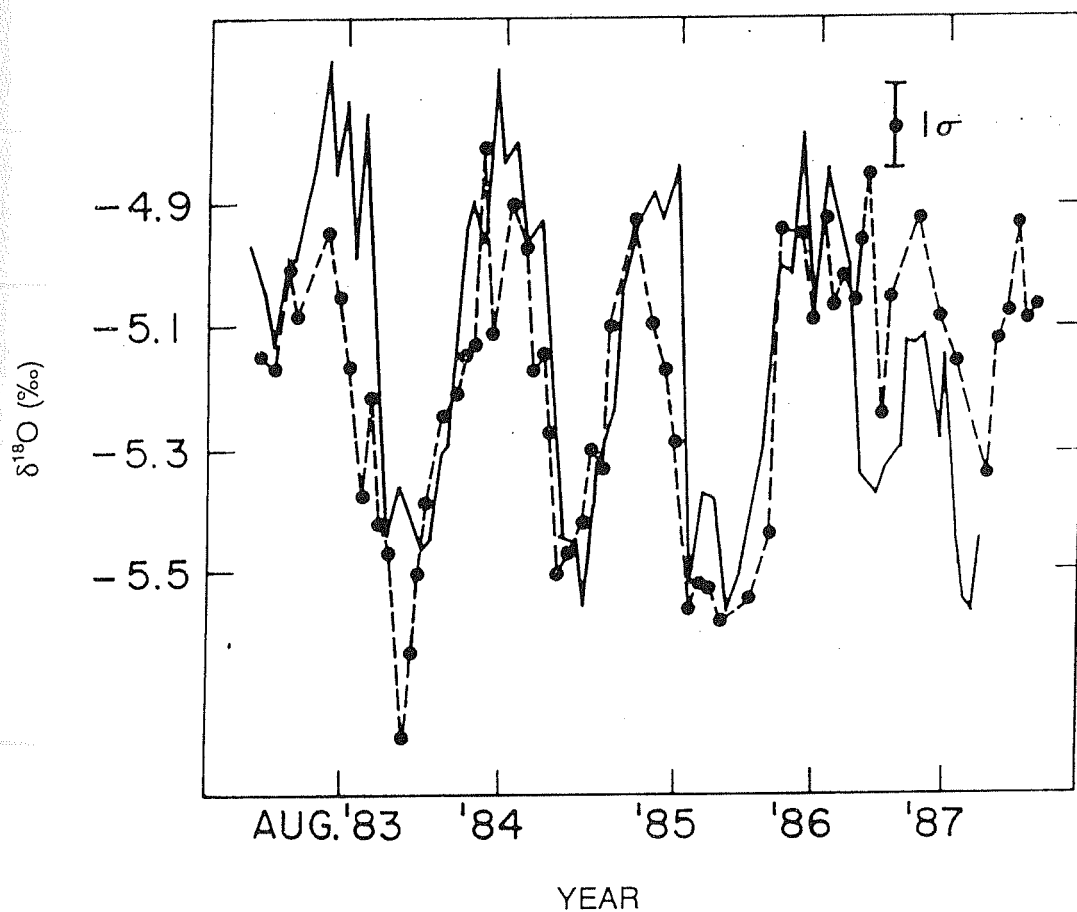


Fig 3.8 Intercomparison of the  $\delta^{18}\text{O}$  of the two *P. compressa* corals (KV-1, KV-2) from the Kavaratti lagoon, Lakshadweep islands. The two profiles resemble very closely. solid line: KV-1; dashed line: KV-2



in drought years (as seen in 1987) and enhanced amplitude during flood years. To check on this we carefully analyzed the  $\delta^{18}\text{O}$  amplitude-rainfall trends in KV-2. The results are not conclusive as a consistent trend was not observed. For example the amplitude in the  $\delta^{18}\text{O}$  for another drought year 1972, did not show a reduction. Similarly the  $\delta^{18}\text{O}$  amplitudes for flood years also exhibit mixed trends. The years 1971 and 1975 show comparatively enhanced amplitude, but 1983, a heavy rainfall year shows a reduced amplitude. Also, a normal rainfall year, 1984 shows a large amplitude. While the reduction in SST in the LDP region during May-Aug is definitely due to upwelling induced by monsoon winds, the monsoon rainfall on the land is a function of several parameters like moisture content of the air masses entering the land, the distribution of rain over land and sea, orographic features, air temperatures etc. Therefore the upwelling induced SST reduction in the LDP does not appear to be correlated directly with the monsoon rainfall.

In summary, the oxygen isotopic records in *Porites* corals of Lakshadweep region provide a useful tool for monitoring the sea surface temperatures in the past with a reasonable accuracy.

## (ii) Carbon isotopes

As mentioned earlier the  $\delta^{13}\text{C}$  of corals is influenced by the isotopic composition of seawater  $\Sigma\text{CO}_2$ , coral growth rate and geometry and biological activities like metabolism and endosymbiotic photosynthesis (Nozaki *et al.* 1978, Fairbanks & Dodge 1979, Aharon 1985, McConnaughey 1989)

The  $\delta^{13}\text{C}$  time series of corals KV-1 and KV-2 are given in Figs 3.3a and 3.6b respectively and presented in Tables III.3 and III.5 of Appendix A. They show annual periodicities with a seasonal amplitude of  $\sim 1\text{‰}$ . We first discuss the seasonal  $\delta^{13}\text{C}$  variations and the timing of density band formation. This is followed by a discussion on the long term trend in  $\delta^{13}\text{C}$  in KV-2.

Coral growth is controlled by various parameters. The favourable factors are higher light intensity resulting in enhancement of photosynthesis; corals are carnivores and live on zooplankton, so availability of zooplankton is another favourable factor for coral

growth. On the other hand the parameters inhibiting the growth include water current, turbidity, sedimentation, rainfall and predators. Suresh & Mathew (1993) made *in-situ* measurements on skeletal extension of a reef building coral *Acropora formosa* which grew in the Kavaratti atoll. They measured variations in temperature, pH, salinity, phosphate, nitrate, nitrite, calcium, water current, suspended matter, rate of sedimentation, rainfall and zooplankton activity for the period of 1988-1989 and correlated the coral extension rate with these environmental parameters. They observed that the extension rate of *A. formosa* is directly related to zooplankton and nitrite availability, though the correlation between the growth rate and nitrite is not clear. In the Lakshadweep region zooplankton are more abundant during Dec-Jan and are least abundant during Aug-Oct (*op cit.*). During the monsoon (JJAS) due to stronger water current and enhanced sediment suspension, the growth rate is adversely affected. Also due to the increased amount of cloud cover photosynthesis decreases causing a decrease in photoinduced calcification and hence coral growth. They give supportive evidence to show that the variation in temperature, pH, salinity, phosphate, nitrate and calcium have relatively minor control on the coral growth. Summarizing, the growth rate is slower during the summer monsoon (JJASO) and higher during the rest of the year.

Figs 3.3a and 3.6b show the  $\delta^{13}\text{C}$  variations of KV-1 and KV-2 respectively. The  $\delta^{13}\text{C}$  in KV-1 starts decreasing from the beginning of summer *i.e.* in Apr, from  $-0.07\text{‰}$  it reduces to  $-1.25\text{‰}$ . The trend reverses in the month of Dec when it starts rising and reaches a maximum during Jan-Feb. This pattern is also seen in case of the KV-2 coral also, though the absolute  $\delta^{13}\text{C}$  values of the two corals are different. The  $\sim 1\text{‰}$  dip in the  $\delta^{13}\text{C}$  in the summer monsoon period can be explained as follows:

The  $\delta^{13}\text{C}$  of the coral is determined by the  $\delta^{13}\text{C}$  of the  $\Sigma\text{CO}_2$  of sea-water in the vicinity of coral. This in turn is controlled by (a) zooxanthallar photosynthesis which uses more  $^{12}\text{C}$  than  $^{13}\text{C}$  and hence enriches the  $\Sigma\text{CO}_2$  of sea-water in  $^{13}\text{C}$ ; (b) respiration of both the coral and the zooxanthellae, which reduces the  $\delta^{13}\text{C}$  of  $\Sigma\text{CO}_2$  of sea-water, (c) upwelling of deeper waters due to monsoon, which deplete the  $\Sigma\text{CO}_2$  in  $^{13}\text{C}$  by mixing deeper waters depleted in  $^{13}\text{C}$ , and (d) oceanic uptake of fossil fuel  $\text{CO}_2$  which also depletes the surface water in  $\delta^{13}\text{C}$ . During SW monsoon the cloudiness increases from 60% during May to more than 80% during Jun-Jul (Hastenrath & Lamb 1979). Due to

monsoon activity currents become stronger causing more sediment suspension. In Jul-Aug suspended matter and sedimentation rate in the Kavaratti atoll are increased by about a factor of 3 to 5 (Suresh & Mathew 1993). These effects cause a substantial reduction in the light intensity and therefore the photosynthesis activity of the zooxanthellae decreases to a great extent. As the photosynthesis slows down, photoinduced calcification is also retarded resulting in the formation of the high density band. Probably during this period the respiration dominates over the photosynthesis fixation of carbon. While photosynthesis is carried out only by the zooxanthellae, the respiration is from both the coral polyp and the zooxanthellae. Under these conditions, the  $\delta^{13}\text{C}$  of coralline  $\text{CaCO}_3$  is expected to decrease.

By the end of May the monsoon induced upwelling increases and a deeper water component depleted in  $^{13}\text{C}$ , is brought along with nutrients like phosphates and nitrates resulting in higher biological productivity in several regions of the Arabian Sea (Sathyendranath *et al.* 1991; Brock & McClain 1992). This causes further reduction in  $\delta^{13}\text{C}$ . Consequently the  $\delta^{13}\text{C}$  reaches a minimum during Oct or early Nov. This is the time when high density bands cease to form. Again after the monsoon season the light level increases. Turbidity, currents and suspended matter are also reduced causing enhancement in the photosynthetic activity which enriches the coral  $\text{CaCO}_3$  in  $^{13}\text{C}$ . During Dec-Jan zooplankton activity reaches its maximum (Suresh & Mathew 1993). These favourable parameters like increased rate of photosynthesis and higher abundance of zooplankton favour the coral growth which result in low density band formation. During rest of the year the mean cloud content is about 30% and hence the  $\delta^{13}\text{C}$  values increase by 0.4‰, due to increased zooxanthallar activity.

Therefore the high (HD) density part of the band formed during the monsoon period shows a depletion in  $\delta^{13}\text{C}$  compared to that of the low density (LD) part. The average  $\delta^{13}\text{C}$  values for the HD and LD bands are shown in Table III.6. The high density bands, in general show systematic depletion in  $\delta^{13}\text{C}$  (except in three cases). While comparing these values we use uncertainties corresponding to the standard deviation of the mean, which is 0.02 to 0.07‰ depending on the number of sample per band.

Table III.6 The average carbon isotopic composition of high and low density bands in coral KV-2

Year	Band type	Average $\delta^{13}\text{C}(\text{‰})$	Year	Band type	Average $\delta^{13}\text{C}(\text{‰})$
1971	HD	-1.11	1980	HD	-1.79
	LD	-1.10		LD	-1.67
1972	HD	-2.42	1981	HD	-1.86
	LD	-1.01		LD	-0.99
1973	HD	-1.14	1982	HD	-1.92
	LD	-0.88		LD	-1.00
1974	HD	-1.19	1983	HD	-2.14
	LD	-0.78		LD	-2.04
1975	HD	-1.27	1984	HD	-2.21
	LD	-1.11		LD	-1.66
1976	HD	-1.10	1985	HD	-2.06
	LD	-0.76		LD	-1.63
1977	HD	-1.45	1986	HD	-1.98
	LD	-1.26		LD	-1.56
1978	HD	-1.88	1987	HD	-1.39
	LD	-1.63		LD	-1.79
1979	HD	-1.90	1988	HD	-2.37
	LD	-1.49		LD	-2.40

Summarizing, the high density band formation takes place during the summer monsoon period viz, Jun-Oct. Due to monsoon activities the growth rate is retarded and the carbon isotopic composition is also depleted. On the other hand the low density bands formed during Nov to May shows a higher growth rate and are enriched in  $^{13}\text{C}$  relative to high

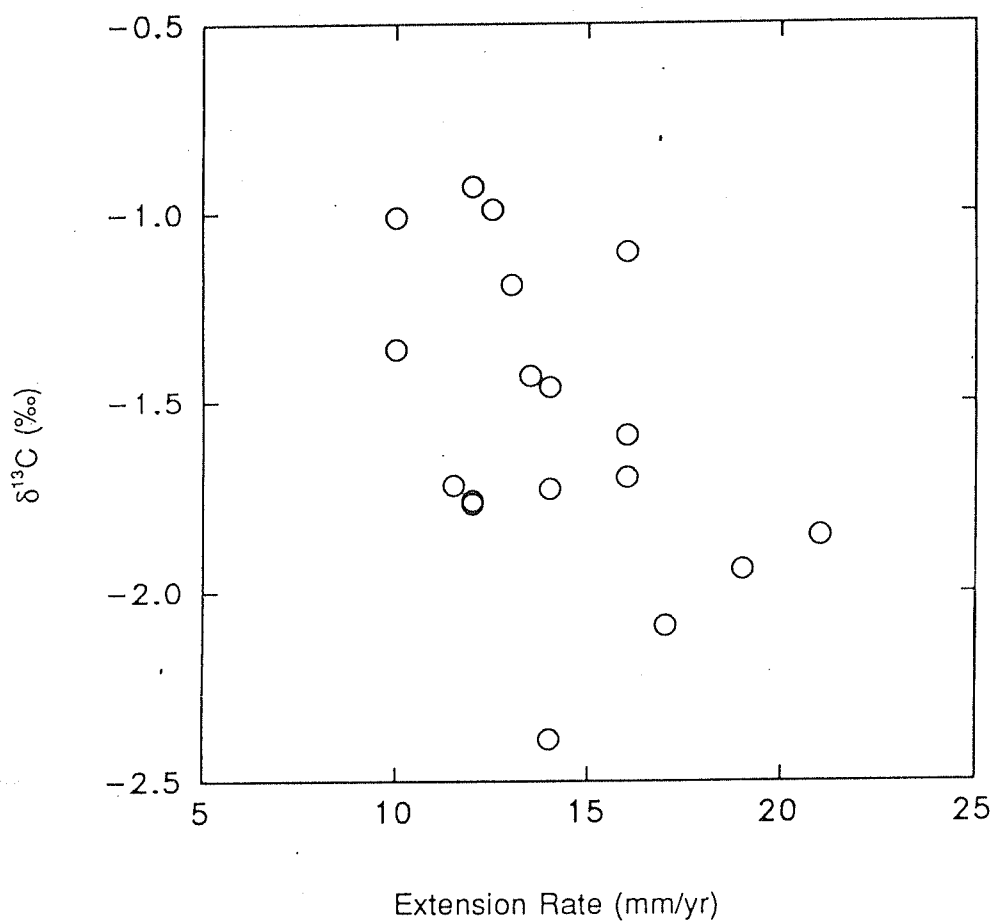


Fig 3.9 Relationship between  $\delta^{13}\text{C}$  and the extension rate in the coral *P.compressa* (KV-2)

density band. The seasonal variation in  $\delta^{13}\text{C}$  is caused by the variation in photosynthetic activity of the zooxanthellae, while the variation in growth rate is controlled by environmental parameters as well as zooxanthallar photosynthesis.

On a longer time scale, the  $\delta^{13}\text{C}$  in KV-2 shows a decreasing trend with time. (KV-1 is only 5 years old and does not show any distinct trend). During the initial stage of its growth KV-2 has a mean  $\delta^{13}\text{C}$  value of 0.5‰, which decreases to a present day value of  $\sim -2.5$ ‰ (Fig 3.6). It is interesting to note that while  $\delta^{18}\text{O}$  does not show any trend,  $\delta^{13}\text{C}$  shows a mean trend of  $-0.12$ ‰ per year. This is similar to the observations of Aharon (1991) who did not find any trend in  $\delta^{18}\text{O}$  but a trend of  $-0.1$ ‰ per year in  $\delta^{13}\text{C}$  for the Palm Island *Porites*. This large negative shift in  $\delta^{13}\text{C}$  appears to be affected by the growth rate related fractionation.  $\delta^{13}\text{C}$  in general shows a negative correlation with the extension rate (Fig 3.9) which conforms to this hypothesis. This growth rate related fractionation is dominant only in interannual time scale; in seasonal time scale the fractionation (of  $^{13}\text{C}$ ) due to changes in photosynthetic activities dominates over the growth rate dependent fractionation. For this reason despite lower growth rate during monsoon time  $\delta^{13}\text{C}$  shows a decrement. Growth rate related fractionation was also proposed by McConnaughey (1989) who observed that the faster growing portions of the skeleton suffered more fractionation. However the exact mechanism of this growth rate related fractionation is yet to be fully understood.

Comparison of the mean  $\delta^{13}\text{C}$  values of KV-1 and KV-2 (both from the Kavaratti lagoon) during 1983-1988, shows distinct differences. The mean  $\delta^{13}\text{C}$  of KV-1 is  $-0.75$ ‰ whereas that of KV-2 is  $-1.8$ ‰. Thus KV-2 is depleted by  $\sim 1$ ‰ compared to KV-1. This could be a depth dependent fractionation. KV-1 grew at a depth of  $\sim 1$ m, whereas KV-2 was from a depth of 7 to 10m. According to Fairbanks and Dodge (1979) corals growing at greater depths get less sunlight and hence their photosynthesis rate is also reduced; consequently they are depleted in  $\delta^{13}\text{C}$  relative to corals growing near the surface. However, this hypothesis is not consistent with our earlier discussion, where higher growth rate is associated with more depleted  $\delta^{13}\text{C}$ . KV-1 has an average growth rate 23.3mm/yr compared to KV-2 which grew slightly slower, 15 mm/yr. This makes it difficult to draw any definitive conclusion about the cause of the difference in the  $\delta^{13}\text{C}$  values of KV-1 and KV-2 and also about the long term trend (in case of KV-2) resulting from growth rate

dependent fractionation discussed earlier.

In spite of these difficulties in explaining the carbon isotopic variations, we see that the  $\delta^{13}\text{C}$  of the *Porites compressa* from Lakshadweep region shows a general behaviour, the seasonal cyclicity due to variations in the photosynthesis modulated by monsoonal activities. This seasonal dip in the  $\delta^{13}\text{C}$  during monsoon and the enhancement of  $\delta^{18}\text{O}$  during the same season due to cooling, induced by upwelling may provide clues to the past upwelling changes, once quantified.

### III.2.b Gulf of Kutch coral

The Gulf of Kutch coral (GK) belongs to the genus *Favia*. Its life span based on X-radiography was 41 years with an average growth rate  $4.3 \pm 1.3$  mm/yr.

The carbon and oxygen isotopic data of samples from annual bands of the Gulf of Kutch coral is presented in Fig 3.10 [data in Appendix-A, Table-III.7]. It is known that the  $\delta^{18}\text{O}$  of coral carbonate is determined by (a) SST and (b)  $\delta^{18}\text{O}$  of the water in which it grows (often when  $\delta^{18}\text{O}$  data for sea water is not available, salinity is used as an index of  $\delta^{18}\text{O}$  as these two in general, are correlated (Craig & Gordon 1965); however this relationship differs from region to region and has to be established for each specific area). To determine the utility of the coral  $\delta^{18}\text{O}$  data for retrieving climatic parameters we need to know how the  $\delta^{18}\text{O}$  of coral responds to the local sea surface temperature and  $\delta^{18}\text{O}$  variations. To quantify these effects for the GK coral we use COADS SST data (Sadler *et al.* 1987) at  $22.6^\circ\text{N}$ ,  $69.5^\circ\text{E}$ , closest available to the Gulf of Kutch. The curve (Fig 3.11) shows maximum SST ( $29^\circ\text{C}$ ) around June and minimum ( $23^\circ\text{C}$ ) around Jan-Feb. During Aug-Sep there is a small trough, ( $\sim 2^\circ\text{C}$ ) which could be due to reduction in air temperature resulting from monsoon activity and the lateral transport of upwelled cooler waters from the open ocean into the Gulf. The  $\delta^{18}\text{O}$  of sea water (relative to PDB) from the coral location was measured periodically (Nov, Dec 1992, Jan, Feb, May & Jun 1993). The values range from  $0.39\text{‰}$  (December) to  $0.71\text{‰}$  (May). Based on these SST and  $\delta^{18}\text{O}$  of water ( $\delta_w$ ) data we calculate the seasonal amplitude in the coral  $\delta^{18}\text{O}$  to be  $1.1 \pm 0.2\text{‰}$ , with a maximum in January and a minimum in June. For making this

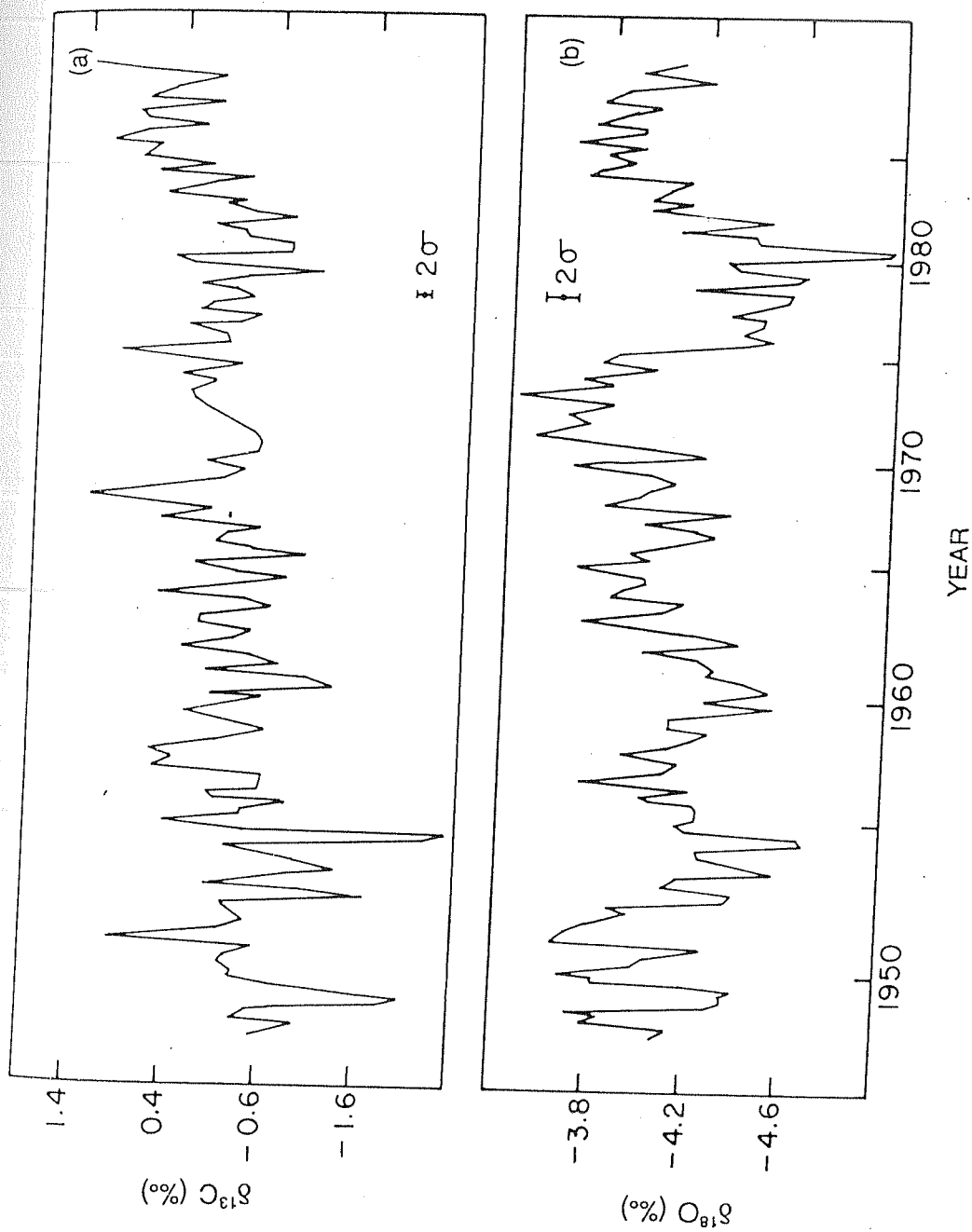


Fig 3.10  $\delta^{13}\text{C}$  (a) and  $\delta^{18}\text{O}$  (b) records of the coral *Favia speciosa* (GK) from the Gulf of Kutch (22.6°N, 70°E)



calculation we have used the relation between SST and  $\delta^{18}\text{O}$  for this coral species (Weber & Woodhead 1972, temperature coefficient  $-0.239\text{‰ }^{\circ}\text{C}^{-1}$ ) and adjusting for the sea water  $\delta^{18}\text{O}$  variation:  $6^{\circ}\text{C}$  change in SST would correspond to  $1.43\text{‰}$  change in the coral  $\delta^{18}\text{O}$ . The change in  $\delta^{18}\text{O}_w$  of  $0.32\text{‰}$  would act in the opposite direction and reduces the coral  $\delta^{18}\text{O}$  amplitude to  $1.1\text{‰}$ . The observed mean seasonal  $\delta^{18}\text{O}$  amplitude is only  $0.3 \pm 0.2\text{‰}$  much less than the calculated value. The apparent discrepancy between the observed and calculated  $\delta^{18}\text{O}$  amplitude could be due to the low resolution sampling resulting from the slow growth rate. This is discussed later based on a model simulation study. The seasonal amplitude is superimposed on an apparent higher order cyclicity of 7-8 years.

It is well established that the coralline  $\delta^{18}\text{O}$  is controlled to a large degree by SST. If there is any relation between SST and rainfall it is likely that the coralline  $\delta^{18}\text{O}$  would also mimic such a relation. To assess this we have compared the  $\delta^{18}\text{O}$  and  $\delta^{13}\text{C}$  of the Gulf of Kutch coral with the rainfall data.

Fig 3.12 shows the minima (corresponding to June) in  $\delta^{18}\text{O}$ ,  $\delta^{13}\text{C}$  and the total monsoon rainfall (approximately same as the annual rainfall) in Kutch for the period 1949-89 A.D. (India Meteorological Division's Records). Kutch and Saurashtra receive almost the entire amount of annual rainfall during the monsoon period (June to September). It can be seen from Fig 3.12 that there is in general negative correlation between the  $\delta^{18}\text{O}$  minima and rainfall. The relationship between the coral  $\delta^{18}\text{O}$  (minima) and rainfall is given by:

$$\delta^{18}\text{O} = -3.9 - 6.5 \times 10^{-4} R \quad (3.6)$$

where R represents rainfall in mm. The correlation coefficient (r) is  $-0.56$  ( $n=41$ ) significant at 0.01 level (P). As the numerical ranges of variation in  $\delta^{18}\text{O}$  ( $0.3\text{‰}$ ) and rainfall (1170 mm) are widely different, we can normalize each of these time series by subtracting the respective means and dividing by the respective standard deviations; this makes both the time series to have identical numerical ranges in variation. (This transform, known as Z transform in statistical literature, makes the mean and standard deviation of the time series to be zero and unity, respectively). Denoting the time series now by  $\delta^{18}\text{O}'$  and  $R'$ , we get a relationship (with the same correlation coefficient as earlier):

$$\delta^{18}\text{O}' = -0.51 R' \quad (3.7)$$

In order to produce a change of  $0.1\text{‰}$  (detection limit) in the coral  $\delta^{18}\text{O}$  rainfall has to

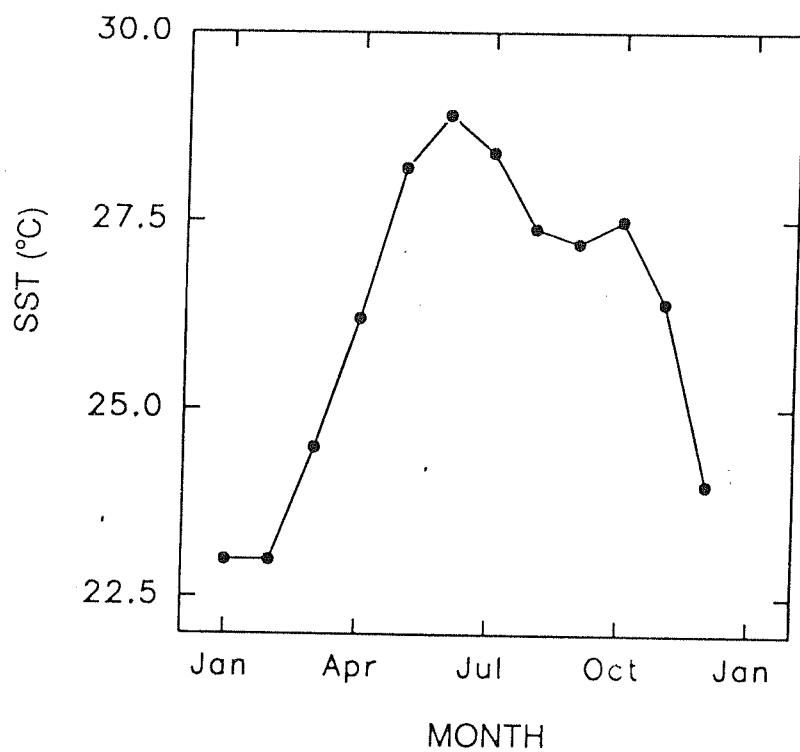


Fig 3.11 Monthly SST variations in the Gulf of Kutch (22.6°N, 69.5°E), near to the coral site. Data from Sadler *et al.* (1987).

change by ~150 mm. The magnitude of year to year variation in rainfall is ~340 mm (one standard deviation, which represents the interannual variability). This will cause a mean interannual change in the coral  $\delta^{18}\text{O}$  of a magnitude 0.22‰. Moreover, the difference in rainfall between two consecutive years can be as large as -700 to +950 mm, as seen from the rainfall record for the period 1949-89 A.D.; therefore the corresponding changes in the coral  $\delta^{18}\text{O}$  can be as large as +0.46 to -0.63‰. We have not been able to observe such large changes in the  $\delta^{18}\text{O}$  record. One possible explanation for this may be coarse resolution of sampling which averages out large changes. This coral has an average growth rate of ~4 mm/yr and a sample of ~1mm thickness corresponds to about 3 month's growth.

The long term changes (*e.g.* 7 to 8 year cyclicality) in the coral  $\delta^{18}\text{O}$ , (Fig 3.10a) may be caused by the long term changes in rainfall. For example the consistently higher than normal rainfall during the late 70's is reflected as a dip in the coral  $\delta^{18}\text{O}$  (Fig 3.12). In order to have a definitive explanation of the periodicity of 7 to 8 years, we need a time series measurement of the  $\delta^{18}\text{O}$  of sea water before and after the monsoon, which is lacking for this region.

The dotted lines in Fig 3.12 a,b and c are fourth order regression lines through the data representing the trends. We used the trend lines to generate points of  $\delta^{18}\text{O}$  and rainfall and found them to be correlated better:  $r = -0.8$  ( $n=41$ ). This shows that while the long term changes in the coral  $\delta^{18}\text{O}$  are related to rainfall, seasonal variations tend to introduce noise in the signal. In addition, the mean annual  $\delta^{18}\text{O}$  of the coral is also significantly correlated with monsoon rainfall over Kutch and Saurashtra ( $r = -0.48$ ,  $P < 0.01$ ) as well as the all India mean monsoon rainfall ( $r = -0.23$ ,  $P < 0.1$ ). This observation is consistent with the theory of Shukla (1975) and observations of Shukla & Mishra (1977) that the increase in SST (reduced coral  $\delta^{18}\text{O}$ ) in the Arabian Sea enhances the evaporation rate and hence the precipitation over India, especially in Gujarat. From the  $\delta^{18}\text{O}$  record we see that the mean difference in the  $\delta^{18}\text{O}$  in decadal time scale (~0.48‰) would correspond to a change of 2.4°C in SST. From this it appears that the GK<sub>h</sub> responds to long term changes in SST probably because of its shallow shelf characteristics. On the other hand the LDP region which is exchanging water with the open Arabian Sea freely, does not show such large long term trends in SST and therefore

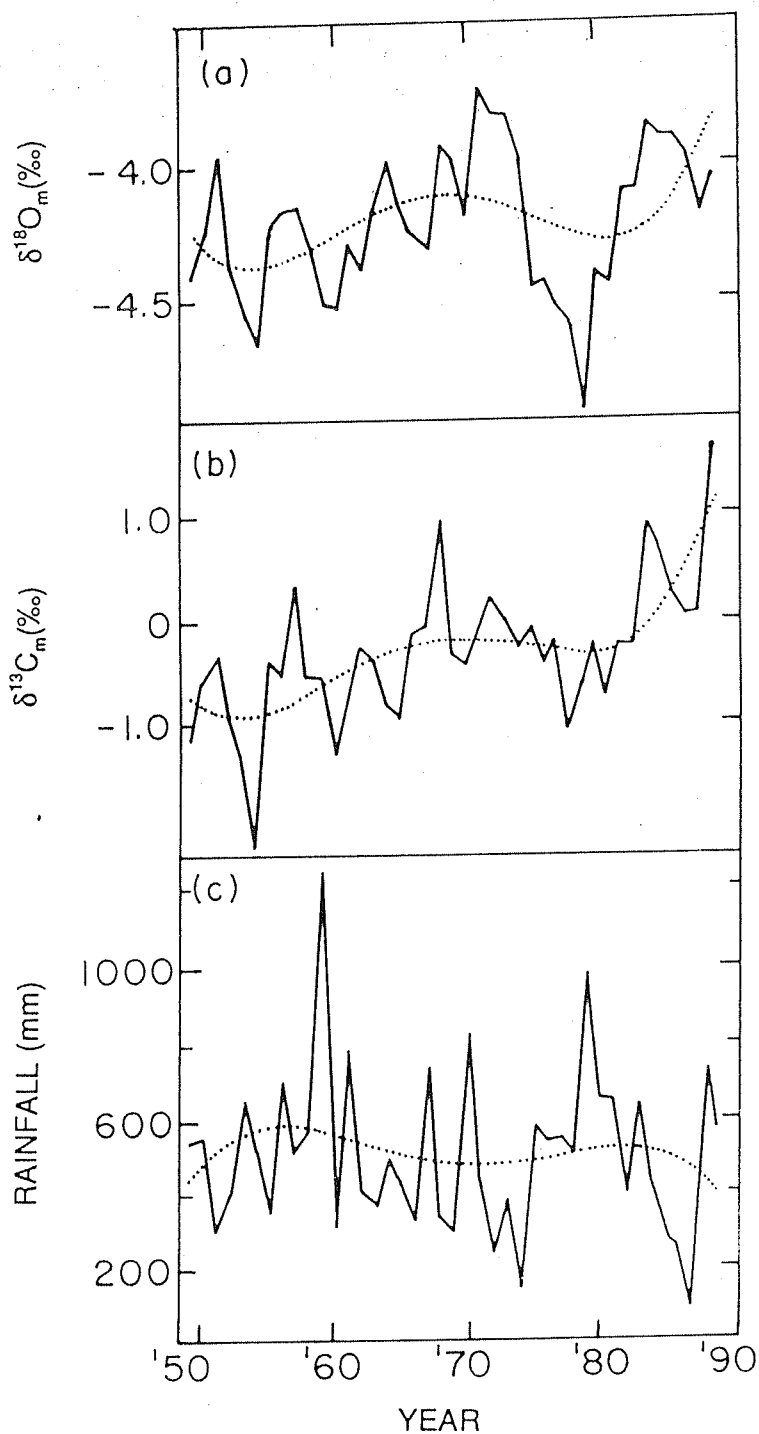


Fig 3.12  $\delta^{18}\text{O}$  minima (a),  $\delta^{13}\text{C}$  minima (b) of the coral *F. speciosa* from the Gulf of Kutch (22.6°N, 70°E). Lower panel (c) shows the interannual variability of monsoon rainfall in the Kutch and Saurashtra region. The dotted lines are fourth order polynomials fitted to the data and indicates the long term trends.

in  $\delta^{18}\text{O}$ . Hence in the case of LDP coral the  $\delta^{18}\text{O}$  is not correlated with monsoon rainfall.

The mean  $\delta^{13}\text{C}$  of the GK coral is  $\sim -0.1\text{‰}$ . Both KV-1 and KV-2 are depleted by about 0.6 and 1.7‰ respectively compared to GK coral. Comparison of the KV-2 data with GK coral is more meaningful as the GK and KV-2 corals had approximately similar life span. The causes for the difference in the  $\delta^{13}\text{C}$  between these two corals are (i) the species dependent fractionation, (ii) the northern Arabian sea, especially the coastal regions are biologically more productive compared to the central and south-eastern Arabian Sea (Qasim 1982) and the  $\delta^{13}\text{C}$  of  $\Sigma\text{CO}_2$  here are expected to be higher than that of the LDP region, and (iii) growth dependent fractionation. The mean growth rate of the GK coral is 4.3 mm/yr whereas that of the KV-2 is 15mm/yr. Since slower growth rate leads to isotopic values which are closer to equilibrium precipitation, the GK coral shows a higher  $\delta^{13}\text{C}$  compared to the KV-2 coral.

The  $\delta^{13}\text{C}$  values of the GK coral show a long term increase of about 2‰ during the 40 years of its growth, from  $\sim -1\text{‰}$  during its early stage of growth to the present day value of  $\sim 1\text{‰}$ . The mechanisms contributing to this long term trends is not well understood, growth-rate related  $^{13}\text{C}$  fractionation may be one of the contributors to this trend. In the earlier stage of growth the mean growth rate was higher ( $\sim 6$  mm/yr) whereas in the later stages the mean growth rate is between 3-4 mm/yr (Fig 3.2). This would contribute to enrichment of  $\delta^{13}\text{C}$  during the later stages.

The  $\delta^{13}\text{C}$  of GK coral shows a seasonal cycle, with a range of  $\sim 1\text{‰}$ . The minimum in  $\delta^{13}\text{C}$  occurs during Jun-Jul, approximately at the same time when the minimum in  $\delta^{18}\text{O}$  occurs. In fact  $\delta^{13}\text{C}$  and  $\delta^{18}\text{O}$  are significantly positively correlated ( $r=0.56$ ). The reason for minimum in  $\delta^{13}\text{C}$  during Jun-Jul is probably due to the reduced rate of photosynthesis during this time of the year compared to the pre SW monsoon (Feb-May) and post SW monsoon (Oct-Jan) seasons.

Qasim (1982) has observed that in general the phytoplankton productivity is high in the coastal regions of the northern Arabian Sea. The average surface productivity for this region is 18.86, 7, and 25.12  $\text{gC m}^{-2} \text{ day}^{-1}$  for the premonsoon, monsoon and NE monsoon period respectively (Table 8 of Qasim 1982). The lowest biological productivity during SW monsoon period, probably leads to a depletion in the coral  $\delta^{13}\text{C}$  during this period. Thus the seasonal changes in  $\delta^{13}\text{C}$  in GK coral hold potential to reconstruct past

changes in surface productivity in this region. Towards this, it is necessary to establish quantitative relation between  $\delta^{13}\text{C}$  and biological productivity of this region.

### III.2.c Effect of sampling on the retrieval of climatic signal

The retrieval of climatic information from the isotopic profiles of coral depends largely on the sampling resolution. Early studies of  $\delta^{18}\text{O}$  records as an SST index were not much successful as observed by Goreau (1977) and Emiliani *et al.* (1978). This apparent drawback of isotopic study was attributed to the (sampling) resolution problem by Fairbanks & Dodge (1979). They showed that with the analyses of as much as 12 samples per annual band they were able to recover the full seasonal amplitude of SST from the  $\delta^{18}\text{O}$  measurements. Lesser the number of samples, more are the chances of missing the maxima and minima in the  $\delta^{18}\text{O}$ . Moreover, in the case of very narrow annual bands, it is difficult to get more than a few samples per band for isotopic analyses. Further, a sample taken by filing or drilling has a finite width (say, 1 mm), which, in the case of a narrow annual band can average the SST signal for a period of as much as 6 months. Thus depending on the sample growth rate (*i.e.* the skeletal extension rate) and the sampling interval, the measured seasonal  $\delta^{18}\text{O}$  amplitude can be greatly reduced compared to its actual value. In order to assess the magnitude of this reduction, we performed a simple computer simulation.

Since the seasonal  $\delta^{18}\text{O}$  profile very closely resembles sinusoidal variations, we generated 20 cycles of a sine wave of unit amplitude and a (spatial) period of 10 mm. This would correspond to a  $\delta^{18}\text{O}$  time series of a coral having a 20 year growth with an annual growth increment (g) of 10mm. Implicit in our use of unit amplitude throughout the 20 cycles is that the seasonality in climate forcing did not change during this period (*i.e.* interannual variability is zero). Also, the constant period represents a constant annual growth increment throughout the 20 years of the coral's life span. In the model we sample this time series for different constant sampling intervals  $\Delta x$  (1, 2, 3, 4 and 5 mm) and consider the sample as a point). The maxima and minima in this sampled time series are identified (Fig 3.13). The sum of the magnitudes of the maxima and minima in each

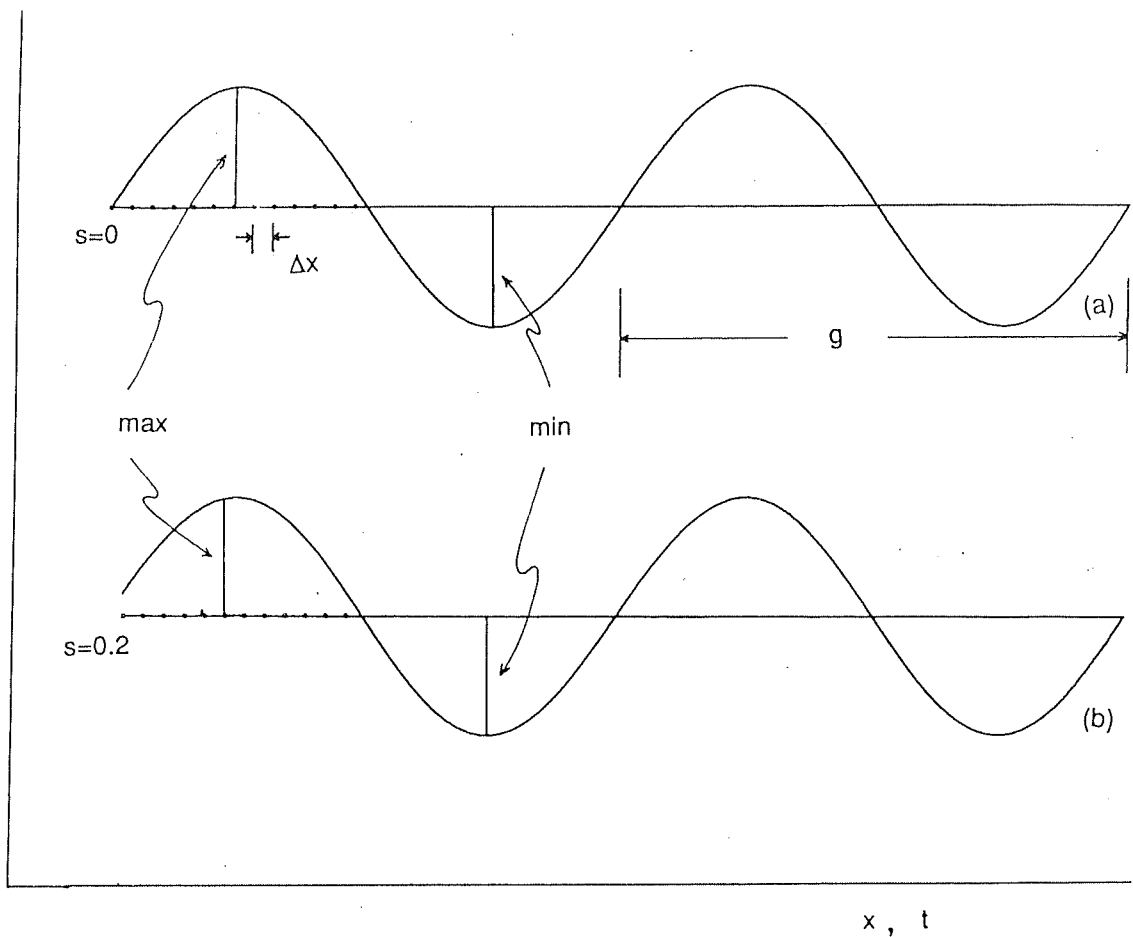


Fig 3.13 Sampling of coral for oxygen isotope study. The seasonal oxygen cycles mimic sine curve.  $s$  is the starting (or phase) of the sampling. (a)  $s=0$  i.e. phase=0 and (b)  $s=0.2$  or phase=7.2°.  $\Delta x$  is the sampling interval and  $g$  stands for annual growth increment.

cycle is divided by 2 to obtain the mean amplitude for each cycle. Then the average of these mean amplitudes over the 20 cycles is calculated and is termed as the 'retrieved amplitude'. We establish a functional relationship between  $\Delta x/g$  (reciprocal of the number of samples per band) and  $A$  (the ratio of the retrieved amplitude to the actual amplitude). Obviously,  $A$  has to be  $\leq 1$ , because the sampling process tends to reduce the signal and at best can reproduce the actual amplitude. The ratio  $A$  gives an estimate of the reduction in the amplitude resulting from variation in sampling interval for a constant annual growth increment. In practice when the coral is collected, the last year's annual cycle may not be complete. So the sampling need not commence at the phase=0 of the sine wave. Therefore the exercise was repeated (i) for different starting values of the distance of the first sampling point  $s$ , (*i.e.* different phases) and (ii) for different  $g$ 's (periods of 5 and 10 mm).

Fig 3.14 shows a plot of  $A$  versus  $\Delta x/g$  when  $g=5\text{mm}$ . Circles denote the values of  $A$  for the sampling case when  $s=0$ , *i.e.* the sampling was started with phase zero and inverted triangles and squares denote cases when sampling was started at phases of  $14.4^\circ$  and  $36^\circ$  respectively. (This was achieved by starting the sampling at distance of 0.2 and 0.5 mm respectively from the origin).

It is obvious that when  $\Delta x/g=0$  (*i.e.* infinitely close sampling) we retrieve the full amplitude (*i.e.*  $A=1$ ) and when  $\Delta x/g=0.5$  or 1 (*i.e.* the sampling interval is half or full period) the retrieved amplitude should be zero, if the sampling starts from origin (*i.e.* zero phase). This is seen in Fig 3.14:  $A=1$  at  $\Delta x/g=0$  and  $A=0$  at  $\Delta x/g=0.5$  and 1 (for  $g=5\text{mm}$ ). For the rest of the values of  $\Delta x/g$  the values of  $A$  lie between 0 and 1. As  $\Delta x/g$  increases, there is a general reduction in  $A$ . For example, when  $\Delta x/g=0.2$ , 5% of the amplitude is lost due to sampling and when  $\Delta x/g=0.8$ , 60% of the amplitude is lost. For the other cases when the sampling was started with non-zero phase, the general trend is the same. However for  $\Delta x/g=0.5$ , we do get  $A$  values above zero. This is because the sample points do not lie on the zeros of the sine curve, but slightly off the zeros providing some "amplitude". Further as the phase increases from 0 to  $36^\circ$ , the scatter in  $A$  increases around  $\Delta x/g=0.5$  and 1. Higher the starting phase, higher is the retrieved amplitude (in these two points). Similar results are shown in Fig 3.15 for the case  $g=10\text{ mm}$ . As before here also it is seen that  $A$  tends to zero as  $\Delta x/g$  equals 0.5 or 1. Fig 3.16 shows a plot of  $A$  versus  $g$  for different  $\Delta x/g$  values. It is seen that for a starting value zero (*i.e.* phase=0)  $A$  is only



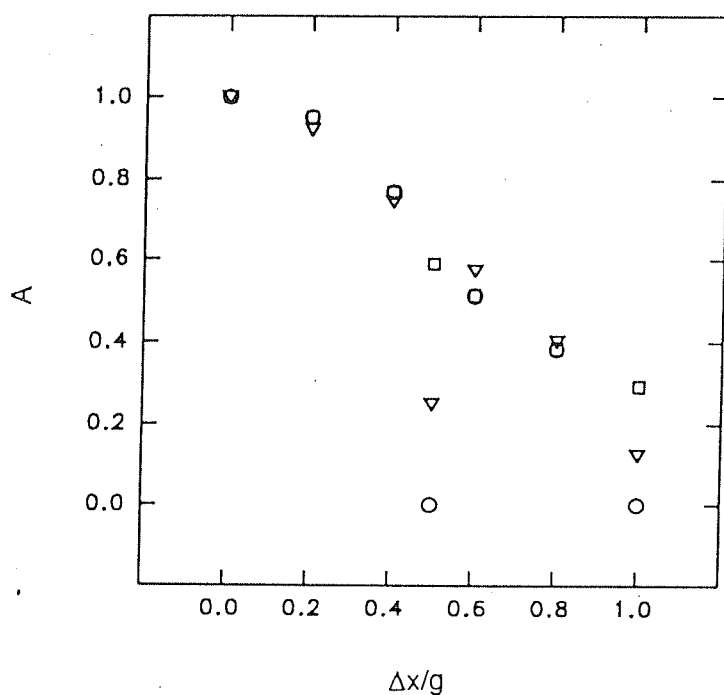


Fig 3.14 Result of the simulation study. Variation in the ratio of the retrieved amplitude to the true seasonal amplitude as a function of  $\Delta x/g$  (the ratio of sampling interval to constant annual increment=5 mm). Different symbols indicate different sample starting(s). Open circle:  $s=0$ ; inverted triangle:  $s=0.2$ ; square:  $s=0.5$ . For  $\Delta x/g=1$  (i.e. sampling interval same as annual growth) and  $s=0$ ,  $A$  becomes equal to 0.  $A$  increases from zero with increasing  $s$ .

a function of  $\Delta x/g$  and not  $g$  itself. However  $A$  shows a small variation with  $\Delta x/g$  when sampling is done at non zero phases. If a 10% reduction in amplitude is accepted, then  $\Delta x/g$  must be at least about 0.3 *i.e.* approximately a minimum of 4 samples per annual band.

In another simulation, we assumed that while year to year climatic changes are absent, the annual growth increment varies in a random fashion between 2.5 to 5 mm (similar to the growth rate variation in the Kutch coral; growth rate varies due to changes in environmental parameters *e.g.* supply of nutrients). Since the sine function has a constant (spatial) period, a variable growth cannot be represented by a single function. In order to circumvent this problem we generated single cycle of 20 sine functions of unit amplitude but with varying period 2.5 to 5 mm. Then we made the composite function by putting the sine functions in the same time sequence as their growth rates in the case of GK coral. The end points of the cycles match because the value of the sine function in a full cycle is zero at either ends ( $0, 2\pi$ ). This curve is then sampled to obtain  $A$  as before for different  $\Delta x$  (1, 2, 3 and 4 mm) and  $s$  ( $0^\circ, 18^\circ, 45^\circ$ ). In this case  $\Delta x/g$  is not a constant as  $g$  varies with time. Therefore we plot  $A$  as a function of  $\Delta x/\bar{g}$ , where  $\bar{g}$  is the average of all  $g$ 's ( $\sim 4$  mm). Fig 3.17 shows the composite plot. We see similar trends as in the earlier case of constant growth increment. Also in general the reduction in amplitude is more or less the same as in the previous case. As shown earlier that  $A$  is independent of  $g$  but only a function of  $\Delta x/g$  (for phase=0). In this case for  $\Delta x/g = 0.2$  we get  $A = 0.92 \pm 0.068$  which is the same within the uncertainty to that of  $A(0.951)$  for  $\Delta x/g = 0.2$  when  $g$  is constant. However direct comparison is slightly difficult because for the cases  $\Delta x/g = 0.5$  and 1 we get significantly higher values of  $A$  even for the case when the sampling starts at zero phase. This is understandable because the annual increment is varying and therefore even for the case  $s=0$ , some "amplitude" will be retrieved for  $\Delta x/g = 0.5$  and  $\Delta x/g = 1.0$ .

In addition to the sampling interval, another factor which reduces the retrieved amplitude is the averaging of the signal due to finite sample thickness. We considered the effect of sampling thickness on the amplitude in the following way: we sampled the data generated for the variable growth rate at different intervals, but now by averaging 1 mm around each sample. For this case the reduction in amplitude was found to be 40% for

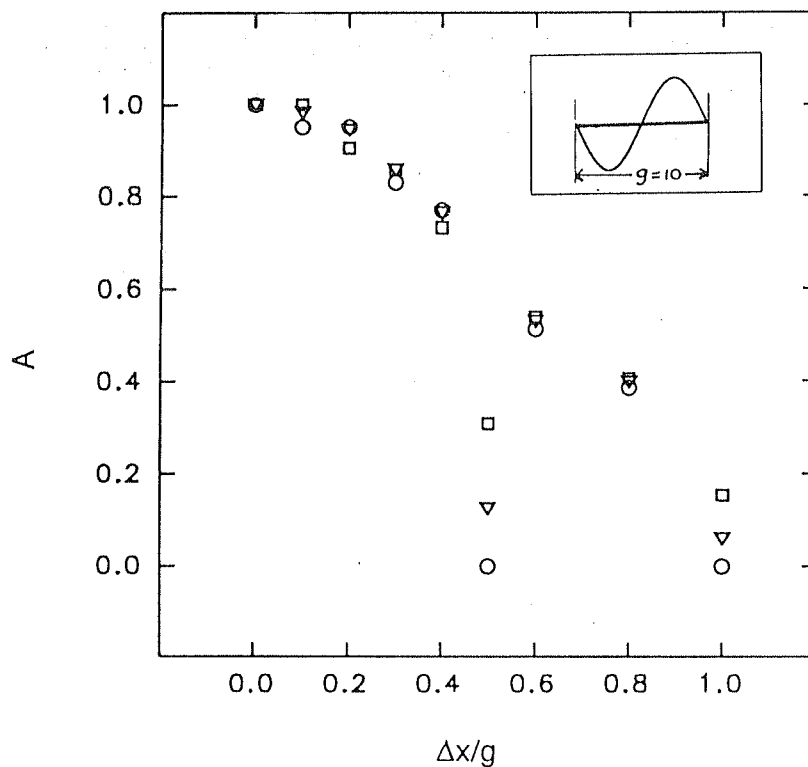


Fig 3.15 Results of the simulation study. Variation in the ratio of the retrieved amplitude to the true seasonal amplitude as a function of  $\Delta x/g$  for the constant annual increment  $g=10$  mm. Symbols indicate different starting of the sampling(s). open circle:  $s=0$ ; inverted triangle  $s=0.2$ ; square:  $s=0.5$ . As shown in the inset that at  $\Delta x=5$  and  $10$ ,  $A$  is zero (for  $s=0$ ), but with increasing  $s$ ,  $A$  increases at these two points.

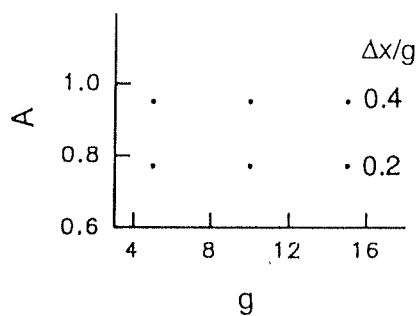


Fig 3.16 Figure shows that the retrieval of amplitude is independent of growth (for zero starting of sampling) but depends on the sampling frequency. Parameters are as described before.

a  $\Delta x/\bar{g}$  value of 0.38 very similar to that in the GK coral. Using this we can compute the approximate magnitude of the actual seasonal  $\delta^{18}\text{O}$  amplitude in the coral studied by us. The observed amplitude (0.3‰) can be considered as 60% of the expected amplitude, therefore the original amplitude can be deduced to be  $0.5 \pm 0.3\text{‰}$ . This is still about a factor of two less than the calculated amplitude of  $1.1 \pm 0.2\text{‰}$  based on SST and the seawater  $\delta^{18}\text{O}$  variations. Considering that there is an uncertainty of 0.2‰ in the measurements (as in case of the  $\delta^{18}\text{O}_{\text{water}}$ ) and hence in the estimate, it may be argued that the expected and observed  $\delta^{18}\text{O}$  amplitudes are comparable within  $\pm 2\sigma$  uncertainties. However, they could be genuinely different for reasons other than sampling. These include (i) The model does not consider year to year changes in  $\delta^{18}\text{O}$  of sea water that may be caused by rainfall (or minor discharges from seasonal rivers), (ii) The calculated coral  $\delta^{18}\text{O}$  amplitude may be an over estimate as (a) the temperature coefficient for our sample may be different from the value we have used, the value reported by Weber & Woodhead (1972); which is the only available data in the literature for the genus *Favia*. However, there may be variations from species to species and from place to place. For instance McConnaughey (1989) reported temperature coefficients deviated by about 30% i.e. 0.205 and 0.15 for *Pavona clavus* samples, one from Champion Island and the other from Punta Pitt, separated by 100 km; (b) We do not have the SST data in the exact location of the coral. Notwithstanding the above possible uncertainties, we get a reasonably good agreement between the calculated and observed  $\delta^{18}\text{O}$  amplitudes.

Our results show that the coralline  $\delta^{18}\text{O}$  and monsoon rainfall are significantly correlated, which can be used for qualitative reconstruction of historical rainfall records and also help understand the role of the Arabian SST in determining the interannual variability of monsoon rainfall over western India. Further higher resolution studies on the Gulf of Kutch corals spanning longer time durations will be useful for such a goal. It is necessary that a very close sampling be done for the  $\delta^{18}\text{O}$  analysis in order to retrieve the full seasonal cycle. The  $\delta^{13}\text{C}$  variations can be a potential indicator of the past surface ocean productivity in this region. In contrast to *Porites* of Lakshadweep the growth related fractionation is less. We have developed a simple model using which it is possible to estimate the reduction in the retrieval of seasonal amplitudes resulting from the averaging and sampling effects.

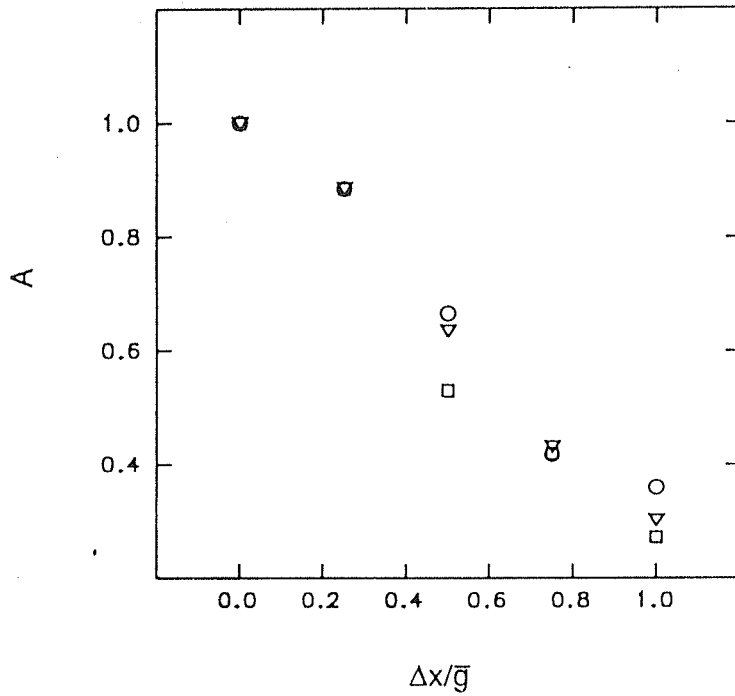


Fig 3.17 Plot of the variation in the ratio of the retrieved amplitude to the true seasonal amplitude as a function of  $\Delta x / \bar{g}$  for the variable annual increment ( $g$ ). Since  $g$  is varying, it has been replaced by average  $g$  i.e.  $\bar{g}$ . Unlike the case of constant growth here  $A$  does not become zero at  $\Delta x = \bar{g}/2$  or at  $\bar{g}$  because of variable nature of  $g$ . However at these points  $A$  shows a wide scatter for different starting values as was observed in case of constant growth.

### III.2.d Stanley Reef coral

A coral *Porites lutea* was collected in December 1988 from the Stanley Reef (19°15'S, 148°07'E), belonging to the Great Barrier Reef, Australia. The coral was about 20 years old and had an average bandwidth of  $11.7 \pm 0.3$  mm as determined from the X-radiographic analysis. In order to determine the extent of intraband isotopic and density variability and their effects on respective records we have analyzed the  $\delta^{18}\text{O}$ ,  $\delta^{13}\text{C}$  and density time series in two tracks of this coral.

It is believed that the coralline isotopic records are influenced by the coral geometry and growth rate. In order to minimize the growth related fractionation it is customary to sample along the axis of maximum growth. However due to various constraints sometimes it is difficult to comply with these requirements. In such cases it is important to know the magnitude of intraband isotopic variability and the factors controlling such variations, *i.e.* climate (external forcing) and non-uniform growth in different directions (internal forcing).

Secondly, the reason for the density band formation in corals has not been clearly understood. For example, Highsmith (1979) and Weber *et al.* (1975) concluded that the density banding is mainly controlled by SST. Others (Buddemeier, 1974; Wellington & Glynn, 1983) have attributed the seasonal variation in growth rate to be the cause of the density banding. But then, growth rate itself may be controlled by the SST. It should be possible to decide between these two alternatives by measuring the stable isotope ratios of oxygen ( $\delta^{18}\text{O}$ ) and carbon ( $\delta^{13}\text{C}$ ) along with the density measurements in the same coral. If the density banding is synchronized with the water temperature, there should be a significant correlation between density and oxygen isotope variations as the latter is related to temperature. On the other hand if the variable growth rate is responsible for the density banding, the density and carbon isotopic variations should be significantly correlated. This is because faster growth rates imply rapid zooxanthallar activity (photosynthesis) which enriches the  $^{13}\text{C}$  in the dissolved inorganic carbon in the neighbourhood of the coral, by removing preferentially the more of the lighter isotope of carbon ( $^{12}\text{C}$ ). Thus the  $\text{CaCO}_3$  secreted by the coral skeleton is enriched in the  $^{13}\text{C}/^{12}\text{C}$

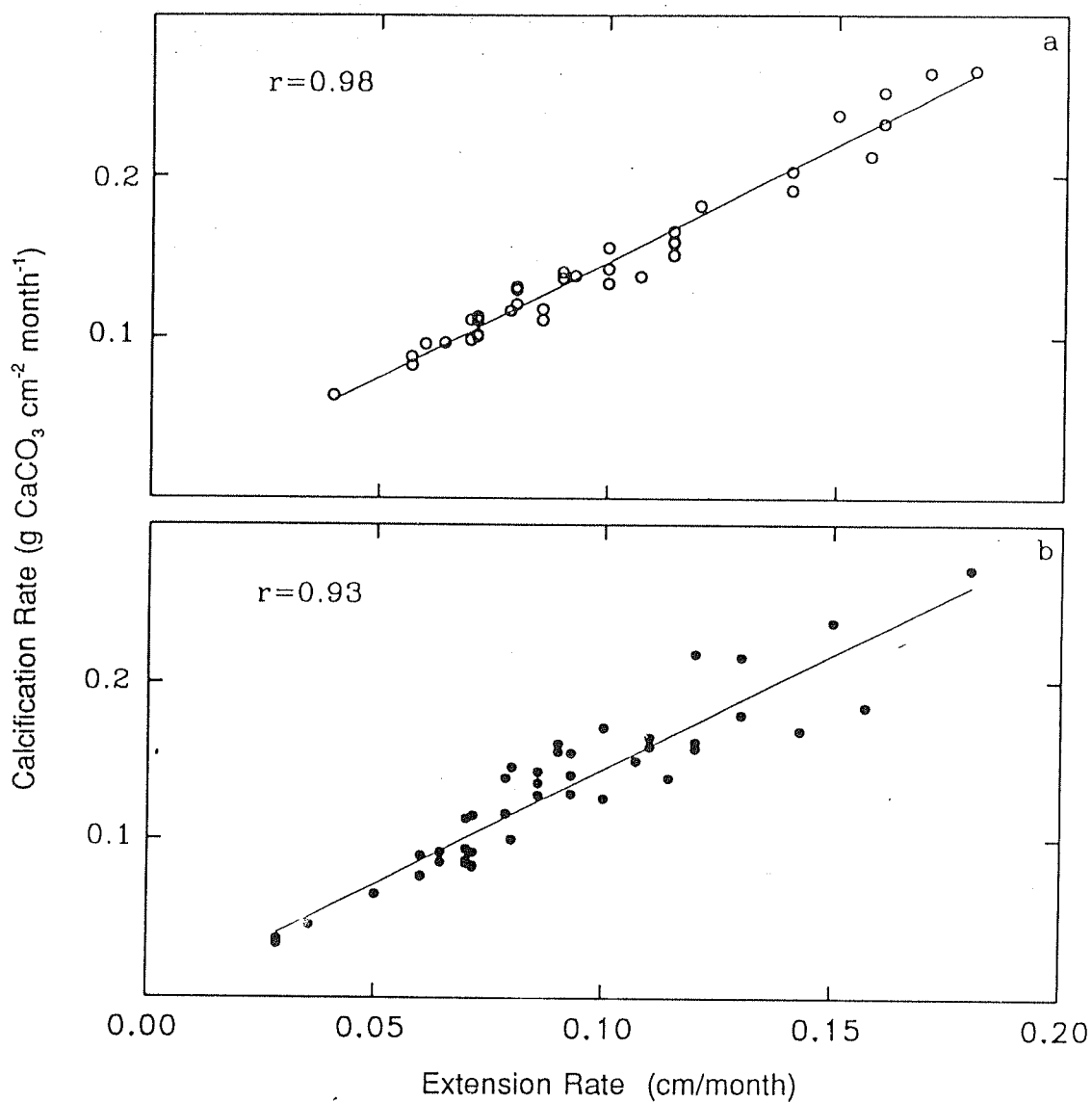


Fig 3.18 Relationship between calcification rate and extension rate of two tracks of coral *P. lutea* collected from the Stanley Reef, east coast of Australia. (a) Track-1, (b) Track-2. The linear trend is clearly evident.

ratio. Again the  $\delta^{13}\text{C}$  is also controlled by variability in growth rate *i.e.* more the growth rate more will be the  $\delta^{13}\text{C}$  fractionation. Clearly the rate of photosynthesis and the rate of growth oppose each other in determining the coral  $\delta^{13}\text{C}$ . The ultimate ratio would be determined by the variable contributions of these two parameters. Precise estimation of the fractionation factors between aragonite-water-bicarbonate system for these two cases would enable to determine their relative contribution which is beyond the scope of this work.

The X-radiography and sampling for stable isotopic measurements were followed as described in previous chapter. The density was measured by J M Lough at the Australian Institute of Marine Science following the procedure described by Barnes & Lough (1989). One of the tracks(Tr-1) was  $\sim 10^\circ$  off the central growth axis, and the other (Tr-2) was away from the growth axis by about  $20^\circ$ . For stable isotopic measurements the sampling was performed along the two tracks approximately at high and low density points. Tr-1 and Tr-2 had 3-4 and 2-3 sampling points per annual band respectively.

The use of growth rate in coral literature has been replaced by appropriate terms like extension rate or calcification rate since sometime they do not show linear relationship. However in our case we use the term growth rate representing both extension rate and calcification rate since they show a strong correlation. Fig 3.18 shows this relation for the two tracks, Track-1(a) and Track-2 (b).

Next we show that the  $\delta^{18}\text{O}$  profiles preserve the environmental parameters. Fig 3.19 shows the covariations between  $\delta^{18}\text{O}$  and SST for Tr-1. The linear regression between these two parameters yield the following equations:

$$\delta^{18}\text{O} = (0.312 \pm 0.44) - (0.21 \pm 0.018) \text{ SST} \quad \text{for Tr-1} \quad (3.8)$$

$r = -0.855$ ,  $n = 51$ ,  $p = 0.1$ , and

$$\delta^{18}\text{O} = (2.20 \pm 1.02) - (0.28 \pm 0.06) \text{ SST} \quad \text{for Tr-2} \quad (3.9)$$

$r = -0.64$ ,  $n = 35$ ,  $p = 0.1$ .

The temperature coefficient ( $0.2 \pm 0.018$ ) in Tr-1 is equal to that of the original palaeotemperature equation of Epstein *et al.* (1953). The temperature coefficient in Tr-2 ( $0.28 \pm 0.06$ ) shows a little more scatter; however it also agrees with the equation of Epstein *et al.* (1953) within  $\pm 1\sigma$  uncertainty. The mean seasonal amplitude in SST in this region is  $\sim 5^\circ\text{C}$ , whereas the observed SST variations from coralline the  $\delta^{18}\text{O}$  is  $3.5 \pm 1^\circ\text{C}$ . In extreme cases they agree within  $\pm 1\sigma$  uncertainties. However a better agreement would



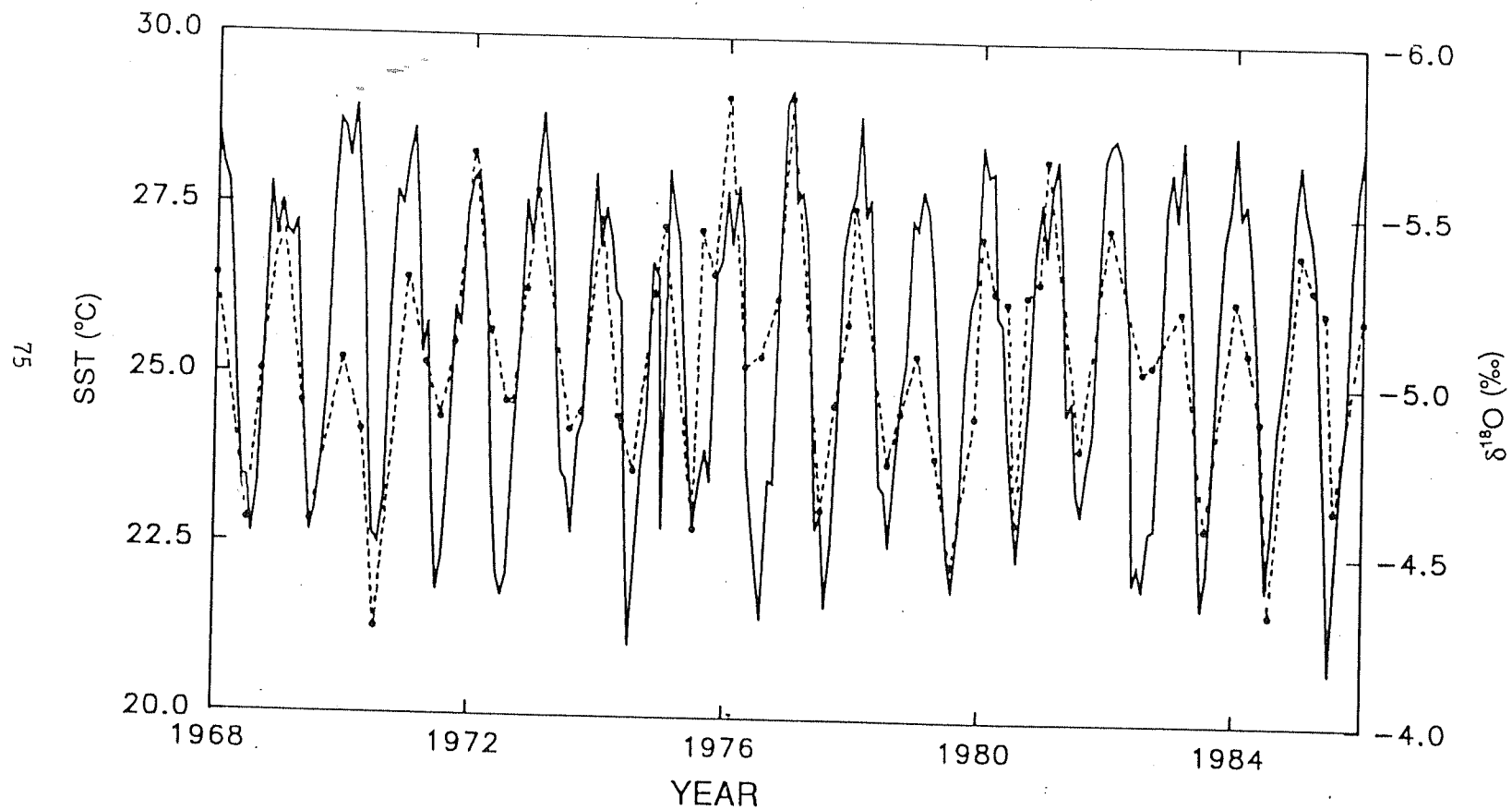


Fig 3.19 Covariation of SST and  $\delta^{18}\text{O}$  of *Porites lutea* from the Stanley Reef, Australia. solid line: SST; dotted line:  $\delta^{18}\text{O}$

have been possible with higher sampling resolution. Using the results of simulation presented in the previous section III.2.c we observe that for a ratio of  $\Delta x/g = 0.27$  (typical for Tr-1) the  $\delta^{18}\text{O}$  amplitude can reduce by 22%. When corrected for this reduction, the  $\delta^{18}\text{O}$  amplitude translated to SST variations would yield a value of  $4.35^\circ\text{C}$  consistent (within  $\pm 1\sigma$  errors) with the actual SST variations in this region. Considering the limitations of the model, as already discussed, we can expect this coral as a reliable SST recorder.

The  $\delta^{18}\text{O}$  also shows a linear negative correlation with rainfall of Queensland coast. Regression analyses of this data yield the following Eqns:

$$\delta^{18}\text{O} = -4.65 - 0.002 R \quad \text{for Tr-1} \quad (3.10)$$

( $r = -0.56$ ,  $n=60$ ,  $p=0.1$ ) and

$$\delta^{18}\text{O} = -4.62 - 0.002 R \quad \text{for Tr-2} \quad (3.11)$$

( $r = -0.36$ ,  $n=44$ ,  $p=0.1$ )

where  $R$  is the monthly rainfall in mm. In this we also see that Tr-1 is better correlated with rainfall than Tr-2. Our results are consistent with that of Aharon(1991) who shows that  $\delta^{18}\text{O}$  in *Porites australiensis* from the Palm island (near to the Stanley Reef) is negatively correlated to the local precipitation. On the other hand carbon isotopic variations in this coral seem to be affected by the cloudiness; as was observed in corals from the Lakshadweep and the Gulf of Kutch. During Jan-Feb, the months of maximum cloud (Lough 1993) in the Queensland coast reduces the available light and hence the photosynthesis rate. This results in a reduction of  $\delta^{13}\text{C}$  in coral  $\text{CaCO}_3$ . On a longer time scale, the  $\delta^{13}\text{C}$  values show a decreasing trend. A factor contributing to this decreasing trend in  $\delta^{13}\text{C}$  with time (Fig 3.21) seems to be related to the growth rate dependent fractionation; as was inferred for  $\delta^{13}\text{C}$  data of the Kavaratti coral, KV-2. The coral shows a significant variability in its growth rate, 6-16mm/yr in Tr-1 and 10-16mm/yr in TR-2 (Fig 3.20). The decreasing trend in  $\delta^{13}\text{C}$  in either of the track also explains that higher growth rate cause more fractionation in  $\delta^{13}\text{C}$ . Since the two tracks are close to each other, the variations in growth rate are expected to be the same which is evident from the near symmetric behaviour of the Fig 3.20. Small deviations from the symmetry is partly due to human error arising from the band thickness measurement from the X-ray picture, and partly due to the actual variations in growth rate in two tracks. The Fig 3.21 shows the

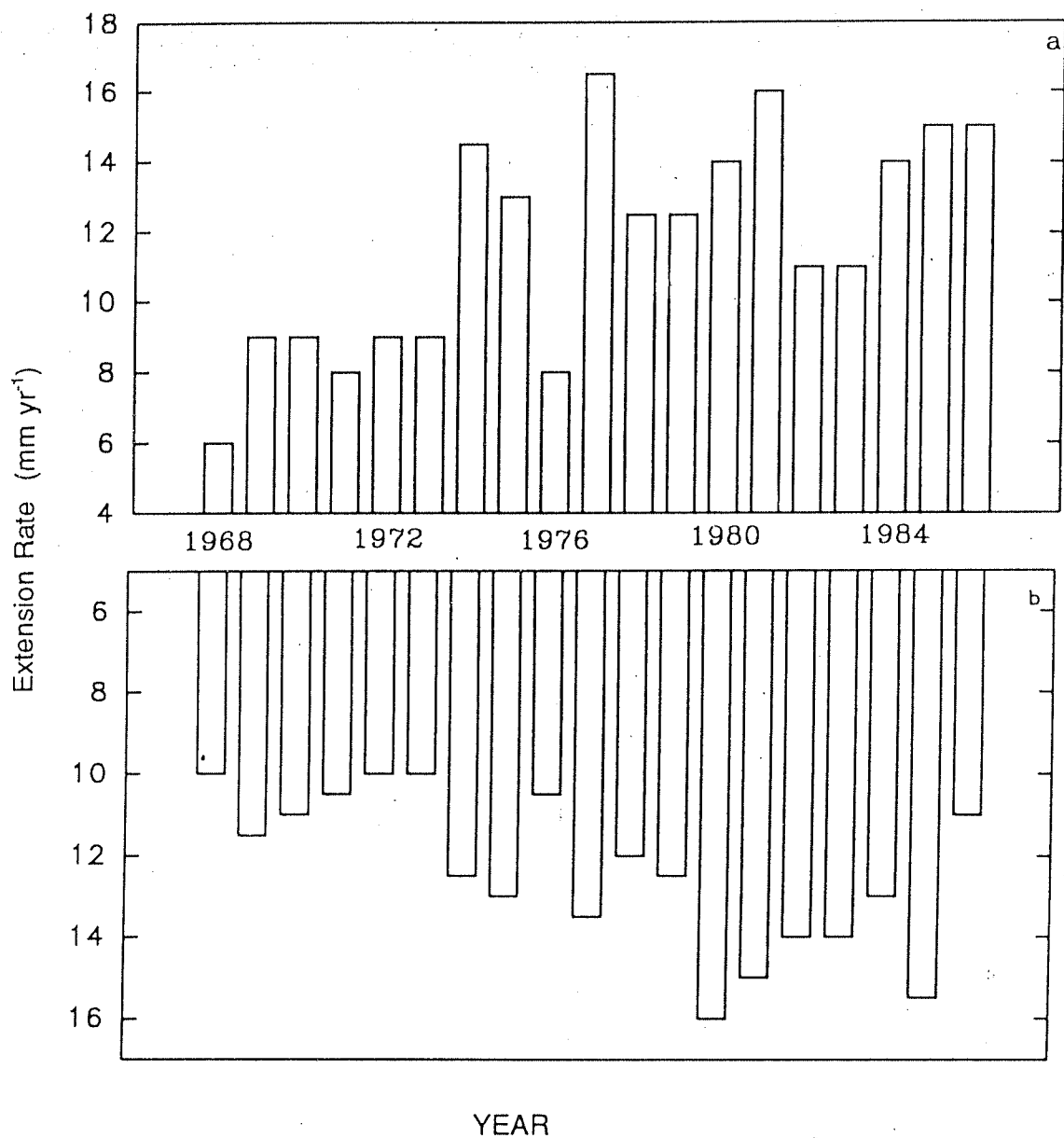


Fig 3.20 Growth rate variability in Track-1 and Track-2 of *P. lutea* from the Stanley Reef, Australia. (a) Track-1, (b) Track-2.

$\delta^{18}\text{O}$ ,  $\delta^{13}\text{C}$  and density variations in Tr-1. And those of Tr-2 are presented in Fig 3.22.[Table III.8 in Appendix A].

The mean  $\delta^{18}\text{O}$  of Tr-1 (no. of analysis  $n=67$ ) is  $-5.07 \pm 0.35\text{‰}$  and that of the Tr-2 ( $n=54$ ) is  $-4.97 \pm 0.39\text{‰}$ . Similarly the mean  $\delta^{13}\text{C}$  values are  $0.95 \pm 0.38\text{‰}$  (Tr-1) and  $-0.83 \pm 0.39\text{‰}$  (Tr-2). The mean densities for the two tracks are  $1.47 \pm 0.11$  and  $1.42 \pm 0.21$  respectively. Within the experimental uncertainties they are in good agreement. The variances in both the isotope ratios in both the tracks are remarkably similar. The smooth lines show the trends in various profiles obtained by fitting the fourth order polynomial. These exhibit the long term trends in the respective time profiles and also represent their resemblances.

Following a procedure of analysis of variance developed for tree rings as outlined by Fritts (1976), we calculate the common variances in the  $\delta^{18}\text{O}$ ,  $\delta^{13}\text{C}$  and density between the two tracks to be 67%, 54% and 68% respectively. This suggests that the intraband isotope variability introduces about 40% noise in the signal. Part of this "noise" could be an experimental artifact. That is, we have assumed that the pair of samples we analyzed from the same annual bands, along the two tracks were precipitated during the same time. In practice it is difficult to confirm this assumption, and errors could be introduced if the samples were precipitated a few weeks apart. This problem will be accentuated when samples are taken from narrow bands and when the samples represent climatic transition zones like winter to summer. Secondly, there could be genuine differences in the isotopic ratios as demonstrated by McConnaughey (1989), who showed progressive enrichment in  $\delta^{13}\text{C}$  of the portion of the coral growing at a lower rate due to the deficiency of sunlight.

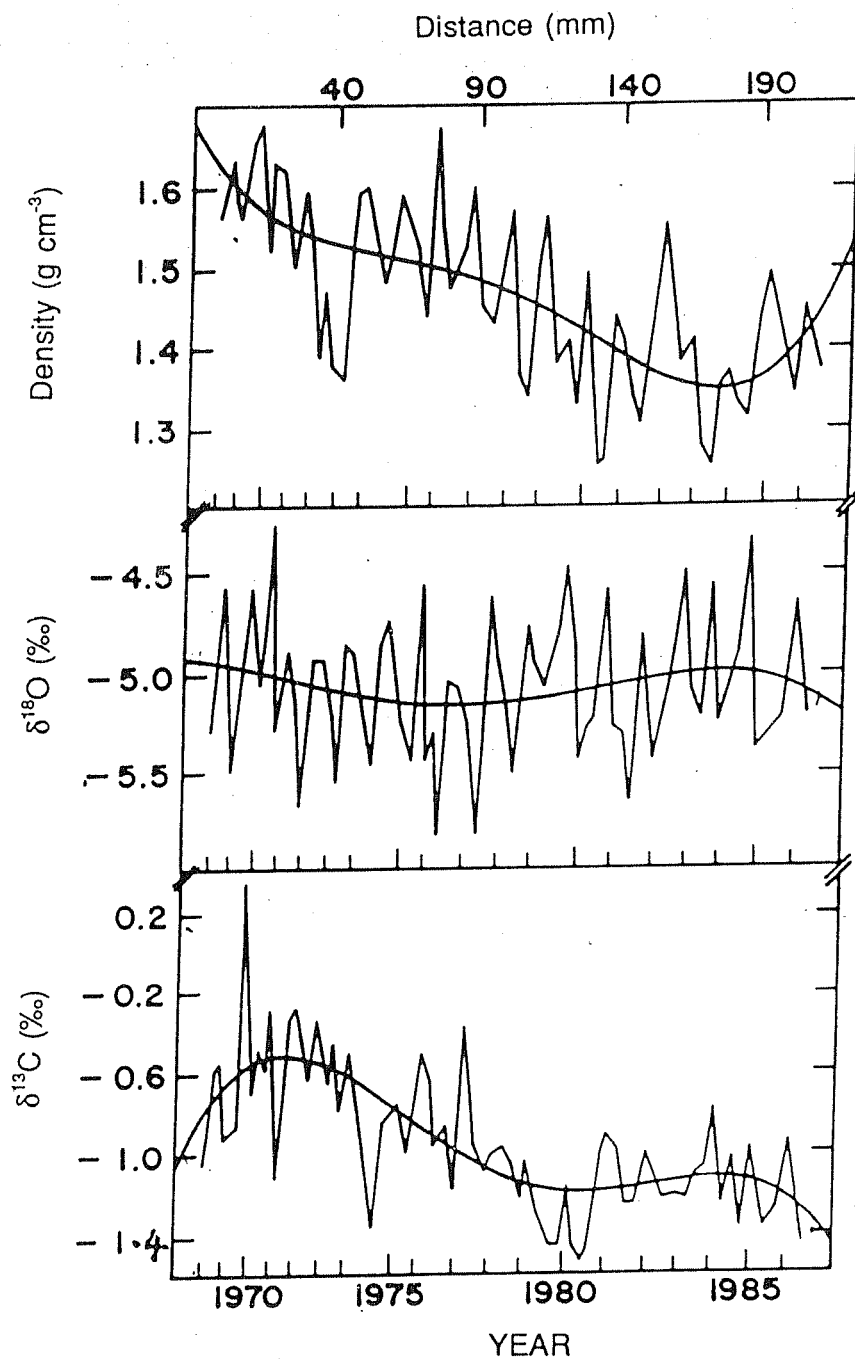


Fig 3.21 Density,  $\delta^{18}\text{O}$  and  $\delta^{13}\text{C}$  variations along Track-1 of coral *P. lutea* from Stanley Reef, Australia. Smooth lines indicate long term trends.

Table III.9 Correlation among the stable isotopes and the density variations.

	Linear correlation coefficient	
	actual data	detrended data
$\delta^{18}\text{O}$ & Density		
Track-1	0.23	0.29
Track-2	0.36	0.18
$\delta^{13}\text{C}$ & Density		
Track-1	0.56	0.20
Track-2	0.54	0.17
$\delta^{18}\text{O}$ & $\delta^{13}\text{C}$		
Track-1	0.02	0.04
Track-2	0.28	0.31

Table III.9 shows the linear correlation coefficients between  $\delta^{18}\text{O}$  & density,  $\delta^{13}\text{C}$  & density,  $\delta^{18}\text{O}$  &  $\delta^{13}\text{C}$  for the two tracks. There are long term trends in the records as shown by smooth lines in Figs 3.21, 3.22. The data have been detrended and the linear correlation coefficients are calculated for the detrended data. There is no significant correlation between  $\delta^{18}\text{O}$  and density in either track, before or after detrending (Table III.9), suggesting that the density band variations are not controlled by SST variations. There is a significant correlation between  $\delta^{13}\text{C}$  and density in each track before the data are detrended. This correlation becomes insignificant when the data are detrended. This has an important implication. As discussed earlier the decreasing trend in  $\delta^{13}\text{C}$  is due to growth rate related fractionation. Hence if density correlates with  $\delta^{13}\text{C}$  but not with  $\delta^{18}\text{O}$  it implies that the density band formation takes place due to the changes in the growth rate rather than SST. The decreasing trend in  $\delta^{13}\text{C}$  is due to the variable growth rate as discussed. Hence detrended profile effectively shows the carbon isotopic variations due to an external factor, like photosynthesis which is governed by availability of sunlight. The lack of a significant correlation between density and  $\delta^{13}\text{C}$  (after detrending) probably implies that density band formation is more influenced by endogenic rather than exogenic factors.

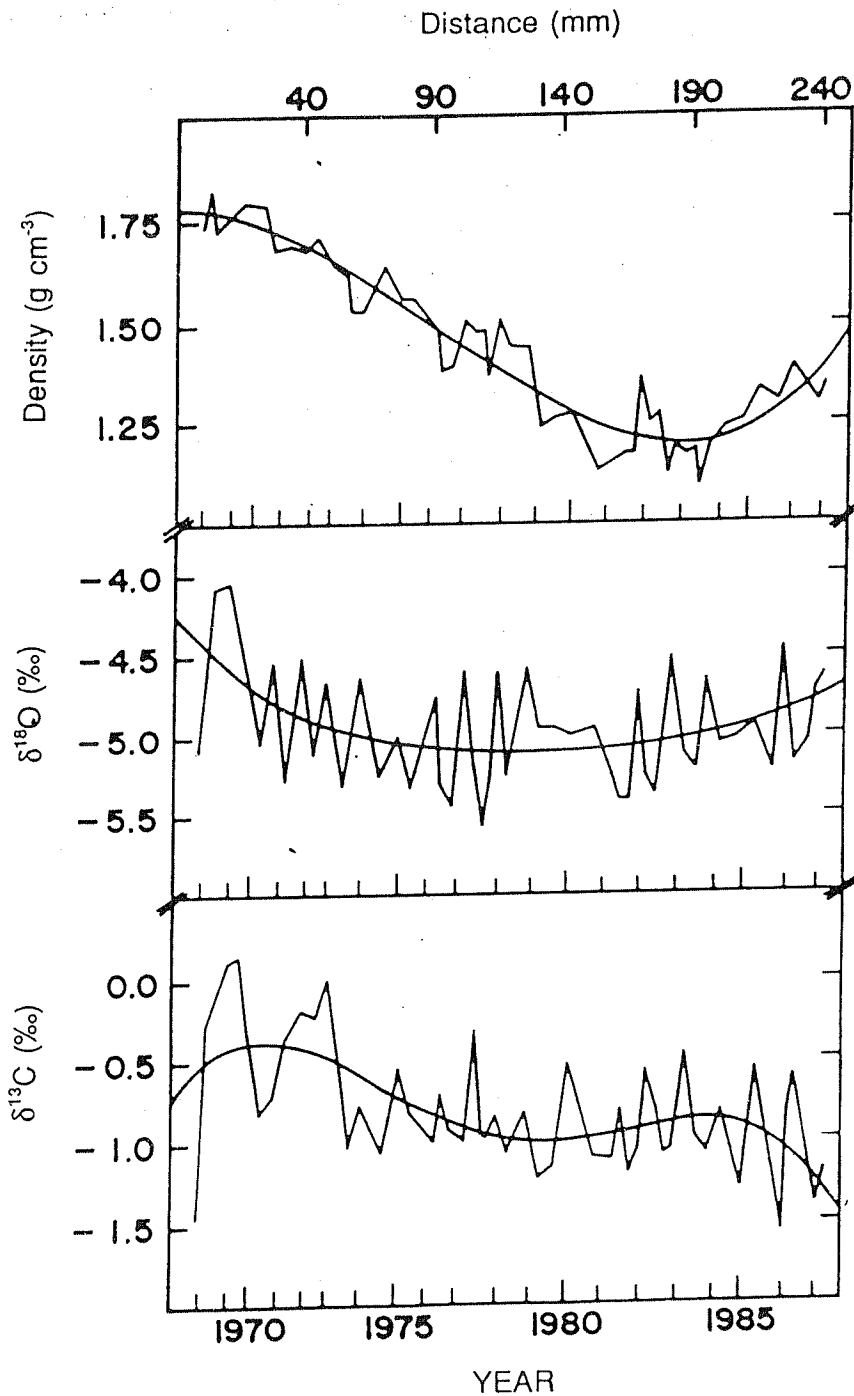


Fig 3.22 Density,  $\delta^{18}\text{O}$  and  $\delta^{13}\text{C}$  variations along Track-2 of coral *P. lutea* from the Stanley Reef, Australia. Smooth lines indicate long term trends.

The corals in this region generally accrete high density bands in summer and low density bands in winter. Lough & Barnes(1991) made detailed investigation on this aspect. The coral density decreases with time in both the tracks (Figs 3.21 & 3.22). The magnitude is about 0.25 g/cm<sup>3</sup> for track 1 and 0.5 g/cm<sup>3</sup> for track 2 between 1968 and 1984 A.D. The reduction in density is more pronounced in the track which is farther away from the central growth axis. The  $\delta^{13}\text{C}$  also decreases by 0.5‰ in both the tracks during this period. The positive correlation between  $\delta^{13}\text{C}$  and density in each of these tracks, therefore, arises due to the long term trend in the data. Slower growth rate corresponds to higher density as seen in the above figure and during 1968-74, the early part of the record. The later part of the record shows higher growth rates and lower densities in general. As shown by McConnaughey (1989), the  $\delta^{13}\text{C}$  values in years of slow growth are isotopically enriched compared to those of years of higher growth rate. Therefore we infer that the density banding is more likely to be determined by variation in growth and rather than by variations in SST. This is to some extent corroborated by the fact that  $\delta^{18}\text{O}$  and  $\delta^{13}\text{C}$  are not correlated. If the kinetic effects were dominant during the fractionation of the isotopes from the sea water to the coral skeleton, one would observe a strong positive correlation between the  $\delta^{18}\text{O}$  and  $\delta^{13}\text{C}$  (McConnaughey 1989). The absence of such a correlation also indicates that metabolic (growth related) fractionation is dominant in the case of  $\delta^{13}\text{C}$ .

Density,  $\delta^{18}\text{O}$  and  $\delta^{13}\text{C}$  time series obtained from two tracks of a *Porites* coral, one close to growth axis (10° off) and another 20° off the axis indicate that there is a small but systematic intraband variability across the central growth axis. Oxygen isotopic ratio, an indicator of the environmental parameter shows a good correlation with SST in both the tracks, however the correlation is weaker in the track 20° off the growth axis. A similar trend is also observed in case of  $\delta^{18}\text{O}$ -rainfall correlation. The carbon isotopic composition seems to be largely controlled by intrinsic factors like metabolism and the variable growth rate. The correlation between density and  $\delta^{13}\text{C}$  implies that the density band formation is controlled more by variable growth rate rather than SST.



### III.3 RADIOCARBON RESULTS

The primary goal of measuring radiocarbon in the Gulf of Kutch coral is to determine the air-sea  $\text{CO}_2$  exchange rate (ASCER) in this region. The  $^{14}\text{C}$  concentrations in the atmosphere and upper layers of the ocean were significantly perturbed by nuclear weapon tests conducted during the 1950's and early 60's. (de Vries 1958, Levin *et al.* 1980) This perturbation and its temporal variation provides a means to determine the ASCER in different regions of the ocean (Broecker *et al.* 1980, Stuiver 1980, Druffel & Suess 1983, Siegenthaler 1983, Cember 1989, Weidman & Jones 1993).

The ASCER can be derived by modelling the temporal variations in  $^{14}\text{C}$  activities of the atmosphere and the surface ocean. The time variations in the surface ocean radiocarbon is derived from  $^{14}\text{C}$  measurements in the annual growth bands of coral; tree rings provide the radiocarbon time history of the atmosphere. With this objective we have measured radiocarbon in the annual bands of corals and tree rings.

#### *Features of the data*

##### III.3.a Gulf of Kutch coral

Fig 3.23 shows the  $\Delta^{14}\text{C}$  time-series in the Gulf of Kutch (GKh, 22.6° N, 70° E) coral for the years 1950-1990 [data in Table III.12, Appendix A]. From a value of -60‰ in the year 1950 it steadily increases to a peak value of 170‰ in 1968, after which it decreases monotonically to a value of 55‰ in 1990. The increase in  $^{14}\text{C}$  activity since 1950 results from the injection of bomb produced radiocarbon from the atmosphere to the surface ocean via air-sea  $\text{CO}_2$  exchange. Moore and Krishnaswami (1974) had reported  $\delta^{14}\text{C}$  time series for a *Favia* coral in the GKh for the years 1951 to 1973. They obtained a peak value of +230‰ for  $\delta^{14}\text{C}$  in 1968. This  $\delta^{14}\text{C}$  when corrected for isotopic fractionation using a  $\delta^{13}\text{C}$  value of -0.27‰ (our measured value in the GKh coral) yields a  $\Delta^{14}\text{C}$  of 169‰ very close to the peak value of 170‰ obtained in this study.

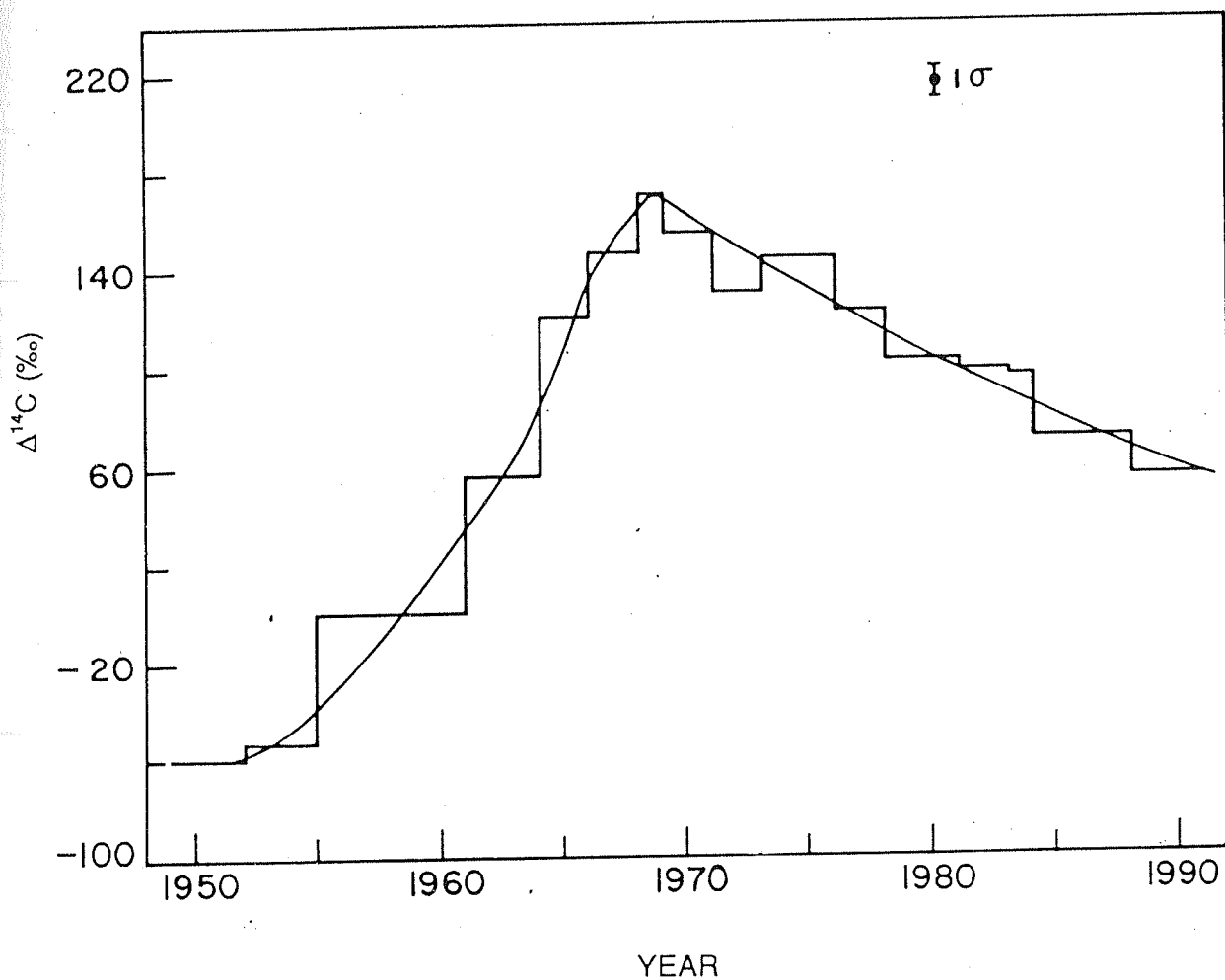


Fig 3.23  $\Delta^{14}\text{C}$  time series in the coral *F. speciosa* from the Gulf of Kutch, northern Arabian Sea. The continuous curve is an eye fit line to the data.

### III.3.b Tree rings

The  $\Delta^{14}\text{C}$  time profile in the annual rings of a teak tree from Thane ( $19^{\circ}14'\text{N}, 73^{\circ}24'\text{E}$ , about 25 km north of Bombay) is shown in Fig 3.24 [data in Table III.12 Appendix A] along with the northern hemispheric (NH) curve (Nydal & Lövseth 1983, Gupta & Polach 1985). The Thane tree ring samples we analyzed cover a time span of 1960 to 1980. In the early sixties, the  $\Delta^{14}\text{C}$  values of the Thane tree rings are indistinguishable from that of NH values, but the two sets of values differ significantly after mid sixties through the year 1980. The Thane tree ring  $\Delta^{14}\text{C}$  reaches a peak value (630‰) during 1964-65, significantly lower than that of the NH peak of ~1000‰. Radiocarbon analyses of air samples from Bombay during 1963-64 (Kusumgar 1965) also show that the  $\Delta^{14}\text{C}$  of Bombay air (~700‰) is similar to the tree ring value but lower than that of the NH curve. Broecker *et al.* (1985) give 3 curves for atmospheric  $\Delta^{14}\text{C}$  time series for the regions:  $>20^{\circ}\text{N}$ ,  $20^{\circ}\text{N}-20^{\circ}\text{S}$ , and  $>20^{\circ}\text{S}$ . The tree analyzed in this study (located at  $19^{\circ}\text{N}$ ) belongs to the middle group, its peak  $\Delta^{14}\text{C}$  value is ~100‰ less compared to that expected from the  $20^{\circ}\text{N}-20^{\circ}\text{S}$  curve. We need to obtain better spatial coverage of tree ring  $\Delta^{14}\text{C}$  data for this region to ascertain the observed lower  $\Delta^{14}\text{C}$  values. If the  $\Delta^{14}\text{C}$  in this region is indeed lower, it could arise from:

- 1) local dilution of  $^{14}\text{C}$  activity of this region. Kusumgar (1965) attributed the lower  $\Delta^{14}\text{C}$  in Bombay air relative to northern hemispheric values to fossil fuel injection of  $\text{CO}_2$ .
- 2) active air-sea exchange of  $\text{CO}_2$  with the adjoining Arabian Sea. The evasion of  $\text{CO}_2$  depleted in  $^{14}\text{C}$  from the Arabian Sea may reduce the  $\Delta^{14}\text{C}$  peak in the atmosphere.

Another reason of reduced peak in the Thane region compared with the NH peak could be the enhanced mixing between stratosphere and troposphere, which result in higher  $^{14}\text{C}$  concentration in the high latitudes relative to that in the lower latitudes (Hagemann *et al.* 1965).

### III.3.b Tree rings

The  $\Delta^{14}\text{C}$  time profile in the annual rings of a teak tree from Thane ( $19^{\circ}14'\text{N}, 73^{\circ}24'\text{E}$ , about 25 km north of Bombay) is shown in Fig 3.24 [data in Table III.12 Appendix A] along with the northern hemispheric (NH) curve (Nydal & Lövseth 1983, Gupta & Polach 1985). The Thane tree ring samples we analyzed cover a time span of 1960 to 1980. In the early sixties, the  $\Delta^{14}\text{C}$  values of the Thane tree rings are indistinguishable from that of NH values, but the two sets of values differ significantly after mid sixties through the year 1980. The Thane tree ring  $\Delta^{14}\text{C}$  reaches a peak value (630‰) during 1964-65, significantly lower than that of the NH peak of ~1000‰. Radiocarbon analyses of air samples from Bombay during 1963-64 (Kusumgar 1965) also show that the  $\Delta^{14}\text{C}$  of Bombay air (~700‰) is similar to the tree ring value but lower than that of the NH curve. Broecker *et al.* (1985) give 3 curves for atmospheric  $\Delta^{14}\text{C}$  time series for the regions:  $>20^{\circ}\text{N}$ ,  $20^{\circ}\text{N}-20^{\circ}\text{S}$ , and  $>20^{\circ}\text{S}$ . The tree analyzed in this study (located at  $19^{\circ}\text{N}$ ) belongs to the middle group, its peak  $\Delta^{14}\text{C}$  value is ~100‰ less compared to that expected from the  $20^{\circ}\text{N}-20^{\circ}\text{S}$  curve. We need to obtain better spatial coverage of tree ring  $\Delta^{14}\text{C}$  data for this region to ascertain the observed lower  $\Delta^{14}\text{C}$  values. If the  $\Delta^{14}\text{C}$  in this region is indeed lower, it could arise from:

- 1) local dilution of  $^{14}\text{C}$  activity of this region. Kusumgar (1965) attributed the lower  $\Delta^{14}\text{C}$  in Bombay air relative to northern hemispheric values to fossil fuel injection of  $\text{CO}_2$ .
- 2) active air-sea exchange of  $\text{CO}_2$  with the adjoining Arabian Sea. The evasion of  $\text{CO}_2$  depleted in  $^{14}\text{C}$  from the Arabian Sea may reduce the  $\Delta^{14}\text{C}$  peak in the atmosphere.

Another reason of reduced peak in the Thane region compared with the NH peak could be the enhanced mixing between stratosphere and troposphere, which result in higher  $^{14}\text{C}$  concentration in the high latitudes relative to that in the lower latitudes (Hagemann *et al.* 1965).

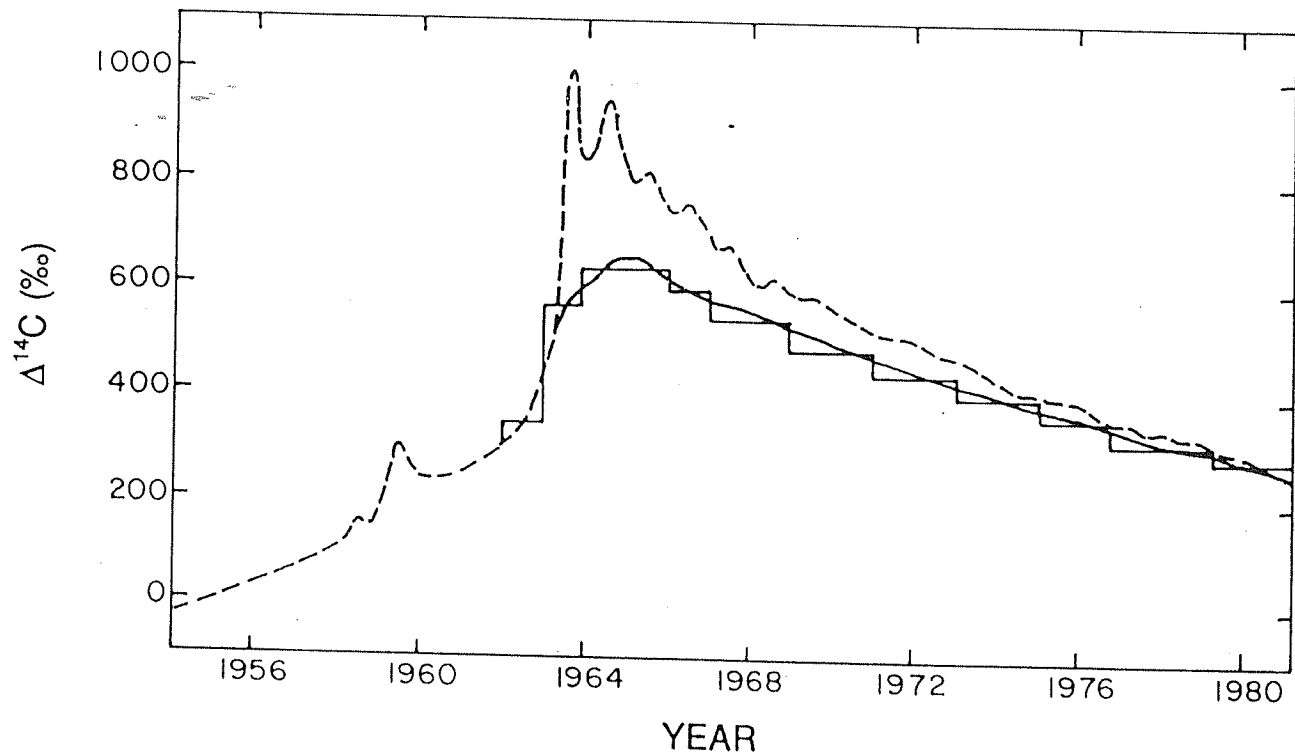


Fig 3.24 Atmospheric  $\Delta^{14}\text{C}$  time variations of the Northern Hemisphere (long dashed line, data from Nydal & Lövseth 1983) and Thane (near Bombay, solid line). The Thane data are based on tree ring measurements. The Thane values are significantly lower than the NH curve. Error bar is too small to be shown.

### III.3.c Air-Sea CO<sub>2</sub> exchange rate (ASCER) in the Gulf of Kutch

Comparison of the  $\Delta^{14}\text{C}$  time series of the coral (representative of surface sea water) and that of the tree ring (atmosphere) shows that  $\Delta^{14}\text{C}$  peak in the GK<sub>h</sub> coral lags behind the atmospheric peak by 4-5 years. This "peak shift" provides information about the CO<sub>2</sub> exchange time scales between the atmosphere and ocean in a particular oceanic region, and is related to the residence time of CO<sub>2</sub> in atmosphere wrt the exchange with the ocean as discussed later. The peak-shift for other oceanic regions range between 4-15 years (Table.III.10). The 4-5 years response time in the GK<sub>h</sub> region probably indicates that the ASCER is greater in this region, resulting from strong monsoon winds.

#### *Model for calculation of ASCER*

Determination of the CO<sub>2</sub> exchange rate between atmosphere and the surface ocean requires a knowledge of sources and sinks of carbon and radiocarbon in the particular oceanic region. The carbon budget in surface water is controlled mainly by air-sea CO<sub>2</sub> exchange, advective processes (lateral and/or vertical mixing of water masses) and biological productivity. The Gulf of Kutch area is a shallow continental shelf region having mean water depth of ~30 m. The GK<sub>h</sub> exchanges water with the adjoining Arabian Sea through tidal currents. The speeds of these currents vary from 0.5 to 0.76 m/sec (Srivastava & John 1977). The mass balance equations for <sup>12</sup>C and <sup>14</sup>C in the Gulf of Kutch between supply and removal is given by:

$$\begin{bmatrix} \text{invasion of CO}_2 + \\ \text{advective transport} \end{bmatrix} = \begin{bmatrix} \text{evasion of CO}_2 + \text{advective transport} \\ + \text{biological removal} \end{bmatrix}$$

For <sup>12</sup>C this is given by (assuming invasion and evasion of CO<sub>2</sub> are equal)

$$F_{12} + w C_s = F_{12} + w C_G + B \quad (3.12)$$

$$w C_s = B + w C_G \quad (3.13)$$

Table: III.10  $\Delta^{14}\text{C}$  minimum, maximum and peak shift for different oceanic regions. The minima of  $\Delta^{14}\text{C}_{\text{coral}}$  represent the pre-bomb values. The time difference between the peaks in  $\Delta^{14}\text{C}$  of the atmosphere and the coral (surface ocean) is termed "peak shift". The atmospheric peak was taken to be in the year 1963.

Oceanic region	$\Delta^{14}\text{C}_{\text{coral}}$		Year of maximum	Peak Shift (yr)	Reference
	min	max			
Bermuda 32°N, 65°W	-50	168	1975	12	Nozaki <i>et al.</i> 1978
Florida 24°57'N 88°33'W	-55	160	1972	9	Druffel & Linik 1978
Oahu 21°N, 158°W	-	175	1973	10	Toggweiler <i>et al.</i> 1991
Belize 16°50'N 83°48'W	-55	160	1972	9	Druffel 1980
North Red Sea 12°N, 43°E	-75	105	1967	4	Cember 1989
South Red Sea 11.5°N, 43°E	-73	~45	1972	>7	Cember 1989
Tarawa 1°N, 172°E	-	103	1978	15	Toggweiler <i>et al.</i> 1991
Galapagos 1°S, 90°W	-72	25	1973	10	Druffel 1981
Fiji 18°S, 179°E	-70	138	1974	11	Toggweiler <i>et al.</i> 1991
Tonga 20°S, 175°W	-	157	1975	12	Toggweiler <i>et al.</i> 1991
Gulf of Kutch 22.6°N, 70°E	-65	172	1968	5	This work

where  $F$  ( $\text{mol m}^{-2} \text{ yr}^{-1}$ ) is the  $\text{CO}_2$  exchange flux,  $w$  ( $\text{m yr}^{-1}$ ) advection velocity,  $C$  ( $\text{mol m}^{-3}$ ) carbon concentration and  $B$  ( $\text{mol m}^{-2} \text{ yr}^{-1}$ ) is biological removal. The subscripts S and G refer to the surface Arabian Sea and the Gulf of Kutch respectively. The above equations assume steady state for  $^{12}\text{C}$  balance. This assumption is an oversimplification as the  $\text{CO}_2$  concentration of atmosphere has been steadily increasing during the past century (Bacastow & Keeling 1981, Siegenthaler & Sarmiento 1993) which would affect the invasion-evasion balance.

The mass balance equation for  $^{14}\text{C}$  is of the following form (neglecting radiocarbon decay, see Appendix-I).

$$D_G \frac{dC_G^*}{dt} = F_{12}(R_A - R_G) + w(C_S R_S - C_G R_G) \quad (3.14)$$

where  $R$  is the  $^{14}\text{C}/^{12}\text{C}$  mol ratio in the respective reservoir. Subscripts A and G stand for the atmosphere and GKh respectively.  $C_G^*$  is the radiocarbon concentration in GKh and  $D_G$  is the mean depth of GKh (Table III.11). The formulation of our model is similar to that used by Cember (1989) for deriving ASCER in the Red Sea region. Eqn 3.14 can be written in the standard  $\Delta^{14}\text{C}$  notation. The first term in the RHS, the net  $^{14}\text{C}$  flux,  $\Delta F_{14}$ , between the atmosphere and the GKh can be expressed as (Stuiver 1980):

$$\Delta F_{12} = k(\Delta^{14}\text{C}_A - \Delta^{14}\text{C}_G)F_{12} \quad (3.15)$$

where  $k$  is a factor which takes into consideration the  $^{14}\text{C}/^{12}\text{C}$  mol ratio of the NBS oxalic acid standard ( $1.176 \times 10^{-12}$ ) and fractionation factor for the inter-reservoir carbon transfer. The numerical value of  $k$  is  $1.24 \times 10^{-15}$  (*op cit.*).  $\Delta^{14}\text{C}_A$  and  $\Delta^{14}\text{C}_G$  are the atmospheric and GKh radiocarbon activities. The second term in the RHS (Eqn 3.14) represents the exchange flux of radiocarbon between the Arabian Sea and GKh by advection. This term can be written as:

$$F_{CG} = u[m(\Sigma\text{CO}_2)_S(1 + \frac{\Delta^{14}\text{C}_S}{1000}) - m(\Sigma\text{CO}_2)_G(1 + \frac{\Delta^{14}\text{C}_G}{1000})] \quad (3.16)$$

where  $m$  is a constant which is obtained by multiplying the  $^{14}\text{C}/^{12}\text{C}$  mol ratio of the NBS



Oxalic acid standard and the fractionation term for transfer of carbon between different reservoirs. That is,  $m=(1.176 \times 10^{-12} \times 1.052)=1.24 \times 10^{-12}$  [vide Appendix II]. The solution of the Eqn 3.14 is given by:

$$\Delta^{14}C_G(t) = \Delta^{14}C_G^0 e^{-Jt} + E e^{-Jt} \int_0^t e^{J\tau} \Delta^{14}C_A(\tau) d\tau + F e^{-Jt} \int_0^t e^{J\tau} \Delta^{14}C_S(\tau) d\tau \quad (3.17)$$

where  $\Delta^{14}C_G^0$  is the initial value (pre-bomb) of  $\Delta^{14}C$  in GKh, J, E and F are constants (Appendix-III). The values of various parameters used in this model are given in Table III.11.

As a first step we calculate  $\Delta^{14}C_G(t)$  using Eqn 3.17 with two simplifications, (i)  $[\Sigma CO_2]_s = [\Sigma CO_2]_G$  and (ii) the advective transport process is negligible, *i.e.* the  $^{14}C$  time variations in the GKh is controlled only by carbon exchange with the atmosphere. Druffel & Suess (1983) also modelled their  $^{14}C$  data in corals from north-west Atlantic and eastern tropical Pacific to derive exchange time scales and  $CO_2$  exchange rate based on a similar simplified model. Eqn 3.14 with  $w=0$  reduces to the model used by Druffel & Suess (1983) *i.e.* the time variations of  $^{14}C$  concentration in sea surface water is proportional to the air-sea gradient of  $\Delta^{14}C$ .

Solving Eqn 3.17 with  $w=0$  and for different  $F_{12}$  values we obtain a family of curves (Fig 3.25). The curve (a) with  $F_{12}=2$  shows that the GKh radiocarbon activity increases monotonically through 1980 without a distinct peak. This is not consistent with our coral data (filled circle in Fig 3.25) which show a distinct peak in 1968. The second and third curves (b) and (c) with  $F_{12}=6$  and 10 respectively, though show peaks in the  $\Delta^{14}C$  time series, they predict much higher radiocarbon concentration in the GKh compared to that observed in the coral. It is clear from these results that the air-sea exchange alone is not able to simulate the observed  $\Delta^{14}C$  variations in the GKh coral. Therefore carbon and radiocarbon supply to the GKh via advection from the Arabian Sea also need to be considered, which would 'dilute' the effects of air-sea exchange and thereby provide a better fit to the coral data.

The advective supply of carbon to the GKh could be from the surface layer or shallow depths of the Arabian Sea. Solution of Eqn 3.17 requires knowledge of time

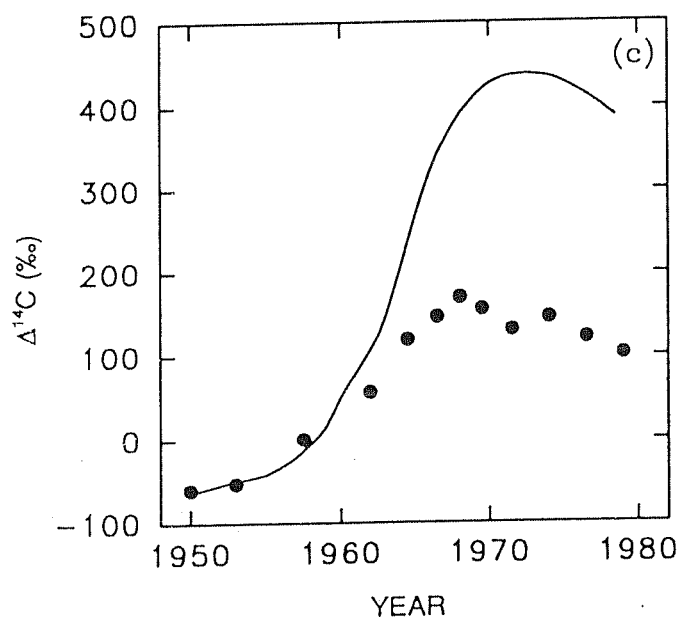
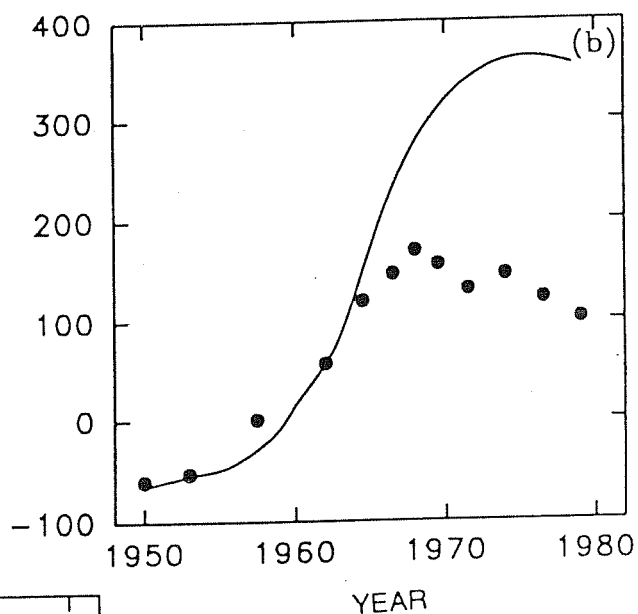
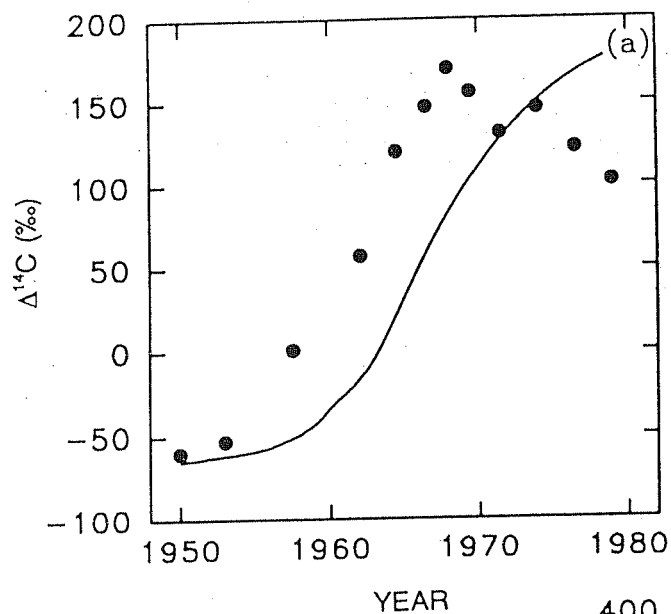


Fig 3.25 Calculated time variations of radiocarbon activity in the Gulf of Kutch considering only air-sea exchange of  $\text{CO}_2$ . (a)  $F_{12}=2$ , (b)  $F_{12}=6$ , (c)  $F_{12}=10 \text{ mol m}^{-2} \text{ yr}^{-1}$ . Solid line: simulated curve; filled circle: coral data.

Table III.11 Symbols, units and values of parameters used in our model

Symbol	Parameter	Unit	Value	Reference
$F_{12}$	air-sea exchange rate of $\text{CO}_2$	$\text{mol m}^{-2}\text{yr}^{-1}$	model derived	
$C_{S,} (\Sigma\text{CO}_2)_S$	total DIC conc. in surface Arab. Sea	$\text{mol m}^{-3}$	2.11	Stuiver & Östlund 1983
$C_{D,} (\Sigma\text{CO}_2)_D$	total DIC conc. of deep Arab. Sea	$\text{mol m}^{-3}$	2.36	-do-
$C_{G,} (\Sigma\text{CO}_2)_G$	total DIC conc. in GKh	$\text{mol m}^{-3}$	2.11	-do-
$R$	$^{14}\text{C}/^{12}\text{C}$ mol ratio	-	variable	
$C^*$	radiocarbon conc.	$\text{mol m}^{-3}$	variable	
$D_S$	mixed layer depth of Arab. Sea	m	60	
$D_G$	mean depth of GKh	m	30	
$(\Delta^{14}\text{C})_A^\circ$	Pre-bomb atmospheric $\Delta^{14}\text{C}$	‰	-25	Stuiver & Quay 1981
$u$	upwelling velocity	$\text{m yr}^{-1}$	model derived	
$w$	advective velocity Arab. Sea to GKh	$\text{m yr}^{-1}$	model derived	

variations in  $R_s$ , the Arabian sea water contributing radiocarbon to GK. Since there is no data on  $\Delta^{14}\text{C}$  time series of the surface Arabian Sea, we need to generate the same for the time period 1953 to 1980, based on input from atmosphere and upwelling from the deep Arabian Sea. We constrain this time series with the 1977 mixed layer  $\Delta^{14}\text{C}$  value of 59‰ based on the GEOSECS (station 416) measurements. We consider the following two box model for the Arabian Sea consisting of surface and deep layers (Fig 3.26).

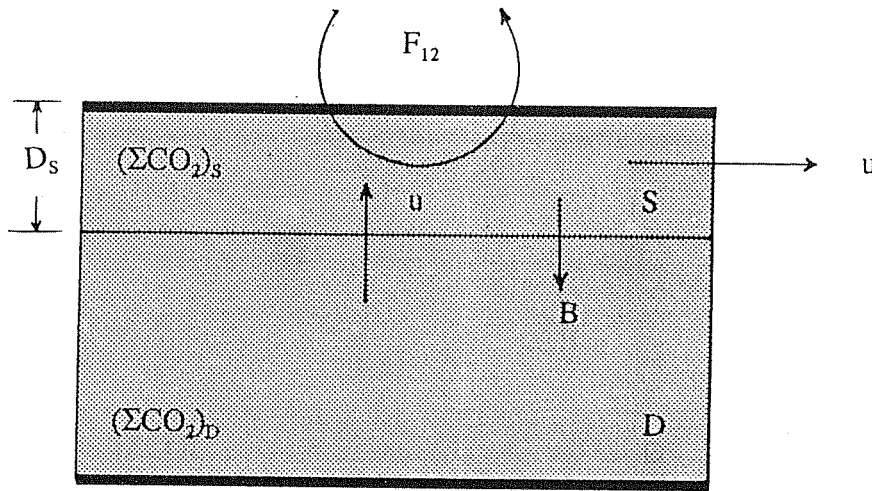


Fig 3.26 Two box model of the (northern) Arabian Sea. S is mixed layer, D is deep ocean, other parameters are defined in Table III.11

The mass balance equation for  $^{14}\text{C}$  for the mixed layer is given by:

$$D_s \frac{dC_s^*}{dt} = F_{12}R_A + uC_D R_D - (uC_S R_S + B R_S + F_{12}R_S + \lambda C_S R_S D_S) \quad (3.18)$$

Neglecting the decay term and substituting,  $uC_D = B + uC_S$  (cf. Eqn 3.13) we get:

$$D_S \frac{dC_S^*}{dt} = F_{12}(R_A - R_S) + u(C_D R_D - C_D R_S) \quad (3.19)$$

Rewriting in terms of  $\Delta^{14}\text{C}$  (c.f. Eqns 3.15 & 3.16),

$$D_S(\Sigma\text{CO}_2)k \frac{d\Delta^{14}\text{C}_S}{dt} = F_{12}k(\Delta^{14}\text{C}_A - \Delta^{14}\text{C}_S) + u(\Sigma\text{CO}_2)_{Dm} \left( \frac{\Delta^{14}\text{C}_D}{1000} - \frac{\Delta^{14}\text{C}_S}{1000} \right) \quad (3.20)$$

Eqn 3.20 has a solution of the form:

$$\Delta^{14}\text{C}_S(t) = e^{-At} \Delta^{14}\text{C}_S^o + B e^{-At} \int_0^t e^{A\tau} \Delta^{14}\text{C}_A(\tau) d\tau + \frac{C}{A} (1 - e^{-At}) \quad (3.21)$$

where A, B, and C are constants (Appendix IV).

Using Eqn 3.21 we generate mixed layer Arabian Sea  $\Delta^{14}\text{C}$  time series based on the atmospheric  $\Delta^{14}\text{C}$  values. The atmospheric  $\Delta^{14}\text{C}$  values for 1950-1960 were taken from Stuiver & Quay (1981) and Gupta & Polach (1985). For 1960-1980, the Thane tree ring  $\Delta^{14}\text{C}$  (Fig 3.21) data were used. The deepwater  $\Delta^{14}\text{C}$  end member value used was -90‰ corresponding to that measured at a depth of ~500 m at GEOSECS station 416 (Stuiver & Östlund 1983). The time series is constrained by fixing the Arabian Sea mixed layer  $\Delta^{14}\text{C}$  value as 59‰ for 1977(*op cit.*) and by the fact that the  $\Delta^{14}\text{C}_{\text{max}}$  should occur around 1968. Typical results for the Arabian Sea time series are given in Fig 3.27. Reasonable estimates for  $F_{12}$  and  $u$  are:

$$F_{12} = 11 \text{ mol m}^{-2} \text{ yr}^{-1} \quad \text{and} \quad u = 10.5 \text{ m yr}^{-1}$$

These values though not unique (as they depend on the  $\Delta^{14}\text{C}$  of the deep water end member used for calculations), they are consistent with other independent estimates.

(i) Broecker *et al.* (1985) has calculated the inventory of bomb  $^{14}\text{C}$  in stn 416 to be  $5.1 \times 10^9 \text{ atom cm}^{-2}$ . According to Stuiver (1980) the inventory is related to the  $\text{CO}_2$  air-sea exchange flux as:

$$Q = 1.24 \times 10^{-15} F_{12} \int (\Delta^{14}\text{C}_A - \Delta^{14}\text{C}_S - 45) dt$$

The value of the integral between 1953-1977 is ~5500 ‰.yr based on our model derived

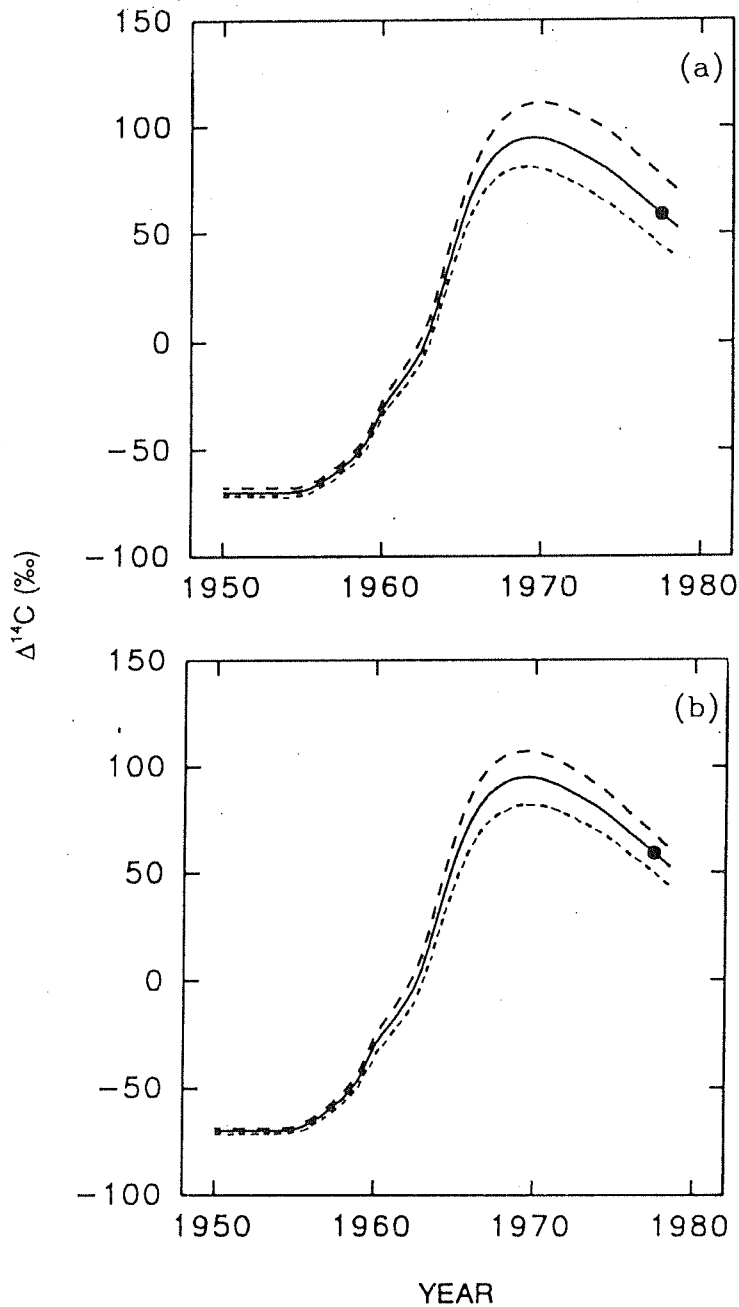


Fig 3.27 Results of box model calculation. The plots show the simulated radiocarbon time series in the mixed layer of the northern Arabian Sea (GEOSECS stn 416) for different sets of parameters. (a) constant  $F_{12}$  ( $11 = \text{mol m}^{-2} \text{ yr}^{-1}$ ) and varying  $u$  ( $=9, 10.5, 12 \text{ m yr}^{-1}$ ), (b) constant  $u$  ( $=10.5$ ) and varying  $F_{12}$  ( $=12, 11, 10$ ). The filled circles represent the 1977 GEOSECS mixed layer  $\Delta^{14}\text{C}$  value (59‰, Stuiver & Östlund 1983). Values of  $F_{12}=11$  and  $u=10.5$  (solid line) appears to be the best (eye) fit curve.

$\Delta^{14}\text{C}$  values of the surface Arabian Sea, atmospheric  $\Delta^{14}\text{C}$  values used in this model, and a steady state  $\Delta^{14}\text{C}$  difference between atmosphere and ocean of about 45‰. This yields a value of  $F_{12} = 12$  similar to that derived using our model.

(ii) the mean annual wind speed in the northern Arabian Sea is about 6 m/s (Esbensen & Kushnir 1981). For this wind speed the expected  $\text{CO}_2$  invasion flux is  $\sim 13 \text{ mol m}^{-2}\text{yr}^{-1}$  using the relationship between windspeed and  $\text{CO}_2$  invasion flux (Broecker *et al.* 1985). Our calculation is in good agreement with this estimate.

(iii) Hasternath & Lamb (1980) estimated the upwelling velocity over the whole of the Arabian Sea and the Bay of Bengal from 200 m depth to be  $\sim 19 \text{ m yr}^{-1}$ . Warren (1992) reports the mean upwelling rate into the bottom of the North Indian Deep Water layer  $\sim 15\text{--}30 \text{ m yr}^{-1}$ ; net upwelling out of the top of the layer to be less than this. Our calculation, the upwelling rate  $10.5 \text{ m yr}^{-1}$  from a depth of  $\sim 500\text{m}$  is not inconsistent with the above estimates.

(iv) the model derived steady state pre-bomb  $\Delta^{14}\text{C}$  value for the surface Arabian Sea is

$$(\Delta^{14}\text{C}_S)_o = \frac{\Delta^{14}\text{C}_D u (\Sigma \text{CO}_2)_D + F_{12} (\Delta^{14}\text{C}_A)_o}{F_{12} + u (\Sigma \text{CO}_2)_D} = -70 \text{ ‰}$$

with  $u = 10.5$  and  $F_{12} = 11$  the value (-70‰) is close to the number -65‰ used by Broecker *et al.* (1985) for the calculation of the bomb  $^{14}\text{C}$  inventory in the station 416.

In addition, other consistency checks on the model can also be made by the following approximations. When  $F_{12} = 0$  (atmospheric exchange is cut off) the  $\Delta^{14}\text{C}_S$  approaches  $\Delta^{14}\text{C}_D$  with a time constant of  $A^{-1}$  [Appendix IV] of 5 yrs. This implies that if the atmospheric exchange is cut off the mixed layer  $\Delta^{14}\text{C}$  will become equal to that of the deep water in about 20-25 years (*i.e.* 4-5 times  $A^{-1}$ ). Similarly for  $u = 0$  (*i.e.* no upwelling)  $\Delta^{14}\text{C}_S$  approaches  $\Delta^{14}\text{C}_A$  with a time constant of about 12 yrs. These time constants are similar to those observed for other oceanic regions for the residence time of carbon in the mixed layer wrt exchange with deep water and the atmosphere.

Now we use the Arabian Sea and the atmospheric  $\Delta^{14}\text{C}$  time series as the two end members contributing carbon and radiocarbon to GKh to generate the  $\Delta^{14}\text{C}$  time series in the Gulf of Kutch; [assuming that the DIC concentrations in these two reservoirs are

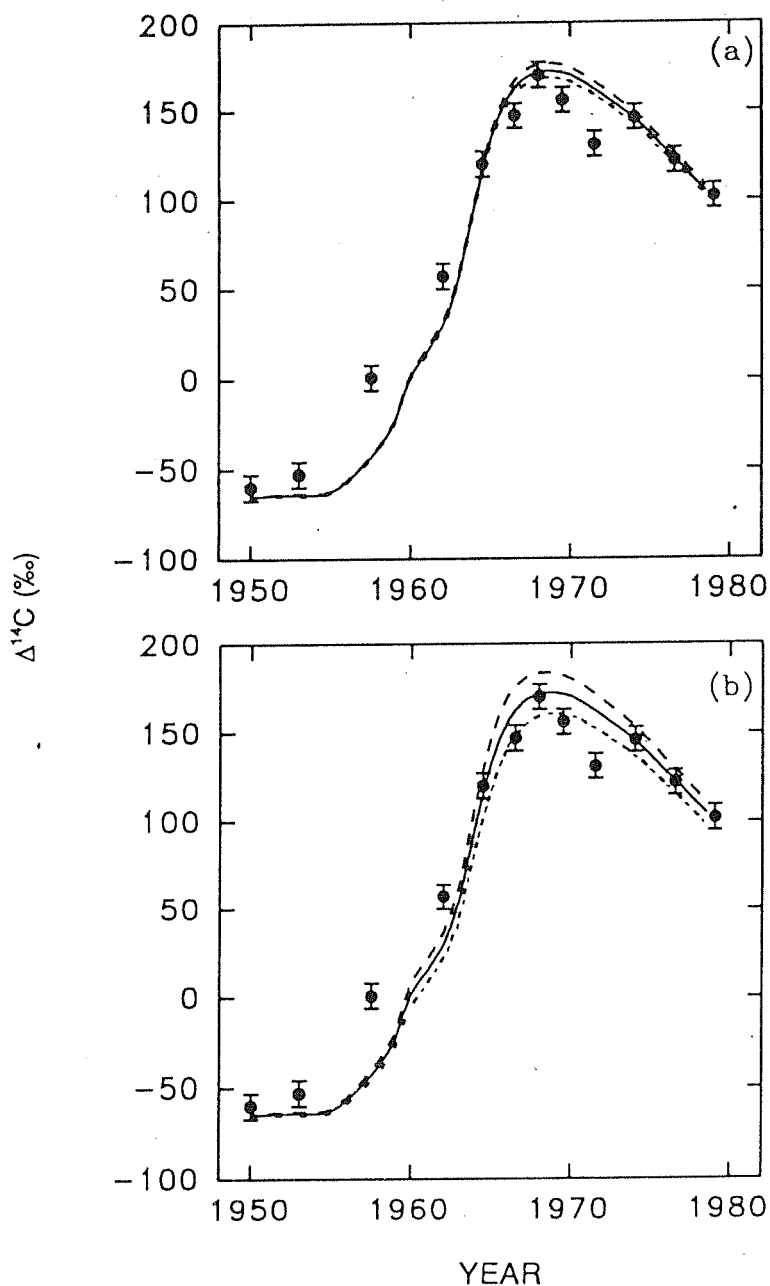


Fig 3.28 Results of box model calculations. The plots show the simulated radiocarbon time series in the Gulf of Kutch (GKh) for different sets of parameters. (a) constant  $F_{12}$  ( $=12 \text{ mol m}^{-2} \text{ yr}^{-1}$ ) and varying  $w$  ( $=26, 28, 30 \text{ m yr}^{-1}$ ) and (b) constant  $w$  ( $=28$ ) and varying  $F_{12}$  ( $=14, 12, 10$ ). Filled circles represent GKh coral data with  $\pm 1\sigma$  errors. Values of  $F_{12} = 12$  and  $w = 28$  (solid line) appear to fit the coral data reasonably well.



equal *i.e.* the biology term  $B=0$ , vide Appendix V ], we generate a family of curves for different sets of values of  $F_{12}$  and  $w$  (Fig 3.28). The solid line is the calculated  $\Delta^{14}\text{C}$  time series for the Gulf of Kutch, filled circles are our coral data.

It is seen from Fig 3.28 that the rise in  $\Delta^{14}\text{C}$  of coral during 1953-1960 is faster than that predicted by the model. A factor which would have contributed to this is an averaging effect. The  $\Delta^{14}\text{C}$  plotted for the year 1957.5 is an average for five coral bands 1955-1960. The steady increase in  $\Delta^{14}\text{C}_A$  during these years is not considered in plotting this data point. Another cause for the discrepancy between the observed  $\Delta^{14}\text{C}$  and the model fit, can be an error in the year assignment for the bands. As we have taken utmost care in sampling and verified the year assignments with the  $\delta^{18}\text{O}$  data this error is unlikely, however, if at all there is an error it is likely to be  $\pm 1$  yr.

The nature of curves in Fig 3.28 shows that the year of  $\Delta^{14}\text{C}$  peak in the GK h is controlled more by  $F_{12}$ , whereas both  $F_{12}$  and  $w$  seem to influence the magnitude of the  $\Delta^{14}\text{C}$  peak.

A reasonable fit to the coral data can be made using the values of  $F_{12} = 12 \text{ mol m}^{-2} \text{ yr}^{-1}$  and  $w = 28 \text{ m yr}^{-1}$  based on the  $\Delta^{14}\text{C}$  time series of the two end members considered. In this case when  $F_{12}=0$  the  $\Delta^{14}\text{C}_G$  approaches  $\Delta^{14}\text{C}_S$  with a time constant of  $\sim 1$  yr and when  $w=0$  the  $\Delta^{14}\text{C}_G$  approaches to that of atmospheric activity with a time constant of about 5 yrs. As already mentioned that the peak shift obtained in our case 4 to 5 yrs is equivalent to this time constant, *i.e.* the residence time of the atmospheric carbon dioxide wrt the exchange between atmosphere and the GK h water when the GK h becomes isolated from the open ocean.

If the  $\Delta^{14}\text{C}$  values of the Arabian Sea end member contributing radiocarbon to GK h is different from that used in the above model, then the values  $F_{12}$  and  $w$  for GK h would also differ correspondingly. There are no reported results on the circulation and hydrographic properties of the GK h and hence it is difficult at present to constrain our model further.

Our estimate of the  $\text{CO}_2$  exchange rate  $11\text{-}12 \text{ mol m}^{-2} \text{ yr}^{-1}$  in this region is in good agreement to that obtained from other investigations elsewhere. The upwelling in the northern Arabian Sea is calculated as  $10.5 \text{ m.yr}^{-1}$  and the Gulf of Kutch and

the Arabian Sea exchange water with each other with an annual mean flow of water mass 40 million cubic metre. This calculation relies on the assumption that the Arabian Sea end member exchanging water with the Gulf of Kutch has a  $\Delta^{14}\text{C}$  time series generated by our model (using GEOSECS stn 416  $\Delta^{14}\text{C}$  for 1977 value as a constraint).

## Appendix I

Relative significance of radiocarbon decay term in mass balance equations (3.7).

In this mass balance equations for  $^{14}\text{C}$  in the GK h and in the surface layers of the Arabian Sea, we have neglected the radiocarbon decay term.

The ratio of radiocarbon decay in the GK h to its atmospheric flux is

$$\alpha = \lambda \frac{C_G R_G D_G}{F_{12} R_A}$$

considering  $R_A \sim R_G$ , a minimum value of  $F_{12} = 1$  and  $C_G D_G \sim 60 \text{ mol } m^{-2}$ , we have  $\alpha \sim 10^{-2}$

Similarly the ratio of the radiocarbon decay term in the mixed layer of the Arabian Sea (depth 60m) to its upwelling flux from deep water is

$$\beta = \lambda \frac{C_S R_S D_S}{u C_D R_D}$$

where  $u$  is the upwelling velocity. Considering  $C_S R_S / C_D R_D \sim 1$  and  $D_S / u \sim 10$  we get  $\beta \sim 10^{-3}$ .

These rough calculations show that the radiocarbon decay is insignificant compared to its supply/removal fluxes in the GK h and in the mixed layer of the Arab. Sea. Therefore it has not been included in our model.

## Appendix-II

The no. of mol of  $^{14}\text{C}$  (i.e.  $C^*$ ) per unit  $m^3$  of ocean water (Stuiver 1980a) is written as:

$$C^* = m \Sigma \text{CO}_2 (1 + \Delta^{14}\text{C}/1000)$$

where  $m$  is constant which is obtained by multiplying the  $^{14}\text{C}/^{12}\text{C}$  mol ratio in the NBS oxalic acid standard and the fractionation term for transfer of carbon between different

reservoirs.

That is,  $m = 1.176 \times 10^{-12} \times 1.052 = 1.24 \times 10^{-12}$

So,

$$\begin{aligned}\frac{dC^*}{dt} &= m \Sigma CO_2 \frac{d}{dt} (1 + \Delta^{14}C/1000) \\ &= \frac{m}{1000} \Sigma CO_2 \frac{d}{dt} \Delta^{14}C \\ &= k \Sigma CO_2 \frac{d}{dt} \Delta^{14}C, [k = \frac{m}{1000}]\end{aligned}$$

### Appendix III

Equation for calculating radiocarbon time series in GKk:

Eqn (3) can be written as follows:

$$\frac{d}{dt} \Delta^{14}C_G = \frac{F_{12}}{D_G \Sigma} (\Delta^{14}C_A - \Delta^{14}C_G) + \frac{W}{D_G} (\Delta^{14}C_S - \Delta^{14}C_G)$$

[considering  $(\Sigma CO_2)_S = (\Sigma CO_2)_G = \Sigma$ ]

$$\frac{d}{dt} (\Delta^{14}C_G) + J (\Delta^{14}C_G) = E \Delta^{14}C_A + F \Delta^{14}C_S$$

where,

$$\begin{aligned}E &= \frac{F_{12}}{D_G \Sigma} \\ F &= \frac{W}{D_G} \\ J &= \frac{\frac{F_{12}}{\Sigma} + w}{D_G} = E + F\end{aligned}$$

## Appendix IV

Equation for radiocarbon time series in surface Arabian Sea:

Eqn (8) can be rearranged as

$$\begin{aligned} \frac{d}{dt} \Delta^{14}C_S + \frac{F_{12} + u(\Sigma CO_2)_D}{D_S(\Sigma CO_2)_S} \Delta^{14}C_S &= \frac{F_{12}}{D_S(\Sigma CO_2)_S} \Delta^{14}C_A + \frac{u(\Sigma CO_2)_D}{D_S(\Sigma CO_2)_S} \Delta^{14}C_D \\ \frac{d\Delta^{14}C_S}{dt} + A(\Delta^{14}C_S) &= B(\Delta^{14}C_A) + C \end{aligned}$$

where,

$$\begin{aligned} A &= \frac{F_{12} + u(\Sigma CO_2)_D}{D_S(\Sigma CO_2)_S} \\ B &= \frac{F_{12}}{D_S(\Sigma CO_2)_S} \\ C &= \frac{u(\Sigma CO_2)_D}{D_S(\Sigma CO_2)_S} \Delta^{14}C_D \end{aligned}$$

## Appendix-V

If the  $CO_2$  invasion and evasion rates in the Gulf of Kutch are equal then the carbon required for precipitation of coral  $CaCO_3$  has to be derived from the incoming water from the Arabian Sea. This requires that the  $\Sigma CO_2$  of incoming Arabian Sea water to be higher than that of GK. This contradicts our assumption  $[\Sigma CO_2]_G = [\Sigma CO_2]_S$ . However as corals covering a very small percentage of the GK area the difference within  $\Sigma CO_2$  between these two waters is likely to be very small, hence we neglect the difference for simplifying the calculations.

### III.4 Cadmium analysis

The coral KV-1 was chosen for Cd analysis. Its high growth rate enabled subseasonal sampling (5 samples/yr) to investigate seasonal changes in the upwelling characteristics of the Lakshadweep region. The Fig 3.29 shows the variations in Cd concentration in subannual bands. In the first two years of its growth (1984-85) the Cd concentration is  $< 2$  nmol Cd/mol Ca, a typical value for corals growing in upwelling regions. Shen *et al.* (1992) observed that the mean Cd concentration was 2-3 nmol Cd/mol Ca in corals from Galapagos island. But in the next two years our coral shows an anomalous behaviour. Two high peaks are seen in each of these two years. They range from 15 to 22 nmol Cd/mol Ca. The figure also shows the  $\delta^{18}\text{O}$  (thin line) of this coral, as  $\delta^{18}\text{O}$  of the corals respond to upwelling. In the first two years there is no significant change in Cd concentration, but in the year 1985 it shows a covariation with  $\delta^{18}\text{O}$ . However in the year 1986 the  $\delta^{18}\text{O}$  peak and Cd peaks are out of phase. This inconsistency in Cd variations could be due to the coral being young. Similar problems with young corals were also noted by other investigators. Shen (pers. comm., 1993) found abnormally high peaks ( $\geq 20$  nmol Cd/mol Ca) in corals from Champion island and Urvina Bay. Unless the behaviour of young corals with respect to the incorporation of Cd is understood, it is not possible to attach environmental significance to Cd measurements from such corals.

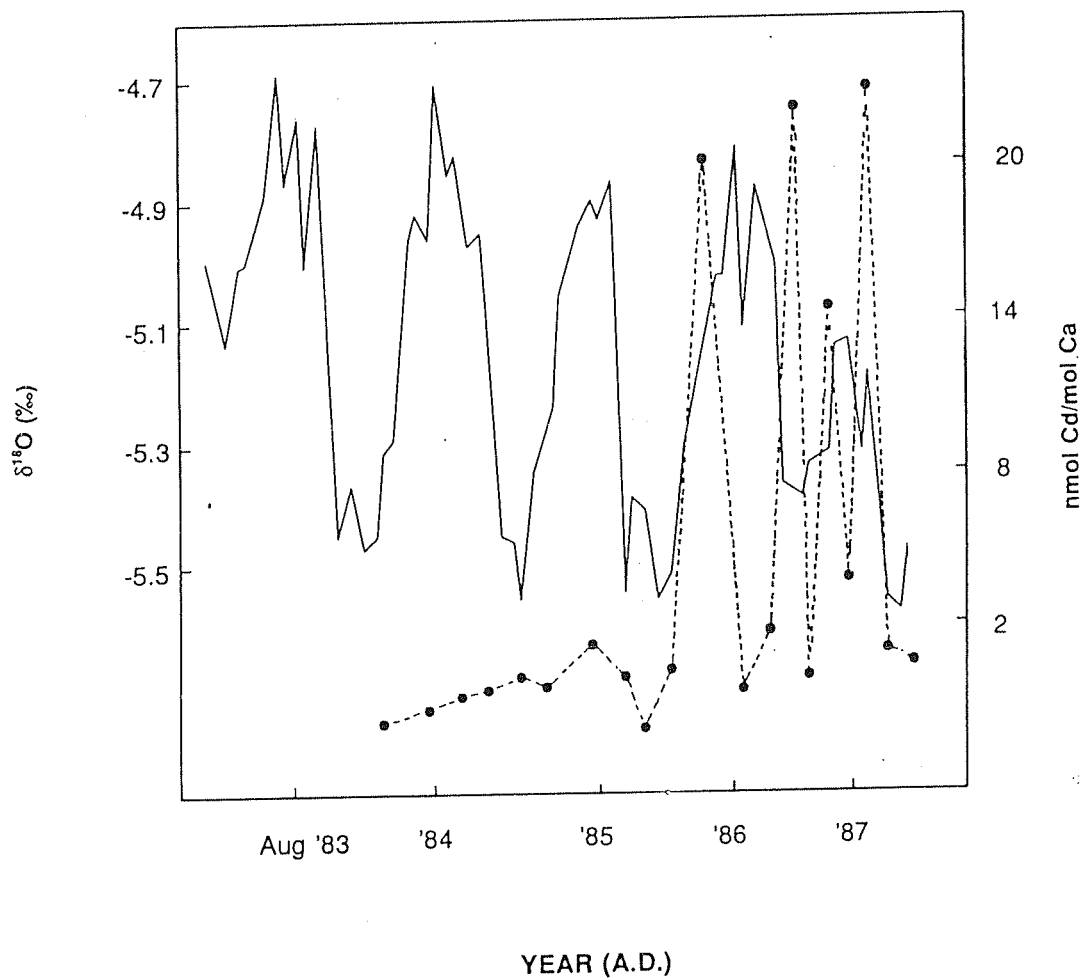


Fig 3.29 The variations of Cd concentration (dotted line) and  $\delta^{18}\text{O}$  (solid line) in coral *P. compressa* (KV-1) from the Kavaratti lagoon, Lakshadweep islands.

### III.5 SYNTHESIS

All the corals analyzed in this thesis are influenced by monsoon systems, the Lakshadweep and the Gulf of Kutch corals by the Indian monsoon and the Stanley Reef coral by the Australian monsoon. Therefore, it would be interesting to compare the isotopic profiles of these samples to look for commonality and the causative factors. However quantitative comparisons are hampered even between the Gulf of Kutch and the Lakshadweep corals (GK & KV2) as the analyses were made on different species, having significantly different growth rates (making it difficult to sample exactly the time contemporaneous sections). Further the SST in these regions is controlled by different factors such as the solar heating (Australia & the Gulf of Kutch) and upwelling (Lakshadweep region). However a qualitative comparison gives the following information:

The oxygen isotope records of the corals (KV2 & GK) from both these locations contain in them monsoon signatures in their oxygen isotopic records in terms of SST and monsoon rainfall respectively. The isotopic profiles of these corals show different trends. This arises because of the different factors which determine the SST in these two regions. The Lakshadweep region is more affected by monsoon induced upwelling and hence sea surface cooling with a minimum SST around Jul-Aug. The coral (*Porites*) from this region accurately records the sea surface temperature variations in their oxygen isotopic ratios registering a maximum in Jul-Aug. The Gulf of Kutch is less influenced by upwelling compared to Lakshadweep region. Here the magnitude of variation in SST is much higher (~6 °C) than in Lakshadweep (~3 to 4°C). The large variation is brought about by summer heating and winter cooling. The lower SST is during Dec-Jan while in Lakshadweep it is in Jul-Aug. The slow growth rate of the GK coral also places a constraint in quantitatively determining the amplitude of seasonal  $\delta^{18}\text{O}$  variation. The  $\delta^{18}\text{O}$  of this coral (GK) also shows an apparent higher order cyclicity.

When we compare the SR coral and Lakshadweep coral (they are of the same genus), we find that the  $\delta^{18}\text{O}$  time series and growth rates are similar. They show a very good resemblance in their oxygen isotopic distributions. The mean  $\delta^{18}\text{O}$  of these two corals are  $-5.07 \pm 0.36$  and  $-5.16 \pm 0.21$  respectively. The mean amplitudes are  $0.75 \pm 0.1$  and

0.55±0.19, corresponding to ~5°C and ~3°C seasonal SST fluctuation respectively. The SR region shows an SST minimum during Austral winter(Jul-Aug) and maximum in summer (Dec-Jan). In case of Lakshadweep the minimum temperature is registered at the same time, Jul-Aug while maximum is around Apr-May. For this reason the  $\delta^{18}\text{O}$  maxima in these two corals coincide while the minima are phase shifted.

Another interesting feature is the  $\delta^{13}\text{C}$  values of these two corals are 180° out of phase. This contrasting behaviour in the  $\delta^{13}\text{C}$  can be explained as follows:

The coral  $\delta^{13}\text{C}$  is to some extent controlled by the rate of photosynthesis, which depends on the availability of sunlight. More cloudiness reduces availability of sunlight and hence the photosynthesis rate. This would result in lower  $\delta^{13}\text{C}$  value. The cloudiness in the Lakshadweep region is maximum during the monsoon period, Jun-Sep when  $\delta^{13}\text{C}$  shows a reduction. During the same period the SR region experiences a relatively cloudfree winter, contributing to a rising trend in the coral  $\delta^{13}\text{C}$ . The long term decreasing trend in both the cases are also remarkably similar. Further investigations on this aspect may be helpful in relating the southwest Indian monsoon and the Australian monsoon, the individual components of the broad-scale Asian monsoon.



## SUMMARY AND CONCLUSIONS

The primary aim of this thesis is to assess the utility of corals from the northern Indian Ocean coasts as a source of high resolution records of climatologic and oceanographic parameters of this region. Towards this, detailed measurements of stable oxygen and carbon isotopes and radiocarbon and preliminary studies of Cd were made in the annual bands of corals collected from the Lakshadweep islands and the Gulf of Kutch. In addition, oxygen and carbon isotope studies on two tracks in a coral from the Stanley Reef, Australia were also done to assess the intraband isotopic variability and its effect on the retrieval of climatic information from the isotopic records, and also for identifying the factors controlling the density band formation. A brief summary of the work and the conclusions arising from it are given below.

The corals studied are from three locations (i) the Lakshadweep islands (10°N, 73°E) (ii) the Gulf of Kutch (22.6°N, 70°E) and (iii) the Stanley Reef (19°15'S, 148°07'E). Of these the Lakshadweep islands and the Gulf of Kutch though are in the Arabian Sea, they are influenced by different climatic regimes. The SST variations in the Lakshadweep are upwelling dominated whereas in the Gulf of Kutch it is controlled mainly by summer heating and winter cooling.

*P. compressa* is the most abundant coral species in the Lakshadweep region. It secretes bands which are clearly discernible in an X-ray picture. These bands are about 15-20 mm thick and are deposited yearly as evidenced from oxygen isotopic studies.

The  $\delta^{18}\text{O}$  of corals from this location shows a seasonal fluctuation of about 0.8‰ corresponding to a 3-4 °C change in SST. This is consistent with the seasonal SST change in this region resulting from the monsoonal upwelling. The absolute values of  $\delta^{18}\text{O}$  and its seasonal amplitude in samples of the same species collected from different locations of Kavaratti lagoon of the Lakshadweep Archipelago are quite similar. This consistent

behaviour and spatial coherency in the oxygen isotope systematics indicate that it is a reliable SST indicator for this region. The absolute values of  $\delta^{18}\text{O}$  of this species of coral, however was found to be depleted by  $\sim 5\text{‰}$  compared to that expected for equilibrium  $\text{CaCO}_3$  precipitation. By comparing the  $\delta^{18}\text{O}$  of *P. compressa* with the  $\delta^{18}\text{O}$  in time contemporaneous samples of a giant clam (*Tridacna maximus*), which is known to precipitate  $\text{CaCO}_3$  in equilibrium, we have quantitatively determined the "disequilibrium offset" in this coral. Using the "disequilibrium offset" we have established a  $\delta^{18}\text{O}$ -SST relation for *Porites* corals from this region. This relation can provide SST with a precision better than about  $\pm 1.4^\circ\text{C}$ .

Comparison of the coral derived SST for the last 17 years with the available instrumental data shows a reasonable agreement between these two sets of data ( $\pm 1^\circ\text{C}$  on an average). This result suggests that the coral  $\delta^{18}\text{O}$  can be used to derive the actual SST of the ambient water. More precise determination of SST is possible if data on temporal variations of the oxygen isotopic composition of water for this region is available.

The carbon isotopic composition of the Lakshadweep coral seems to be controlled by endosymbiotic photosynthesis coupled with growth rate dependent fractionation. The  $\delta^{13}\text{C}$  shows a seasonal cyclicity of about  $1\text{‰}$ . The  $\delta^{13}\text{C}$  seasonality appears to be controlled indirectly by monsoon activity. During the monsoon season cloud cover increases, strong wind enhances the ocean currents and sediment suspension. These factors reduce the light level in the water causing reduction in zooxanthellar photosynthesis and hence  $\delta^{13}\text{C}$  in coral. The reduced  $\delta^{13}\text{C}$  is associated with high density band, as during monsoon reduction in photosynthesis reduces the coral growth resulting in high density band formation.

The absolute values of  $\delta^{13}\text{C}$  among samples collected from locations which are within  $\pm 60\text{km}$  shows significant variability, though all of these exhibit seasonal cyclicity of  $\sim 1\text{‰}$  with a dip in the monsoon season. Thus  $\delta^{13}\text{C}$  does not show spatially consistent behaviour among samples from nearby locations. This is unlike  $\delta^{18}\text{O}$  which shows spatial coherency. However the seasonal cyclicity of both  $\delta^{18}\text{O}$  and  $\delta^{13}\text{C}$  appear to be monsoon related. Therefore studies on the temporal changes in the seasonal cyclicities of  $\delta^{18}\text{O}$  and  $\delta^{13}\text{C}$  would be helpful in monitoring changes in monsoon intensity and upwelling, once quantified.

The coral (*F. speciosa*) from the Gulf of Kutch is characterized by lower growth rate

(~ 4mm/yr) compared to the Lakshadweep corals. The oxygen isotopic composition of this coral shows an average seasonal cyclicity of ~ 0.3‰, much less than the expected value (1.1‰) for a 6°C change in SST and ~ 0.3‰ change in oxygen isotopic composition of water between summer and winter. A major contributor to this damping in the seasonal  $\delta^{18}\text{O}$  amplitude seems to be the artifact of sampling corals having a slow growth rate. Sampling of corals having a growth rate of ~ 4mm/yr can yield only 2-4 months resolution which is insufficient to retrieve the full seasonal amplitude. Model simulation on the effect of sampling interval and sample thickness on the retrieval of seasonal amplitude suggests that for corals having growth rate of ~ 4mm/yr and sampled similar to the GKh coral, the seasonal amplitude could be damped by as much as ~ 50% because of sampling.

The  $\delta^{18}\text{O}$  time variations of the GKh coral show a higher order cyclicity (~ 7 yrs) a result not observed in the Lakshadweep corals. This long term change in  $\delta^{18}\text{O}$  shows a negative correlation with interannual rainfall variability. This can be explained in terms of SST-rainfall relationship. Since  $\delta^{18}\text{O}$  of coral decreases with increase in SST which also enhances the evaporation rate and hence precipitation, coral  $\delta^{18}\text{O}$  shows a negative correlation with rainfall.

The  $\delta^{13}\text{C}$  of the GKh coral also shows a seasonal cyclicity ~ 1‰, and appears to be controlled by endosymbiotic photosynthesis. The absolute  $\delta^{13}\text{C}$  values of GKh coral is significantly higher (~ 0.6-1.7 ‰) compared to the LDP corals. This could be because of several factors, species dependent fractionation, higher  $\delta^{13}\text{C}$  of ambient water resulting from enhanced rate of biological productivity and slower growth rate of the GKh coral. The coastal regions of the northern Arabian Sea has a higher productivity which can enrich the  $\Sigma\text{CO}_2$  of water (in  $\delta^{13}\text{C}$ ) and hence the coralline  $\delta^{13}\text{C}$ . Another reason for the  $\delta^{13}\text{C}$  enrichment in the GKh coral is its slower growth rate. Slower growth rate leads to isotopic values which are closer to equilibrium precipitation, hence the GKh coral shows higher values of both the  $\delta^{13}\text{C}$  and  $\delta^{18}\text{O}$  compared to the LDP corals.

Density and stable isotopic analyses were carried out in a coral *P. lutea* from the Stanley Reef, Australia in order to assess the intraband isotopic variability and their effect on the retrieval of climatic information from the isotopic records. Two tracks, one close to the central growth axis (~10°) and another ~ 20° off the growth axis were analyzed. The  $\delta^{18}\text{O}$  shows inverse relation with SST and rainfall variability of the surrounding region. The

carbon isotopic variation is related to insolation. This study reveals that the  $\delta^{18}\text{O}$ -SST correlation shows a progressive regression off the central growth axis. The lack of significant correlation between  $\delta^{18}\text{O}$  and density in either track suggests that the density band variations are not controlled by the SST variations.

Radiocarbon analyses were made in the annual bands of the GK<sub>h</sub> coral and in the rings of a teak tree collected from Thane (19°14'N, 73°24'E) near Bombay. These measurements were made to obtain the rates of air-sea exchange of  $\text{CO}_2$  and the advective mixing of water in this region. The  $\Delta^{14}\text{C}$  peak value of the Thane tree in the year 1964 is  $\sim 630$  ‰, significantly lower than that of the atmospheric  $\Delta^{14}\text{C}$  of the northern hemisphere ( $\sim 1000$  ‰). The radiocarbon time series of the GK<sub>h</sub> coral was modelled considering the supply of  $^{12}\text{CO}_2$  and  $^{14}\text{CO}_2$  to the gulf (GK<sub>h</sub>) through air-sea exchange and advective water transport from the Arabian Sea. Reasonable fit for the GK<sub>h</sub> coral data was obtained with air-sea exchange rate of  $11\text{-}12 \text{ mol m}^{-2} \text{ yr}^{-1}$ , upwelling velocity  $\sim 10 \text{ m yr}^{-1}$  (in the Arabian Sea) and advective velocity of  $28 \text{ m yr}^{-1}$  between Arabian Sea and the Gulf of Kutch. The model results also suggest that it is not possible to reproduce the radiocarbon time series in the GK<sub>h</sub> coral without considering the advective supply of carbon and radiocarbon to the gulf from the Arabian Sea. Further the model also predicts that with the typical  $\text{CO}_2$  exchange rate of  $8\text{-}25 \text{ mol m}^{-2} \text{ yr}^{-1}$  the  $\Delta^{14}\text{C}$  in corals would be much higher than commonly observed if dilution by advective supply is not considered. The deduced velocity ( $\sim 28 \text{ m/yr}$ ) of the advective transport of water between the gulf and the Arabian Sea is much lower than the surface current velocity in this region, but can be understood in terms of fluxes of carbon and radiocarbon to the gulf to match the observed coral  $\Delta^{14}\text{C}$  time series.

## SCOPE FOR FURTHER WORK

The work presented in this thesis represents the first detailed study of stable isotopic and radiocarbon systematics in corals from the Indian coasts. The study was conducted to explore the utility of these corals as a source of climatic and oceanographic recorders for this region. The results, as summarized in the earlier pages are very encouraging and attest to the use of corals as high resolution records of "ocean climate".

The reconstruction of the historical SST data using the coralline  $\delta^{18}\text{O}$  in both spatial and temporal domain would be important for climate models aimed at establishing relation between the SST and monsoon and eventually predicting monsoon rainfall. Such models would naturally require high precision historical data, which at present are difficult to retrieve from coral studies. Availability of data of the temporal variability of  $\delta^{18}\text{O}$  of ambient water, and more precise estimate of the disequilibrium offset should help retrieve the historical SST with better precision. An independent approach would be to use the Sr/Ca thermometry in coral.

One of the important climate systems in the tropics is monsoon. To understand the monsoon dynamics, its characteristic behaviour in seasonal and interannual time scale, it is essential to have a detailed knowledge of its past variability. Analysis of longer cores of corals from the Lakshadweep region will be extremely helpful in this aspect. The present work has revealed that the  $\delta^{18}\text{O}$  of coral faithfully records the seasonal sea surface cooling induced by monsoon upwelling. Our results show that the enhancement of the  $\delta^{18}\text{O}$  and the depletion in the  $\delta^{13}\text{C}$  of coral take place during the monsoon period. Detailed investigation in this direction is necessary to quantify the  $\delta^{18}\text{O}$ - $\delta^{13}\text{C}$  relationship. These characteristics can be used as indices to quantify the changes in monsoon intensity. This can be further augmented by the combined analyses of stable isotope and cadmium data, since cadmium concentration is a measure of upwelling.

The interpretation of carbon isotopic records, as already mentioned has been difficult since the factors contributing to its fractionation are not well understood. We have shown that in the Lakshadweep region the seasonal cyclicity in the  $\delta^{13}\text{C}$  of coral is controlled by zooxanthellar photosynthesis modulated by monsoon activities. However the

causes for difference in the  $\delta^{13}\text{C}$  absolute values among samples collected from nearby locations and its long term trends need to be better understood. It is essential to know more about the causative mechanisms of the spatial and temporal (decadal timescale) trend in  $\delta^{13}\text{C}$  which would help in developing better models for the oceanic uptake of fossil fuel  $\text{CO}_2$ . To gain a better knowledge on the controlling factors of the coralline  $\delta^{13}\text{C}$ , better data on seasonal variability of water column productivity and  $\delta^{13}\text{C}$  of  $\Sigma\text{CO}_2$  of water are needed.

The *Favia* coral from the Gulf of Kutch is characterized by lower growth rate, which limits its utility for retrieving climatic information on seasonal time scale. However the analysis of oxygen isotopes seems to be promising in retrieving qualitative information of rainfall variability and the carbon isotope would be useful to estimate the past productivity. Combined analyses of time contemporaneous samples of the coralline  $\delta^{13}\text{C}$  and sea surface productivity is warranted to quantify the  $\delta^{13}\text{C}$ -productivity relation. Analysis of other coral species having higher growth rate like *Porites* from this region will be useful to understand the monsoon related phenomena in finer resolution.

The extension of the radiocarbon analysis in coral bands dated back to 30's or 40's will provide the pre-bomb surface sea  $\Delta^{14}\text{C}$ . Since many of the oceanic models deal with steady state conditions, an accurate determination of the steady state difference in atmosphere and oceanic  $\Delta^{14}\text{C}$  would be essential to constrain these models. A longer time series of coral bands back in time would provide information of "Suess effect" in the Arabian Sea vis-a-vis in other oceanic regions. High resolution measurements of oceanic and atmospheric  $\Delta^{14}\text{C}$  may give valuable information about the seasonal dependence of the  $\text{CO}_2$  exchange rate, and also the role of the Arabian Sea in the overall air-sea exchange and carbon budget. Extension of the modelling work on  $\Delta^{14}\text{C}$  from steady state to transient case, incorporating the temporal change in atmospheric  $\text{CO}_2$  concentration would provide better constraints on the  $\text{CO}_2$  air-sea exchange and ocean water mixing rates.

## REFERENCES

- Aharon P. (1985) Carbon isotope record of late Quaternary coral reefs: possible index of sea surface paleoproductivity. In: ET Sundquist and WS Broecker (eds), *The Carbon Cycle and Atmospheric CO<sub>2</sub>: Natural Variations Archean to Present*. Geophysical Monograph 32. Am. Geophys. Union, Washington, DC, pp 343-355.
- Aharon P. (1991) Recorders of reef environment histories: stable isotopes in corals, giant clams, and calcareous algae. *Coral Reefs* 10:71-90.
- Aharon P. and Chappel J. (1986) Oxygen isotopes, sea level changes and the temperature history of a local reef environment in New Guinea over the last 10<sup>5</sup> years. *Palaeogeogr. Palaeoclimatol. Palaeoecol.* 56:337-379.
- Bacastow R.B. and Keeling C.D. (1981) Atmospheric carbon dioxide concentration and the observed airborne fraction. In: B. Bolin (ed) *Carbon Cycle Modelling*. John Wiley, New York, pp 103-112.
- Barnes D.J. and Lough J.M. (1989) The nature of skeletal density banding in scleractinian corals: fine banding and seasonal patterns. *J. Exp. Mar. Biol. Ecol.* 126:119-134.
- Beatty R.D. (1978) Concepts, Instrumentation and Techniques in Atomic Absorption Spectrometry, Perkin-Elmer, 49 pp.
- Beck J.W., Edwards R.L., Ito E., Taylor F.W., Recy J., Rougerie F., Joannot P., and Henin C. (1992) Sea-surface temperature from coral skeletal strontium/calcium ratios. *Science* 257:644-647.
- Bhushan R., Chakraborty S. and Krishnaswami S. (1993) Physical Research Laboratory (Chemistry) radiocarbon date list CH-1 Submitted to *Radiocarbon*.
- Boyle E.A., Sclater F.R. and Edmond J.M. (1976) On the marine geochemistry of cadmium. *Nature* 263:42-44.
- Brock J.C. and McClain C.R. (1992) Interannual variability in phytoplankton blooms observed in the northwestern Arabian Sea during the south-west monsoon *J. Geophys. Res.* 97:733-750.
- Broecker W.S., Peng T.H., Mathieu G., Hesselin R. and Torgersen T. (1980) Gas exchange rate measurements in natural systems. *Radiocarbon* 22:676-683.
- Broecker W.S., Peng T.H., Östlund G. and Stuiver M. (1985) The distribution of bomb radiocarbon in the ocean. *J. Geophys. Res.* 90:6953-6970.
- Bruland K.W. (1983) Trace elements in seawater. In: *Chemical Oceanography* vol 8 JP

- Riley and R. Chester (eds), Academic Press, London, pp 157-220.
- Buddemeier R.W. (1974) Environmental Controls Over Annual and Lunar Monthly Cycles in Hermatypic Coral Calcification. *Proc. 2nd Int. Coral Reef Symp.* 259-267.
- Buddemeier R.W., Maragos J.E. and Knutson D.W. (1974) Radiographic studies of reef coral exoskeletons: rates and patterns of coral growth. *J. Exp. Mar. Biol. Ecol.* 14:179-200.
- Cain W.F. and Suess H.E. (1976) Carbon-14 in tree rings. *J. Geophys. Res.* 81:3688-3694.
- Cember R.P. (1989) Bomb radiocarbon in the Red Sea: a medium scale gas exchange experiment. *J. Geophys. Res.* 94:2111-2123.
- Cole J.E. and Fairbanks R.G. (1990) The southern oscillation recorded in the  $\delta^{18}\text{O}$  of corals from Tarawa Atoll. *Paleoceanography* 5:669-683.
- Cole J.E., Shen G.T., Fairbanks R.G. and Moore M. (1992) Coral monitors of El Niño/Southern Oscillation dynamics across the equatorial Pacific. In: H Diaz and V Markgraf (eds), El Niño: Historical and Paleoclimatic aspects of the Southern Oscillation. Cambridge University Press, Cambridge, UK, pp 349-375.
- Craig H. (1957) Isotopic standards for carbon and oxygen and correction factors for mass spectrometric analysis of carbon di-oxide. *Geochim. Cosmochim. Acta* 12:133-149.
- Craig H. (1965) The measurement of oxygen isotope paleotemperatures. In: E Tongiorgi (ed), Stable isotopes in Oceanographic Studies and Paleotemperatures. Third SPOLETO Conference on Nuclear Geology. Pisa, Italy, pp 161-181.
- Craig H. and Gordon L.I. (1965) Deuterium and oxygen 18 variations in the ocean and the marine atmosphere. In: E Tongiorgi (ed), Stable isotopes in Oceanographic Studies and Paleotemperatures. Third SPOLETO Conference on Nuclear Geology. Pisa, Italy, pp 161-181.
- de Villiers S., Shen G.T., and Nelson B.K. (1993) Sr/Ca thermometry in corals: method calibration and evaluation of  $(\text{Sr}/\text{Ca})_{\text{seawater}}$  and interspecies variability. *Geochim. Cosmochim. Acta*. (in press).
- de Vries H. (1958) Variations in concentration of radiocarbon with time and location on earth. *K. Ned. Akad. Wet., Proc. Ser. B*, 61:94-102.
- Dodge R.E. and Thomson J. (1974) The natural radiochemical and growth records in contemporary hermatypic corals from the Atlantic and Caribbean. *Earth Planet. Sci. Lett.* 23:313-322.
- Druffel E.M. (1980) Radiocarbon in annual coral rings of Belize and Florida. *Radiocarbon*



- Druffel E.M. (1981) Radiocarbon in annual coral rings from the eastern tropical Pacific Ocean. *Geophys. Res. Lett.* 8:59-62.
- Druffel E.M. (1985) Detection of El Nino and decade time scale variations of sea surface temperature from banded coral records :implication for the carbon dioxide cycle. In: ET Sundquist and WS Broecker (eds), *The Carbon Cycle and Atmospheric CO<sub>2</sub>: Natural Variations Archean to Present*. Geophysical Monograph 32, Am. Geophys. Union, Washington, DC, pp 111-122.
- Druffel E.M. (1987) Bomb radiocarbon in the Pacific: Annual and seasonal time scale variations. *J. Mar. Res.* 45:667-698.
- Druffel E.M. (1989) Decade time scale variability of ventilation in the North Atlantic: high precision measurements of bomb radiocarbon in banded corals. *J. Geophys. Res.* 94:3271-3285.
- Druffel E.M. and Linick T.W. (1978) Radiocarbon in annual coral rings of Florida. *Geophys. Res. Lett.* 5:913-916.
- Druffel E.M. and Suess H.E. (1983) On the radiocarbon record in banded corals: exchange parameters and net transport of <sup>14</sup>CO<sub>2</sub> between atmosphere and surface ocean. *J. Geophys. Res.* 8:1271-1280.
- Dunbar R.B. and Wellington G.M. (1981) Stable isotopes in a branching coral monitor seasonal temperature variation. *Nature* 293:453-455.
- Duplessy J.C., Be A.W.H., and Blanc P.L. (1981) Oxygen and carbon isotopic composition and biogeographic distribution of planktonic foraminifera in the Indian Ocean. *Palaeogeogr. Palaeoclimatol. Palaeoecol.* 33:9-46.
- Emiliani C. (1956) Oxygen isotopes and paleotemperature determinations. IVth Congr.Int. Assoc. Quat. Res., pp 831-843.
- Emiliani C., Hudson J.H., Shinn E.A., and George R.Y. (1978) Oxygen and carbon isotopic growth records in a reef coral from the Florida Keys and a deep sea coral from Blake Plateau. *Science* 202:627-629.
- Epstein S., Buchsbaum R., Lowenstam H.A., and Urey H.C. (1953) Revised carbonate-water-isotopic temperature scale. *Geol. Soc. Am. Bull.* 64:1315-1326.
- Esbensen S.K. and Kushnir Y. (1981) The heat budget of the global ocean: an atlas based on estimate from surface marine observations, Rep 29, Clim. Res. Inst. Oreg State Univ., Corvallis.
- Fairbanks R.G. and Dodge R.E. (1979) Annual periodicity of the <sup>18</sup>O/<sup>16</sup>O and <sup>13</sup>C/<sup>12</sup>C

- ratios in the coral *Montastrea annularis*. *Geochim. Cosmochim Acta* **43**:1009-1020.
- Fritts H.C. (1976) Tree rings and climate. Academic Pres, London, 567 pp.
- Gat J.R. and Gonfiantini R.(eds) (1981) Stable isotope hydrology, deuterium and oxygen-18 in the water cycle. Int. Hydro. Prog. Technical Report Series 210, IAEA, Vienna, 337 pp.
- Goreau T.J. (1977) Coral skeleton chemistry : physiological and environmental regulation of stable isotopes and trace metals in *Montastrea annularis*. Proc. Roy. Soc. London B, **196**:291-315.
- Grossman E.L. and Ku T.L. (1986) Oxygen and carbon isotope fractionation in biogenic aragonite: temperature effects. *Chem. Geol.* **59**:59-74.
- Gupta S.K. and Polach H.A. (1985) Radiocarbon dating practices at ANU, Radiocarbon Laboratory handbook, Research School of Pacific Studies, Australian National University, Canberra, 173 pp.
- Hagemann F.T., Gray J., Jr, and Machta L. (1965) Carbon-14 measurements in the atmosphere 1953 to 1964, *U. S. At. Energy Comm. Rep. HASL-159*, 124 pp.
- Hastenrath S. and Lamb P.J. (1979) Climatic atlas of the Indian Ocean Part I: Surface climate and atmospheric circulation, The university of Wisconsin Press, Madison, Wisconsin, USA.
- Hastenrath S. and Lamb P.J. (1980) On the heat budget of the hydrosphere and atmosphere in the Indian Ocean. *J. Phys. Oceanogr.* **10**:694:708.
- Highsmith R.C. (1979) Coral growth rates and environmental control of the density banding *J. Exp. Mar. Biol. Ecol.* **37**:105-125.
- Kessler M.J. (1989) Liquid Scintillation Analysis Science and Technology. Packard Instrument Company. Publication No. 169-3052, 413 pp.
- Knutson D.W., Buddemeier R.W., and Smith S.V. (1972) Coral chronometers:seasonal growth bands in reef corals. *Science* **177**:270-272.
- Kusumgar S. (1965) Study of the geophysical processes based on  $C^{14}/C^{12}$  ratios in the atmosphere. M. Sc thesis, University of Bombay, Bombay, 55 pp.
- Land L.S., Lang J.C. and Barnes D.J., (1975) Extension rate: a primary control on the isotopic composition of West Indian (Jamaican) scleractinian reef coral skeletons. *Mar. Biol.* **33**:221-233.
- Lea D.W., Shen G.T., and Boyle E.A. (1989) Coralline barium records temporal variability in Equatorial Pacific upwelling. *Nature* **340**:373-376.

- Leder J.J., Szmant A.M., and Swart P.K. (1991) The effect of prolonged "bleaching" on skeletal banding and stable isotopic composition in *Montastrea annularis*. *Coral Reefs* 10:19-27.
- Levin I., K.O. Munnich and W. Weiss (1980) The effect of anthropogenic CO<sub>2</sub> and <sup>14</sup>C sources on the distribution of <sup>14</sup>C in the atmosphere. *Radiocarbon* 22:379-391
- Lough J.M. and Barnes D.J. (1990) Possible relationship between environmental variables and skeletal density in a coral colony from the Central Great Barrier Reef. *J. Exp. Mar. Biol. Ecol.* 134:221-241.
- Lough J.M. (1993) Climate variability and El Niño-Southern Oscillation events in the vicinity of the Great Barrier Reef : 1958 to 1987 (pre-print).
- Macintyre I.C. and Smith S.V. (1974) X-radiographic studies of skeletal development in coral colonies. *Proc. 2nd Int. Symp. on Coral Reefs*. pp 269-276.
- McConnaughey T. (1989) <sup>13</sup>C and <sup>18</sup>O isotopic disequilibrium in biological carbonates: I. Patterns. *Geochim. Cosmochim. Acta* 53:151-162.
- Moore W.S. and Krishnaswami S. (1974) Correlation of X-radiography revealed banding in corals with radiometric growth rates. *Proc. 2nd Int. Coral Reef Symp.* Brisbane, pp 269-276.
- Moore W.S., Krishnaswami S., and Bhat S.G. (1973) Radiometric determination of coral growth rates. *Bull. Mar. Sci.* 23:157-176.
- Noakes J.E., Kim S. and Stipp J.J. (1965) Chemical and counting advances in liquid scintillation age dating. In: RM Chatters and EA Olson (eds), *Proc. Int. Conf. on <sup>14</sup>C and Tritium Dating*. NBS, Washington, DC, USAEC 650-652. pp 68-92.
- Nozaki Y., Rye D.M., Turekian K.K., and Dodge R.E. (1978) A 200 year record of carbon-13 carbon-14 variations in a Bermuda coral. *Geophys. Res. Lett.* 5:825-828.
- Nydal R. and Lövseth K. (1983) Tracing bomb <sup>14</sup>C in the atmosphere 1962-1980 *J. Geophys. Res.* 88:3621-3642.
- Pant G.B. and Borgaonkar H.P. (1983) Growth rings of teak tree and regional climatology (an ecological study of Thane region) In: LR Singh *et al.* (eds). *Environmental Management*, Allahabad Geographical Society, Univ. Allahabad, India pp. 153-158.
- Pätzold J. (1984) Growth rhythms recorded in stable isotopes and density bands in the reef coral *Porites lobata* (Cebu, Philippines). *Coral Reefs* 3:87-90.
- Paul D.K., Bhide U.V., Ghanekar S.P. and Sikka D.R. (1992) Variability of sea surface temperature over the Arabian Sea and organised convection over Indian region during summer monsoon, In: BN Deasi (ed), *Oceanography of the Indian Ocean*.

Oxford and IBH Publishing Co. (P) Ltd. New Delhi, pp 627-635.

- Pillai C.S.G. and Patel M.I. (1988) Scleractinian corals from the Gulf of Kutch. *J. Mar. Biol. Ass. India* 30:54-74.
- Qasim S.Z. (1982) Oceanography of the northern Arabian Sea. *Deep Sea Res.* 9:1041-1068.
- Ramesh R., Bhattacharya S.K. and Pant G.B. (1989) Climatic significance of  $\delta D$  variations in a tropical tree species from India. *Nature* 337:149-150.
- Romanek C.S., and Grossman E.L. (1989) Stable isotopes profile of *Tridacna maxima* as environmental indicators. *Palaios* 4:402:413.
- Sadler J.C., Lander M.A., Hori A.M., and Oda L.K. (1987) Tropical marine climatic atlas Vol 1. Indian Ocean and Atlantic Ocean. Department of Meteorology, University of Hawaii.
- Sarkar A. (1989) Oxygen and carbon isotopes in Indian Ocean sediments and their paleoclimatic implications. PhD Thesis. Gujarat University, Ahmedabad, 164 pp.
- Sarkar A, Ramesh R., Bhattacharya S.K., and Rajagopalan G. (1990)  $\delta^{18}O$  evidence for a stronger north-east monsoon current during the last glaciation. *Nature* 433:549-551.
- Sathyendranath S., Gouveia A.D., Shetye S.R., Ravindran P. and Platt T. (1991) Biological control of surface temperature in the Arabian Sea. *Nature* 349:54-55.
- Shen G.T., Boyle E.A. and Lea D.W. (1987) Cadmium in corals as a tracer of historical upwelling and industrial fallout. *Nature* 328:794-796.
- Shen G.T. and Boyle E.A. (1988) Determination of lead, cadmium and other trace elements in annually-banded corals. *Chem. Geol.* 67:47-62.
- Shen, G.T. and Sanford C. L. (1990) Trace element indicators of climatic variability in reef building corals. In: PE Glynn (ed), Global Ecological Consequences of the 1982-83 El Niño-Southern Oscillation. Elsevier, New York. pp 255-284.
- Shen G.T., Cole J.E., Lea D.W., Linn L.J., McConnaughey T., and Fairbanks R.G. (1992) Surface ocean variability at Galapagos from 1936-1982: calibration of geochemical tracers in corals. *Paleoceanography* 7:563-588.
- Shukla J. (1975). Effect of Arabian sea surface temperature anomaly on Indian summer monsoon : a numerical experiment with the GFDL model. *J. Atmos. Sci.* 32:503-511.
- Shukla J. and Mishra B.N. (1977) Relationship between sea surface temperature and

- wind speed over the central Arabian sea and monsoon rainfall over India. *Mon. Wea. Rev.* **105**:998-1002.
- Siegenthaler U. (1983) Uptake of excess CO<sub>2</sub> by an outcrop-diffusion model of the ocean. *J. Geophys. Res.* **88**:3599-3608.
- Siegenthaler U. and Sarmiento J.L. (1993) Atmospheric carbon dioxide and the ocean. *Nature* **365**:119-125
- Smith S.V. Buddemeier R.W., Redalje R.C. and Houck J.E. (1979): Strontium-calcium thermometry in coral skeletons. *Science* **204**:404-407.
- Srivastava P.S. and John V.C. (1977) Current regime in the Gulf of Kutch. *Ind. J. Mar. Sci.* **6**:39-48.
- Stuiver M (1980) <sup>14</sup>C distribution in the Atlantic Ocean. *J. Geophys. Res.* **85**:2711-2718.
- Stuiver M. (1980a) Workshop on <sup>14</sup>C data reporting *Radiocarbon* **22**:964-966.
- Stuiver M. and Polach H.A. (1977) Discussion Reporting <sup>14</sup>C data. *Radiocarbon*, **19**: 355-363.
- Stuiver M. and Quay P.D. (1981) Atmospheric <sup>14</sup>C changes resulting from fossil fuel CO<sub>2</sub> release and cosmic ray flux variability. *Earth Planet. Sci. Lett.* **53**:349-362.
- Stuiver M. and Östlund H.G. (1983) GEOSECS Indian Ocean and Mediterranean radiocarbon. *Radiocarbon* **25**:1-29.
- Suresh V.R. and Mathew K.J. (1993) Skeletal extension of staghorn coral *Acropora formosa* in relation to environment at Kavaratti atoll (Lakshadweep). *Ind. J. Mar. Sci.* **22**:176-179.
- Swart P.K. (1983) Carbon and oxygen isotope fractionation in scleractinian corals: a review. *Earth Sci. Rev.* **19**:51-80.
- Toggweiler J.R., Dixon K. and Broecker W.S. (1991) The Peru upwelling and the ventilation of the south Pacific thermocline. *J. Geophys. Res.* **96**:20467-20497.
- Urey H.C. (1947) The thermodynamic properties of isotopic substances. *J. Chem. Soc.* pp 562-581.
- Wafar M.V.W. (1986) Corals and coral reefs of India *Proc. Indian Acad. Sci. (Animal/Plant Sci)* suppl. pp. 19-43.
- Warren B.A. (1992) Circulation of north Indian deep water in the Arabian Sea. In: Oceanography of the Indian Ocean. BN Desai (ed). Oxford and IBH Publishing Co. Pvt. Ltd. New Delhi. pp 575-582.

- Weber J.N. (1974)  $^{13}\text{C}/^{12}\text{C}$  ratios as natural isotopic tracers elucidating calcification processes in reef building and non-reef-building corals. *Proc. 2nd Int. Coral Reef Symp*, Great Barrier Reef Committee, Brisbane, pp 289-298.
- Weber J.N., and Woodhead P.M.J (1972). Temperature dependence of oxygen-18 concentration in reef coral carbonates. *J. Geophys. Res.* **77**:463-473.
- Weber J.N. (1974)  $^{13}\text{C}/^{12}\text{C}$  Ratios as Natural Isotopic tracers Elucidating Calcification Processes in Reef-building and Non Reef-building Corals. *Proc. 2nd Int. Coral Reef Symp.*, pp 289-298.
- Weber J.N., Eugene W.W., and Weber P.H. (1975) Correlation of density banding in reef coral skeletons with environmental parameters: the basis for interpretation of chronological records preserved in the coralla of corals. *Paleobiology* **1**:137-149.
- Weidman C.R. and Jones G.A. (1993) A shell derived time history of bomb  $^{14}\text{C}$  on Georges Bank and its Labrador Sea implications. *J. Geophys. Res.* **98**:14577-14588.
- Wellington G.M. and Glynn P.W. (1983) Environmental influences on skeletal banding in eastern Pacific (Panama) corals. *Coral Reefs* **1**:215-222.
- Wyrtki K. (1971) Oceanographic atlas of the International Indian Ocean Expedition NSF, Washington DC, 531 pp.

# Appendix - A

Table III.2 Oxygen isotopic records of KV-1; Am and GC

Year & Month	Kavartti coral		Amini coral		Giant Clam	
	Dis. (mm)	$\delta^{18}\text{O}(\text{‰})$	Dis. (mm)	$\delta^{18}\text{O}(\text{‰})$	Dis. (mm)	$\delta^{18}\text{O}(\text{‰})$
					clam collected	
			coral collected		0.0	-0.29
					2.2	-0.37
Aug '88			0.0	-5.29	3.7	-0.20
			3.6	-5.03	5.5	-0.11
			6.1	-5.13		
			8.5	-5.07	7.4	-0.21
			10.9	-5.34	8.6	-0.18
					10.1	-0.43
May '88					11.4	-0.55
			13.7	-5.67	12.9	-1.25
					14.3	-0.96
					15.6	-1.04
					17.0	-0.73
					18.9	-0.84
					20.7	-0.91
					22.6	-0.67
					24.1	-0.85
			16.6	-5.38	25.7	-0.84
					27.7	-0.81
			19.3	-5.53	29.7	-0.68
					31.4	-0.67
					33.1	-0.67
			21.8	-5.23	34.8	-0.58
			24.7	-5.09	36.6	-0.47
					38.1	-0.62
Aug '87	11.2	-5.14	26.5	-5.10	40.0	0.43
	12.1	-5.15	29.5	-5.14		



Table III.2 contd.

Year & Month	Kavartti coral		Amini coral		Giant Clam	
	Dis. (mm)	$\delta^{18}\text{O}(\text{‰})$	Dis. (mm)	$\delta^{18}\text{O}(\text{‰})$	Dis. (mm)	$\delta^{18}\text{O}(\text{‰})$
May '87	13.8	-5.15	31.8	-5.18	42.8	-0.87
	15.0	-5.33				
	17.2	-5.36	34.7	-5.18		
	18.2	-5.39				
	19.0	-5.42	37.3	-5.35	44.7	-0.87
	20.1	-5.34			46.4	-0.76
	21.0	-5.38			48.1	-0.87
	21.8	-5.29	40.4	-5.12	49.8	-0.62
					51.3	-0.72
	22.8	-5.03			53.2	-0.69
	23.5	-5.17			55.8	-0.51
	24.2	-4.97				
	25.3	-5.22	43.1	-5.20	57.8	-0.31
	26.4	-4.86			59.7	-0.37
					62.3	-0.63
Aug '86	27.5	-5.29	45.8	-5.14	64.3	-0.26
	28.3	-5.11	48.5	-4.92	66.3	-0.34
					68.2	-0.50
	29.2	-5.25			69.5	-0.46
	29.8	-4.81	51.2	-4.63	71.4	-0.25
	31.0	-5.14				
	31.6	-5.04				
	32.3	-5.07	53.6	-4.93	72.9	-0.35
	33.2	-5.02			74.3	-0.43
	34.2	-5.20				
	35.1	-5.11				
	35.8	-5.23				

Table III.2 contd.

Year & Month	Kavartti coral		Amini coral		Giant Clam	
	Dis. (mm)	$\delta^{18}\text{O}(\text{‰})$	Dis. (mm)	$\delta^{18}\text{O}(\text{‰})$	Dis. (mm)	$\delta^{18}\text{O}(\text{‰})$
Aug '85	36.5	-5.32	56.5	-4.81	76.1	-0.92
	37.7	-5.33				
	38.5	-5.44				
	39.5	-5.64	59.1	-5.52	78.1	-1.21
	40.2	-5.53				
	41.1	-5.56	62.1	-5.24		
	42.2	-5.59				
	43.2	-5.53				
	44.0	-5.41				
	44.9	-5.49	64.3	-5.39		
	45.9	-5.39				
	46.9	-5.69	67.5	-4.81		
	48.0	-5.58				
	48.8	-4.93				
	49.7	-4.87	70.4	-4.75	79.9	-0.53
	50.7	-5.01				
	51.6	-4.94				
	52.3	-4.90				
	53.2	-4.90	72.6	-4.92		
	54.0	-5.13				
	54.7	-4.93				
	55.5	-4.98	74.9	-5.00		
	56.2	-4.98				
	57.0	-5.04				
	58.0	-5.08	77.5	-4.99		
	58.7	-5.13				
	59.5	-5.25				

Table III.2 contd.

Year & Month	Kavartti coral		Amini coral		Giant Clam	
	Dis. (mm)	$\delta^{18}\text{O}(\text{‰})$	Dis. (mm)	$\delta^{18}\text{O}(\text{‰})$	Dis. (mm)	$\delta^{18}\text{O}(\text{‰})$
May '85	60.2	-5.37				
	61.0	-5.34	81.0	-5.25		
	61.9	-5.56				
	62.5	-5.34				
	63.5	-5.62	83.8	-5.55	82.0	-1.19
	64.4	-5.57			84.0	-1.08
	65.1	-5.42				
	66.1	-5.46				
	66.8	-5.46			86.2	-1.07
	67.7	-5.46			87.9	-0.98
	68.4	-5.20				
	69.2	-5.25			89.9	-0.78
	70.2	-5.10				
	71.0	-4.94			92.1	-0.72
	72.0	-5.01				
	72.8	-4.99				
	73.9	-5.03	87.2	-5.21	95.5	-0.49
	74.9	-4.81				
	75.5	-4.82				
	76.3	-4.85			98.0	-0.73
	77.0	-4.85				
Aug '84	77.6	-4.69	89.8	-4.60	100.4	-0.22
	78.5	-5.00			102.4	-0.38
	79.3	-4.97			105.1	-0.53
	80.2	-4.92	coral starts growing			
	81.0	-4.90				
	81.5	-5.10				
	82.3	-4.96			108.5	-0.70

Table III.2 contd.

Year & Month	Kavartti coral		Amini coral		Giant Clam	
	Dis. (mm)	$\delta^{18}\text{O}(\text{‰})$	Dis. (mm)	$\delta^{18}\text{O}(\text{‰})$	Dis. (mm)	$\delta^{18}\text{O}(\text{‰})$
May '84	83.2	-5.19			108.5	-0.70
	83.9	-5.12				
	84.5	-5.39			111.5	-0.53
	85.5	-5.30				
	86.2	-5.48			115.3	-0.66
	87.0	-5.33				
	87.7	-5.52			118.2	-0.56
	88.5	-5.47			121.0	-0.94
	89.3	-5.44				
	90.0	-5.49				
	91.0	-5.32				
	91.7	-5.41				
	92.5	-5.33				
	93.3	-5.37				
	94.1	-5.18				
	94.8	-5.46				
	95.7	-5.28				
	96.2	-5.21				
	97.4	-4.80				
	98.1	-4.75				
	98.9	-4.84				
	99.7	-5.00				
Aug '83	100.4	-4.61			124.1	-0.44
	101.2	-4.74				
	102.2	-4.84				
	102.8	-4.86				
	103.5	-4.78				
	104.2	-4.67				

Table III.2 contd.

Year & Month	Kavartti coral		Amini coral		Giant Clam	
	Dis. (mm)	$\delta^{18}\text{O}(\text{‰})$	Dis. (mm)	$\delta^{18}\text{O}(\text{‰})$	Dis. (mm)	$\delta^{18}\text{O}(\text{‰})$
May '83	105.0	-4.89			126.6	-0.99
	105.7	-4.84			clam starts growing	
	106.7	-4.90				
	107.4	-4.92				
	108.3	-4.89				
	109.2	-5.00				
	110.0	-4.94				
	110.7	-4.99				
	111.5	-4.91				
	112.2	-5.14				
	113.1	-4.82				
	114.0	-5.03				
	115.0	-4.77				
	116.0	-4.97				

Table III.3 Carbon isotopic data of coral KV-1

Year & month	distance (mm)	$\delta^{13}\text{C}(\text{‰})$	Year & month	distance (mm)	$\delta^{13}\text{C}(\text{‰})$
	0.0	-0.84		36.5	-1.33
	2.0	-0.61		37.7	-1.31
	3.5	-0.91		38.5	-1.12
	5.0	-0.93	May '86	39.5	-0.59
	6.0	-0.70		40.2	-0.44
	7.5	-0.91		41.1	-0.38
	8.9	-1.19		42.2	-0.33
Aug '87	11.2	-0.96		43.2	-0.22
	12.1	-1.09		44.0	-0.15
	13.8	-0.70		44.9	-0.10
	15.0	-1.31		45.9	-0.43
	17.2	-1.21		46.9	-0.66
	18.2	-0.11		48.0	-0.78
May '87	19.0	-0.22		48.8	-0.33
	20.1	-0.27	Aug '85	49.7	-0.30
	21.0	-0.40		50.7	-0.16
	21.8	-0.40		51.6	-0.24
	22.8	-0.54		52.3	-0.41
	23.5	-0.46		53.2	-0.73
	24.2	-0.50		54.0	-0.90
	25.3	-0.56		54.7	-1.27
	26.4	-0.91		55.5	-1.22
	27.5	-0.97		56.2	-1.27
	28.3	-0.73		57.0	-1.06
	29.2	-0.43		58.0	-1.15
Aug '86	29.8	-0.80		58.7	-1.12
	31.0	-1.21		59.5	-1.42
	31.6	-0.83		60.2	-1.16
	32.3	-0.83		61.0	-1.40
	33.2	-1.01		61.9	-1.09
	34.2	-1.33		62.5	-0.78
	35.1	-1.14	May '85	63.5	-0.57
	35.8	-1.39		64.4	-0.48

Table III.3 contd.

Year & month	distance (mm)	$\delta^{13}\text{C}(\text{‰})$	Year & month	distance (mm)	$\delta^{13}\text{C}(\text{‰})$
	65.1	-0.28		91.0	-0.53
	66.1	-0.29		91.7	-0.58
	66.8	-0.30		92.5	-0.63
	67.7	-0.29		93.3	-0.59
	68.4	-0.52		94.1	-0.72
	69.2	-0.61		94.8	-0.80
	70.2	-0.41		95.7	-0.61
	71.0	-0.43		96.2	-0.57
	72.0	-0.52		97.4	-0.27
	72.8	-0.51		98.1	-0.52
	73.9	-0.48		98.9	-0.48
	74.9	-0.52		99.7	-0.63
	75.5	-0.93	Aug '83	100.4	-0.31
	76.3	-0.88		101.2	-0.46
	77.0	-0.65		102.2	-0.85
Aug '84	77.6	-0.85		102.8	-1.06
	78.5	-0.78		103.5	-1.20
	79.3	-0.71		104.2	-1.02
	80.2	-0.82		105.0	-1.25
	81.0	-0.77		105.7	-1.23
	81.5	-0.84		106.7	-1.03
	82.3	-0.91		107.4	-1.23
	83.2	-1.40		108.3	-0.99
	83.9	-1.14		109.2	-0.97
	84.5	-0.86		110.0	-0.69
	85.5	-0.90		110.7	-0.83
	86.2	-0.57		111.5	-0.65
	87.0	-0.45	May '83	112.2	-0.87
May '84	87.7	-0.46		113.1	-0.46
	88.5	-0.37		114.0	-0.61
	89.3	-0.32		115.0	-0.31
	90.0	-0.43		116.0	-0.51

Table III.5 Oxygen and carbon isotope data of KV-2 coral

Year	$\delta^{18}\text{O}$ (‰)	$\delta^{13}\text{C}$ (‰)	Year	$\delta^{18}\text{O}$ (‰)	$\delta^{13}\text{C}$ (‰)
1966.08	-4.72	0.19	1968.74	-4.83	-0.34
1966.20	-4.82	0.36	1968.83	-4.84	-0.42
1966.40	-5.15	0.81	1968.93	-5.04	-0.72
1966.45	-5.05	0.73	1969.04	-5.16	-0.40
1966.50	-5.04	0.47	1969.14	-5.16	-0.27
1966.55	-5.01	0.35	1969.22	-5.33	-0.30
1966.60	-4.85	0.20	1969.31	-5.06	-0.61
1966.65	-4.70	0.22	1969.40	-5.57	-0.89
1966.77	-4.98	-0.01	1969.46	-5.39	-1.06
1966.87	-4.99	0.06	1969.52	-5.16	-0.89
1966.97	-4.95	-0.21	1969.58	-5.01	-1.46
1967.08	-5.18	-0.36	1969.65	-4.98	-1.40
1967.18	-5.24	0.62	1969.74	-5.08	-1.68
1967.29	-5.25	0.77	1969.83	-5.07	-1.94
1967.40	-5.27	0.69	1969.92	-5.08	-1.82
1967.43	-4.92	0.23	1970.00	-5.10	-1.93
1967.47	-4.94	-0.30	1970.08	-5.10	-1.74
1967.50	-5.18	-0.11	1970.17	-5.09	-0.91
1967.54	-5.04	0.39	1970.24	-5.22	-0.78
1967.58	-5.24	0.58	1970.32	-5.46	-0.95
1967.61	-4.95	-0.17	1970.40	-5.48	-1.08
1967.65	-4.75	0.18	1970.44	-5.45	-0.16
1967.90	-4.90	0.16	1970.48	-5.26	-1.36
1968.13	-4.83	0.05	1970.52	-5.16	-1.40
1968.25	-5.11	0.43	1970.56	-5.03	-1.50
1968.40	-5.26	0.33	1970.61	-4.99	-1.42
1968.46	-5.12	-0.13	1970.65	-4.85	-1.47
1968.53	-4.94	-0.77	1970.77	-5.02	-1.74
1968.58	-4.91	-0.77	1970.88	-5.06	-1.78
1968.65	-4.75	-0.30	1970.00	-5.23	-1.39



Table III.5 contd.

Year	$\delta^{18}\text{O}$ (‰)	$\delta^{13}\text{C}$ (‰)	Year	$\delta^{18}\text{O}$ (‰)	$\delta^{13}\text{C}$ (‰)
1970.08	-5.10	-1.74	1972.40	-5.58	-0.84
1970.17	-5.09	-0.91	1972.48	-5.05	-0.99
1970.24	-5.22	-0.78	1972.56	-4.91	-0.62
1970.32	-5.46	-0.95	1972.65	-4.98	-0.79
1970.40	-5.48	-1.08	1972.77	-5.12	-1.21
1970.44	-5.45	-1.06	1972.88	-5.07	-1.60
1970.48	-5.26	-1.36	1973.00	-5.06	-1.37
1970.52	-5.16	-1.40	1973.12	-5.04	-0.98
1970.56	-5.03	-1.50	1973.22	-5.08	-0.81
1970.61	-4.99	-1.42	1973.31	-5.22	-0.58
1970.65	-4.85	-1.47	1973.40	-5.41	-0.47
1970.77	-5.02	-1.74	1973.44	-5.36	-0.62
1970.88	-5.06	-1.78	1973.48	-5.30	-0.86
1971.00	-5.23	-1.39	1973.52	-5.23	-1.03
1971.12	-5.40	-1.17	1973.56	-5.17	-1.03
1971.22	-5.14	-0.92	1973.61	-4.99	-1.13
1971.31	-5.20	-0.76	1973.65	-4.96	-0.85
1971.40	-5.50	-0.78	1973.77	-5.05	-1.15
1971.44	-5.38	-0.82	1973.87	-5.22	-1.24
1971.48	-5.21	-1.04	1973.97	-5.29	-1.25
1971.52	-4.06	-0.95	1974.08	-5.72	-1.22
1971.56	-4.98	-0.90	1974.18	-5.68	-1.10
1971.61	-4.80	-0.91	1974.29	-5.76	-1.01
1971.65	-4.79	-1.02	1974.40	-5.60	-0.75
1971.77	-4.99	-1.25	1974.44	-5.25	-1.05
1971.87	-5.07	-1.38	1974.48	-5.21	-1.60
1971.97	-5.16	-1.55	1974.52	-5.09	-1.40
1972.08	-5.32	-1.55	1974.56	-5.04	-1.20
1972.18	-5.49	-0.84	1974.61	-4.97	-1.05
1972.29	-5.49	-0.69	1974.65	-4.84	-0.78

Table III.5 contd.

Year	$\delta^{18}\text{O}$ (‰)	$\delta^{13}\text{C}$ (‰)	Year	$\delta^{18}\text{O}$ (‰)	$\delta^{13}\text{C}$ (‰)
1974.80	-5.12	-1.28	1978.28	-5.39	-1.13
1975.00	-5.40	-0.89	1978.40	-5.46	-1.55
1975.20	-5.34	-0.91	1978.53	-5.06	-2.11
1975.40	-5.41	-0.55	1978.65	-4.86	-1.79
1975.45	-5.38	-0.42	1978.78	-5.24	-2.13
1975.50	-5.20	-1.20	1978.90	-5.07	-1.81
1975.55	-5.12	-1.74	1979.03	-5.06	-1.84
1975.60	-4.94	-1.51	1979.15	-5.23	-1.69
1975.65	-4.86	-1.35	1979.28	-5.27	-1.35
1975.80	-4.95	-1.40	1979.40	-5.30	-1.23
1975.94	-5.06	-1.69	1979.48	-5.36	-1.48
1976.10	-5.05	-1.67	1979.56	-5.03	-1.56
1976.28	-5.21	-0.96	1979.65	-4.88	-1.80
1976.40	-5.40	-0.77	1979.78	-5.02	-1.94
1976.47	-5.42	-0.62	1979.90	-5.05	-2.30
1976.54	-5.41	-0.53	1980.03	-5.21	-2.08
1976.60	-5.43	-1.02	1980.15	-5.27	-1.52
1976.65	-5.04	-1.16	1980.28	-5.38	-1.52
1976.80	-5.08	-1.18	1980.40	-5.39	-1.42
1976.97	-5.22	-1.49	1980.44	-5.18	-1.52
1977.17	-5.25	-1.27	1980.49	-5.10	-1.66
1977.28	-5.36	-0.80	1980.53	-5.17	-2.19
1977.40	-5.59	-0.71	1980.57	-5.18	-2.39
1977.46	-5.43	-1.02	1980.61	-5.11	-2.15
1977.52	-5.27	-1.72	1980.65	-4.91	-1.36
1977.58	-5.14	-1.62	1980.08	-5.23	-1.09
1977.65	-4.78	-1.16	1981.40	-5.30	-1.46
1977.80	-4.84	-1.73	1981.48	-5.28	-1.88
1977.97	-4.78	-1.51	1981.57	-5.03	-1.36
1978.15	-5.26	-1.13	1981.65	-4.89	-1.80

Table III.5 contd.

Year	$\delta^{18}\text{O}$ (‰)	$\delta^{13}\text{C}$ (‰)	Year	$\delta^{18}\text{O}$ (‰)	$\delta^{13}\text{C}$ (‰)
1981.65	-4.89	-1.80	1984.48	-5.40	-2.28
1981.78	-4.91	-2.39	1984.51	-5.36	-2.16
1981.90	-4.96	-2.28	1984.54	-5.26	-2.19
1982.03	-5.17	-2.01	1984.57	-5.22	-2.04
1982.15	-5.22	-1.29	1984.60	-5.16	-1.87
1982.28	-5.22	-0.68	1984.63	-5.15	-1.93
1982.40	-5.40	-0.85	1984.65	-4.83	-2.12
1982.48	-5.25	-1.44	1984.73	-5.13	-2.72
1982.57	-5.08	-1.88	1984.81	-5.05	-2.66
1982.65	-4.99	-2.20	1984.89	-4.94	-2.44
1982.78	-5.00	-2.12	1984.97	-4.91	-2.26
1982.90	-5.05	-2.46	1985.06	-4.97	-1.89
1983.03	-4.97	-2.12	1985.15	-5.19	-1.83
1983.15	-5.02	-1.42	1985.23	-5.16	-1.69
1983.28	-5.16	-1.28	1985.31	-5.30	-1.79
1983.40	-5.18	-0.97	1985.40	-5.52	-1.72
1983.48	-5.01	-1.03	1985.43	-5.49	-1.25
1983.57	-5.09	-1.72	1985.46	-5.44	-1.31
1983.65	-4.95	-1.74	1985.49	-5.32	-1.85
1983.74	-5.06	-2.06	1985.52	-5.35	-1.78
1983.83	-5.17	-2.46	1985.55	-5.12	-2.08
1983.93	-5.39	-2.41	1985.58	-5.05	-2.24
1984.04	-5.22	-2.28	1985.61	-5.02	-2.26
1984.14	-5.43	-2.31	1985.65	-4.93	-2.23
1984.22	-5.44	-2.24	1985.77	-5.11	-2.24
1984.31	-5.47	-2.07	1985.87	-5.19	-2.29
1984.34	-5.79	-2.03	1985.97	-5.31	-2.31
1984.40	-5.78	-1.84	1986.08	-5.58	-1.61
1984.42	-5.65	-1.88	1986.18	-5.54	-1.63
1984.45	-5.53	-2.02	1986.29	-5.55	-1.62

Table III.5 contd.

Year	$\delta^{18}\text{O}$ (‰)	$\delta^{13}\text{C}$ (‰)	Year	$\delta^{18}\text{O}$ (‰)	$\delta^{13}\text{C}$ (‰)
1986.40	-5.61	-1.39	1989.58	-5.14	-1.94
1986.46	-5.57	-1.48	1989.65	-4.91	-1.85
1986.53	-5.46	-1.77	1989.78	-4.95	-2.55
1986.58	-4.96	-1.90	1989.90	-5.14	-2.90
1986.65	-4.96	-1.61	1990.04	-5.15	-2.63
1986.74	-5.11	-1.81	1990.16	-5.20	-2.61
1986.83	-4.95	-2.10	1990.28	-5.37	-2.36
1986.92	-5.10	-2.14	1990.40	-5.42	-2.41
1987.00	-5.04	-2.22	1990.44	-5.26	-2.32
1987.10	-5.09	-1.88	1990.48	-5.35	-2.15
1987.20	-4.99	-1.58	1990.52	-4.95	-2.58
1987.30	-4.89	-1.53	1990.56	-5.12	-2.41
1987.40	-5.27	-1.25	1990.61	-4.88	-2.67
1987.53	-5.08	-1.60	1990.65	-4.91	-2.80
1987.65	-4.95	-1.66	1990.74	-4.99	-2.75
1987.90	-5.11	-1.04	1990.83	-5.22	-3.09
1988.15	-5.25	-0.72	1990.92	-5.31	-3.23
1988.40	-5.37	-1.26	1991.00	-5.20	-2.94
1988.49	-5.15	-1.34	1991.10	-5.04	-2.72
1988.57	-5.12	-1.53	1991.20	-5.10	-2.29
1988.65	-4.96	-1.64	1991.30	-5.34	-2.05
1988.80	-5.15	-1.70	1991.40	-5.44	-1.91
1988.95	-5.12	-2.00	1991.43	-5.31	-1.76
1989.10	-5.17	-1.83	1991.47	-5.43	-1.54
1989.25	-5.29	-1.64	1991.50	-5.34	-1.72
1989.40	-5.40	-1.66	1991.54	-5.15	-2.12
1989.46	-5.30	-1.72	1991.58	-5.05	-1.80
1989.53	-5.27	-1.87	1991.61	-5.01	-1.85

Table III.7  $\delta^{18}\text{O}$  and  $\delta^{13}\text{C}$  records of Gk coral

Year	Distance (mm)	$\delta^{18}\text{O}$ (‰)	$\delta^{13}\text{C}$ (‰)	Year	Distance (mm)	$\delta^{18}\text{O}$ (‰)	$\delta^{13}\text{C}$ (‰)
1948	0.00	-4.08	-0.54	1956	49.90	-4.22	-0.81
	1.70	-4.15	-1.12		50.70	-4.03	-0.04
	3.30	-3.78	-0.36		51.80	-3.99	0.02
	4.40	-3.86	-0.44		52.50	-4.07	-0.57
1949	5.40	-3.73	-0.71	1957	53.00	-4.19	-0.56
	6.30	-4.27	-1.82		54.00	-4.07	-0.58
	7.50	-4.37	-2.14		55.30	-3.75	-0.59
	8.40	-4.36	-1.54		57.20	-4.06	0.62
1950	9.50	-4.42	-1.14	1958	58.80	-4.16	0.35
	10.70	-4.25	-0.72		61.00	-3.91	0.65
	11.80	-3.82	-0.50		62.50	-4.10	-0.05
	12.70	-3.84	-0.30		63.80	-4.19	-0.42
1951	13.70	-3.69	-0.35	1959	65.10	-4.29	-0.57
	15.40	-3.99	-0.22		66.60	-4.11	-0.26
	17.00	-4.04	-0.23		68.50	-4.10	0.27
	18.80	-4.28	-0.55		70.50	-4.53	-0.58
1952	20.60	-3.65	1.02	1960	72.00	-4.25	0.00
	22.60	-3.70	-0.09		73.80	-4.54	-1.34
	24.50	-3.80	-0.43		75.60	-4.42	-1.01
	26.20	-3.97	-0.29		77.10	-4.27	0.04
1953	27.80	-3.88	-0.20	1961	78.80	-4.29	-0.77
	29.20	-4.36	-1.72		80.30	-4.22	-0.46
	30.50	-4.40	-0.94		82.30	-3.98	-0.31
	32.00	-4.10	-0.03		83.90	-4.40	-0.26
1954	34.00	-4.16	-0.99	1962	85.60	-4.23	-0.45
	35.00	-4.57	-1.41		87.50	-3.95	0.13
	36.30	-4.48	-1.41		89.00	-3.73	0.12
	38.60	-4.25	-0.54		90.80	-4.08	-0.66
1955	40.20	-4.23	-0.26	1963	92.40	-4.16	-0.39
	41.60	-4.68	-2.23		94.00	-3.85	0.54
	42.70	-4.65	-2.52		95.50	-3.90	-0.09
	44.00	-4.20	-0.41		96.90	-4.00	-0.81
1956	45.70	-3.94	0.48	1964	98.60	-3.98	-0.27
	49.60	-4.23	-0.34		100.40	-3.70	0.19
	48.20	-4.24	-0.37		102.10	-4.17	-0.98

Table III.7 contd.

Year	Distance (mm)	$\delta^{18}\text{O}$ (‰)	$\delta^{13}\text{C}$ (‰)	Year	Distance (mm)	$\delta^{18}\text{O}$ (‰)	$\delta^{13}\text{C}$ (‰)
1966	103.4	-3.92	-0.42	1978	160.0	-4.15	0.20
	105.2	-4.09	-0.03		161.5	-4.57	-0.01
	106.7	-4.28	-0.15		162.9	-4.62	-1.10
	108.2	-4.20	-0.56		164.3	-4.34	0.26
1967	110.0	-3.98	0.53	1979	165.7	-4.28	0.52
	111.9	-4.34	-0.03		166.9	-4.94	-0.72
1968	113.5	-3.82	0.88		168.4	-4.98	-0.73
	115.0	-3.94	0.94	1980	170.0	-4.41	-0.28
1969	116.8	-3.99	0.40		171.5	-4.39	-0.24
	118.2	-4.10	-0.06	1981	172.8	-4.08	0.07
	120.2	-4.01	-0.34		174.4	-4.47	-0.76
1970	121.9	-3.67	0.19		175.6	-4.26	-0.37
	123.8	-4.22	-0.46	1982	177.2	-3.96	-0.06
	125.5	-4.00	-0.5		178.3	-4.14	-0.26
1971	128.2	-3.51	-0.41	1983	179.4	-3.96	0.57
	131.0	-3.74	-0.13		181.2	-4.03	-0.06
1972	132.8	-3.65	0.05		182.9	-4.13	-0.29
	135.0	-3.84	0.22	1984	184.1	-3.69	0.65
1973	137.1	-3.44	0.36		185.6	-3.76	0.09
	139.2	-3.84	-0.02		187.3	-3.88	0.84
1974	140.8	-3.70	0.34	1985	188.5	-3.77	0.75
	142.7	-4.02	-0.30		189.8	-3.94	0.61
1975	144.4	-3.78	0.65	1986	191.0	-3.63	1.16
	145.8	-3.85	1.05		192.8	-3.93	0.76
	147.4	-4.24	-0.14		193.9	-3.93	0.18
	149.0	-4.49	-0.10	1987	195.2	-3.71	0.80
1976	150.6	-4.35	0.32		196.4	-3.88	0.88
	152.0	-4.43	-0.21		198.6	-4.00	-0.02
	153.1	-4.45	-0.48	1988	199.8	-3.74	0.77
1977	154.4	-4.30	0.21		201.7	-3.85	0.49
	156.0	-4.41	0.06		203.9	-4.21	0.00
	157.2	-4.54	-0.47	1989	205.9	-3.90	0.96
	158.8	-4.56	-0.22		208.0	-4.09	1.57

Table III.8a Oxygen and carbon isotopic records of the SR coral in Track-1

Year	Distance(mm)	$\delta^{18}\text{O}(\text{‰})$	$\delta^{13}\text{C}(\text{‰})$	density(g cm <sup>-3</sup> )
1968	0.0	-5.29	-1.05	1.56
	4.1	-4.57	-0.58	1.63
	5.3	-5.01	-0.56	1.59
1969	6.9	-5.49	-0.93	1.56
	11.3	-4.92	-0.86	1.66
	13.1	-4.57	0.35	1.68
1970	16.4	-5.05	-0.71	1.52
	18.3	-4.84	-0.49	1.63
	21.3	-4.26	-0.59	1.62
1971	22.5	-5.29	-0.28	1.59
	25.3	-5.04	-1.11	1.50
	27.2	-4.88	-0.72	1.54
	29.2	-5.10	-0.37	1.59
1972	31.2	-5.66	-0.28	1.53
	34.2	-5.14	-0.45	1.39
	36.0	-4.93	-0.62	1.47
	38.6	-4.93	-0.35	1.38
1973	42.8	-5.26	-0.64	1.36
	44.3	-5.55	-0.46	1.47
	46.5	-4.85	-0.77	1.59
1974	50.0	-4.90	-0.51	1.60
	56.3	-5.47	-1.10	1.48
	59.4	-4.89	-1.36	1.53
	62.1	-4.73	-0.85	1.59
1975	67.2	-5.25	-0.75	1.53
	70.8	-5.45	-0.99	1.44
	74.3	-4.56	-0.72	1.61
1976	75.6	-5.44	-0.51	1.57

Table III.8a contd.

Year	Distance (mm)	$\delta^{18}\text{O}(\text{‰})$	$\delta^{13}\text{C}(\text{‰})$	Density(g cm <sup>-3</sup> )
1977	78.8	-5.31	-0.66	1.47
	80.7	-5.83	-0.96	1.49
	83.8	-5.04	-0.86	1.52
	87.3	-5.07	-1.17	1.60
	90.6	-5.24	-0.38	1.46
	94.5	-5.83	-0.97	1.43
1978	97.8	-4.62	-1.09	1.51
	100.5	-4.93	-1.01	1.57
	104.4	-5.17	-0.97	1.37
	106.7	-5.51	-1.01	1.34
1979	110.7	-4.76	-1.22	1.51
	112.7	-4.91	-1.04	1.56
	116.7	-5.08	-1.29	1.38
	121.5	-4.78	-1.46	1.41
	124.3	-4.96	-1.45	1.33
	127.4	-4.90	-1.16	1.49
1980	129.0	-5.43	-1.41	1.42
	132.1	-5.27	-1.54	1.25
	134.2	-5.24	-1.47	1.26
	138.0	-4.59	-1.06	1.44
1981	140.5	-5.26	-0.91	1.41
	144.3	-5.30	-0.98	1.34
	147.1	-5.66	-1.25	1.30
	150.9	-4.81	-1.25	1.42
1982	155.1	-5.46	-1.00	1.55
	160.5	-5.04	-1.23	1.38
	165.3	-4.50	-1.21	1.41
1983	168.3	-5.06	-1.23	1.28



Table III.8a contd.

Year	Distance (mm)	$\delta^{18}\text{O}(\text{‰})$	$\delta^{13}\text{C}(\text{‰})$	Density( $\text{g cm}^{-3}$ )
1984	172.0	-5.22	-1.11	1.25
	174.8	-4.58	-1.08	1.35
	177.7	-5.25	-0.77	1.37
	181.2	-5.10	-1.25	1.33
	184.7	-4.90	-1.02	1.31
	188.0	-4.33	-1.36	1.42
1985	191.1	-5.39	-0.97	1.49
	196.2	-5.29	-1.37	1.42
	200.3	-5.22	-1.27	1.34
1986	204.3	-4.64	-0.94	1.45
	209.4	-5.20	-1.45	1.37

Table III.8b Oxygen and carbon isotopic record of SR coral (Track-2)

Year	distance (mm)	$\delta^{18}\text{O}(\text{‰})$	$\delta^{13}\text{C}(\text{‰})$	Density(g cm <sup>-3</sup> )
1968	0.0	-5.09	-1.46	1.74
	3.0	-4.46	-0.31	1.83
1969	6.0	-4.09	-0.22	1.73
	11.5	-4.05	0.09	1.77
	16.0	-4.46	0.14	1.80
1970	24.0	-5.05	-0.84	1.79
	28.5	-4.54	-0.74	1.68
1971	34.0	-5.29	-0.37	1.69
	40.0	-4.54	-0.19	1.68
1972	45.0	-5.11	-0.23	1.71
	50.0	-4.67	0.00	1.66
1973	56.5	-5.34	-0.83	1.62
	59.0	-5.10	-1.03	1.53
1974	63.0	-4.64	-0.78	1.53
	71.0	-5.28	-1.09	1.64
1975	78.0	-5.02	-0.57	1.56
	83.0	-5.34	-0.85	1.56
1976	92.0	-4.76	-1.01	1.48
	94.0	-5.33	-0.73	1.38
	98.5	-5.47	-0.95	1.39
1977	102.5	-4.61	-1.01	1.51
	107.0	-5.27	-0.32	1.48
	110.5	-5.58	-0.96	1.48
	112.0	-5.48	-0.99	1.37
1978	116.0	-4.61	-0.85	1.51
	120.0	-5.26	-1.08	1.44
1979	127.0	-5.49	-0.83	1.44
	132.5	-4.97	-1.23	1.24
	138.0	-4.96	-1.16	1.26

Table III.8b contd.

Year	Distance (mm)	$\delta^{18}\text{O}(\text{‰})$	$\delta^{13}\text{C}(\text{‰})$	Density(g cm <sup>-3</sup> )
1980	144.0	-5.01	-0.53	1.27
	154.0	-4.96	-1.10	1.13
1981	161.0	-5.26	-1.12	1.16
	164.5	-5.43	-0.81	1.17
	168.0	-5.42	-1.21	1.17
1982	171.0	-4.74	-1.09	1.36
	174.5	-5.26	-0.59	1.25
	178.0	-5.40	-0.79	1.27
	181.0	-4.99	-1.11	1.12
1983	184.0	-4.53	-1.06	1.19
	189.0	-5.12	-0.48	1.17
	192.0	-5.19	-0.85	1.18
	194.0	-5.25	-0.99	1.09
1984	197.0	-4.66	-1.10	1.19
	203.0	-5.07	-0.83	1.23
1985	210.5	-5.03	-1.31	1.25
	216.5	-4.95	-0.59	1.33
	223.2	-5.25	-1.16	1.30
	226.8	-4.49	-1.57	1.37
1986	228.0	-4.58	-0.95	1.39
	231.5	-5.20	-0.63	1.37
	237.0	-5.07	-1.19	1.31
	239.5	-4.74	-1.38	1.29
	241.5	-4.66	-1.22	1.34

Table III.12A  $\Delta^{14}\text{C}$  records of the Gulf of Kutch coral

Sample code	Year of Growth	$\Delta^{14}\text{C}(\text{‰})$	Sample code	Year of Growth	$\Delta^{14}\text{C}(\text{‰})$
CH:88	1949-51	-60 $\pm$ 5	CH:80	1971-72	131 $\pm$ 7
CH:87	1952-54	-53 $\pm$ 6	CH:78	1973-75	146 $\pm$ 7
CH:86	1955-60	0.8 $\pm$ 6	CH:77	1976-77	122 $\pm$ 6
CH:85	1961-63	57 $\pm$ 7	CH:76	1978-80	102 $\pm$ 7
CH:84	1964-65	120 $\pm$ 7	CH:69	1981-82	99 $\pm$ 7
CH:83	1966-67	147 $\pm$ 8	CH:68	1983	96 $\pm$ 7
CH:82	1968	170 $\pm$ 6	CH:67	1984-87	71 $\pm$ 6
CH:81	1969-70	156 $\pm$ 7	CH:66	1988-90	55 $\pm$ 7

Table III.12B  $\Delta^{14}\text{C}$  records of Thane tree rings

Sample code	Year of Growth	$\Delta^{14}\text{C}(\text{‰})$	Sample code	Year of Growth	$\Delta^{14}\text{C}(\text{‰})$
CH:191	1960	238 $\pm$ 6	CH:180	1971-72	434 $\pm$ 7
CH:190	1961	260 $\pm$ 6	CH:179	1973	400 $\pm$ 7
CH:187	1962	338 $\pm$ 6	CH:178	1974	420 $\pm$ 7
CH:186	1963	565 $\pm$ 8	CH:177	1975	354 $\pm$ 6
CH:185	1964-65	630 $\pm$ 8	CH:176	1976	340 $\pm$ 7
CH:184	1966	587 $\pm$ 8	CH:173	1977	311 $\pm$ 6
CH:183	1967	560 $\pm$ 7	CH:172	1978	299 $\pm$ 6
CH:182	1968	534 $\pm$ 7	CH:171	1979-80	260 $\pm$ 7
CH:181	1969-70	476 $\pm$ 7			

## List of Publications of the author

- Chakraborty S. and Ramesh R. (1992)** Climatic significance of  $\delta^{18}\text{O}$  and  $\delta^{13}\text{C}$  variations in a banded coral (*Porites*) from Kavaratti, Lakshadweep Islands. In: BN Desai (ed) *Oceanography of the Indian Ocean*. Oxford and IBH Publication (P) Ltd. New Delhi, pp 473-478.
- Chakraborty S. and Ramesh R. (1993)** Monsoon records in Indian corals. In: *Proc. Int. Symp. on Global Change (IGBP)* Waseda Univ., Tokyo pp 648:653.
- Chakraborty S. and Ramesh R. (1993)** Monsoon induced sea surface temperature changes recorded in Indian coral. *Terra Nova* (in press).
- Chakraborty S. and Ramesh R. (1993)** Stable isotopes variations in a coral from the Gulf of Kutch: environmental implications. ID-GBP special publication. DOS, Bangalore (in press)
- Bhushan R., Chakraborty S. and Krishnaswami S. (1993)** Physical Research Laboratory (Chemistry) radiocarbon date list CH-1 Submitted to *Radiocarbon*.
- Chakraborty S., Ramesh R. and Lough J.M. (1993)** Effect of intraband variability on stable isotope and sensity time series obtained from banded corals. Submitted to *Geophys. Res. Lett.*
- Chakraborty S., Ramesh R. and Krishnaswami S. (1993)** Air-sea exchange of  $\text{CO}_2$  in the Gulf of Kutch based on bomb carbon in corals and tree rings. MS in preparation